70-14,423

O'REILLY, Patrick Daniel, 1940-
THE INTERACTIONS OF 16.2 BeV NEGATIVE PIONS WITH EMULSION NUCLEI.

The University of Oklahoma, Ph.D., 1970
Physics, elementary particles

University Microfilms, Inc., Ann Arbor, Michigan

THE UNIVERSITY OF OKLAHOMA

GRADUATE COLLEGE

THE INTERACTIONS OF 16.2 BEV NEGATIVE PIONS WITH EMULSION NUCLEI

A DISSERTATION

SUBMITTED TO THE GRADUATE FACULTY

in partial fulfillment of the requirements for the

degree of

DOCTOR OF PHILOSOPHY

BY

PATRICK D. O'REILLY

Norman, Oklahoma

1969

THE INTERACTIONS OF 16.2 BEV NEGATIVE

PIONS WITH EMULSION NUCLEI

A DISSERTATION

APPROVED BY

J. R. Burwell

J. M. Caufield

Joseph Cohn

William N. Huff

Dennis Slag

DISSERTATION COMMITTEE

ACKNOWLEDGEMENTS

The author would like to thank Dr. James R. Burwell, who directed this research, for his advice and guidance throughout the course of the research. He would also like to express his thanks to Dr. Jalal Samimi for the use of the data from his research project. Many thanks go to the other members of the high energy laboratory staff who contributed in any way, no matter how small, to this research.

A special debt of gratitude is owed the author's wife, Leona, who typed this manuscript. Her patience and understanding during the course of this project are deeply appreciated. The author would also like to thank his parents, Gabe and Esther O'Reilly for the many sacrifices, financial and otherwise, they have made on his behalf. Without them, achievement of this educational goal would not have been possible.

Finally, the support of an NDEA fellowship for part of the period of research is acknowledged.

TABLE OF CONTENTS

LIST OF TABLES

LIST OF TABLES (Cont.)

LIST OF ILLUSTRATIONS

LIST OF ILLUSTRATIONS (Cont.)

THE INTERACTIONS OF 16.2 BEV NEGATIVE PIONS WITH EMULSION NUCLEI

CHAPTER I

INTRODUCTION

In elementary particle physics, two problems which have attracted the attention of many researchers are the structure of the nucleon and the characteristics of the pion. Since the pion is a quantum of the force field which is exchanged between two nucleons in the nucleus of an atom, a study of its characteristics should lead to a better understanding of the nuclear force. One way in which the characteristics of elementary particles can be studied is through the observation of interactions which involve the particles of interest.

During the last several years, a large number of experiments have been performed to study high energy pion-nucleon and nucleon-nucleon collisions. From these experiments such quantities as the partial cross section for the production of certain types of events and for the multiplicities of secondary particles created by the interaction process have been determined. The results have been compared with theoretical models and from the comparisons a better understanding of the interaction process and the particles involved has been obtained.

Most of the secondary particles which are produced in high energy pion-nucleon and nucleon-nucleon collisions are pions. For this reason a study of the kinematical characteristics of the secondary pions should yield much information about the strong interaction mechanism. A great deal of literature has been published up to now for that purpose.

However, if one considers a slightly different type of interaction involving the same incident particle; namely, a pion-nucleus interaction, a quite dissimilar situation arises. There are comparatively few results on this type of interaction in the literature. A possible explanation for this lack of publications lies in the fact that the pion-nucleus collision process itself can be more complex than that of the pion-nucleon collision. Since all the secondary pions which are created in pion-nucleus collisions may not be products of the primary interaction, these two types of interactions can be different from a physical viewpoint.

Therefore, an investigation of pion-nucleus interactions and a comparison of the results with available published results should lead to a better understanding of the interaction process. A comparison with the results obtained from pion-nucleon interactions will point out any similarities or differences which may exist between the two types of interactions.

The purpose of this dissertation is to examine pion-nucleus interactions and to compare the results both with available theories and with published results. The results are also compared with those obtained from a study of pion-nucleon interactions at the same incident pion energy.

Chapter II begins with a discussion of the existing theoretical ideas on the mechanism of pion-nucleus interactions which involve multiple pion production. This is followed by a summary of the theoretical and experimental work which has been done on the transverse momentum of secondary pions produced in high energy interactions. The chapter concludes with a brief discussion of resonances and the possibility of the formation of multi-pion resonances in the pion-nucleus interaction process.

Chapter III contains a description of the experiment and the equipment used for measurements. An outline of the experimental procedure is then presented. The determination of experimental error is discussed in the last section.

The data which was obtained in the experiment is presented and analyzed in detail in Chapter IV. A comparison is made of these results with the theoretical predictions and experimental observations of pion-nucleus interactions discussed in Chapter II. These experimental results are also compared with the results of investigations of pion-nucleon interactions, in particular, with the results from interactions at the same incident pion energy.

A summary of the experimental results and the conclusions which can be made on the basis of these results are presented in the last chapter.

CHAPTER II

DISCUSSION OF THEORY AND PREVIOUS RESULTS

Particle-Nucleus Interactions Theory

In the analysis of the interactions of high energy nucleons or mesons with atomic nuclei which result in secondary meson production, two basic theoretical models have been used almost exclusively. These are the inter-nuclear cascade model and the tube model.

Cascade Model

The cascade model of high energy particle-nucleus interactions was developed from a theory proposed by Heisenberg[1] in 1943 and restated by Serber[2] four years later. This theory was formulated as a description of the mechanism of high energy nucleon-nucleus interactions. It was concerned with paired interactions between the incident nucleon and the individual nucleons of the nucleus. The physical principles underlying this theory are as follows: the incident nucleon has a small wavelength. Because of this, there is a high probability that the interaction is concentrated on one of the nucleons in the nucleus. Since the duration of the collision is short, the recoil nucleon does not have enough time to transfer the interaction to the remainder of the nucleus. As a result, in the scattering which takes place, the recoil nucleon behaves almost as if it were in a free state and not bound to the nucleus. The difference is connected with the momentum distribution of nucleons in the nucleus and with the Pauli principle. To high energy nucleons, the nucleus appears like a gas of non-interacting nucleons which is located in a potential field of definite configuration[3].

Since its wavelength is so short, the motion of the incident nucleon can be treated classically and a definite trajectory in the nuclear matter can be ascribed to it. The recoil nucleons, which have received a significant amount of energy from the primary nucleon, can be treated in a similar manner. From the viewpoint of the cascade model, the first stage of the interaction consists of collisions of high energy nucleons with the nucleons of the nucleus. A part of the cascade is then emitted from the nucleus in the form of experimentally observed high energy secondary particles--mostly mesons. The remaining parts, having lost an appreciable amount of their energy, are absorbed by the nucleus. This forms an excited nucleus and the cascade process is completed. The last stage of the interaction now occurs, namely the evaporation process in which the excited nucleus loses its energy in the form of nucleons, deuterons and α particles.

This model also applies to the case where the incident particle is a pion[4]. The description of the interaction is analagous to that of the nucleon-nucleus interaction only the initial stage of the reaction consists of a pion-nucleon interaction instead of a nucleon-nucleon interaction.

Exact analytic calculations of the cascade process do not exist at the present time simply because many of the characteristics of the cascade have no analytic expressions to represent them. One example of this is the cross section for the nucleon-nucleon collisions occurring in the cascade.

However, Goldberger[5] proposed the use of the Monte Carlo method of statistical testing to simulate the real process. Since it is possible in this method to analyze complex processes, the individual elements of which can be specified either analytically or numerically, the computational difficulties are lessened to a certain degree. With the advent of high speed electronic computers, the task became even easier. A brief discussion of the published results of the Monte Carlo calculations using the cascade model will be presented in a later section in this chapter.

Tube Model

The tube model of high energy particle-nucleus reactions was first proposed in 1954 by Rozental and Chernavskii[6]. At that time two of the major theories of multiple meson production in high energy interactions were the thermodynamical models of Fermi[7] and Heisenberg[8]. Then, in 1953, Landau[9] proposed a different theory of multiple production which was based on relativistic hydrodynamics instead of thermodynamics. In 1955 Feinberg[10] claimed that the cascade model of nucleon-nucleus interactions was inconsistent with the wave properties of the particles involved in the interactions. He suggested that for incident nucleons with energies between 10^{10} and 10^{12} eV colliding with atomic nuclei the tube model is a better description of the interaction mechanism. The following year, Belen'kji and Landau[11] published a paper which applied the hydrodynamical theory to a high energy nucleon-nucleon collision. They then extended this treatment to the case of a nucleon-nucleus collision. Here they combined the hydrodynamical theory of multiple production with the tube model. Further calculations concerning nucleon-nucleus interactions have been made by Belen'kji and Milekhin[12] and by Milekhin[13]. Their results will be presented in the next section.

The basic features of the tube model are the following: the collision of a high energy nucleon with a nucleus is not considered as a series of collisions between nuclear nucleons. Because the separation distance between the nucleons in the nucleus is of the order of the radius of the nuclear force and in each collision several new particles are created, the collision must therefore lead to a process of simultaneous creation of particles in the whole range through which the nucleon passes in the nucleus. The incident nucleon will interact with only a part of the nucleus and not always with the whole nucleus. In other words, it will cut a tube through the nucleus. This tube is actually an excited system which emits its energy in the form of secondary particles which are experimentally observable.

Although the tube model in its original form was proposed to explain high energy nucleon-nucleus collisions, it has also been applied to the interactions of high energy pions with nuclei[(14)].

According to Barashenkov _et al._[(15)], confusion sometimes arises in the analysis of particle-nucleus interactions when the two theoretical models are applied to the data. Since the duration of an interaction between a high energy particle and a target nucleus is very short, the interaction may have no time to spread out in the direction perpendicular to the velocity of the incident particle. This will result in the interaction being concentrated in the tube of nuclear matter. This phenomena is often advanced as an argument in support of the tube model. It is important to realize that such a physical picture is related only to the kinematics of the process and therefore does not contradict either the cascade or the tube model.

The chief characteristic of the tube model is the simultaneous interaction of the primary particle with a major part of the target nucleus or even with the whole nucleus in some cases. This interaction takes place in the tube and the tube then becomes a coherent excited system as a whole. This is different from the main characteristics of the cascade model--namely successive interactions with separated nucleons within a conical or tubular shaped portion of nuclear matter.

Predictions of the Models and Previous Results

As was mentioned earlier, no complete analytical calculations using the cascade model are available. However, many authors[3,4,15-22] have used the Monte Carlo method to simulate particle-nucleus interactions. The energies of the primary particles in these calculations have varied from several MeV (low-energy) to several BeV (high energy) to cosmic ray energies. In order to make the calculations it was first necessary to assume the applicability of one of the theoretical models of multiple particle production in high energy particle-nucleon collisions: a thermodynamical model[7,8], the hydrodynamical model[9], the excited nucleon[23]*, the fireball model[24,25], or some modified version of one of these which can be found in one of the reviews of multiple production theory[25-28]. The

*Valid model only for E_0>100 BeV.

model chosen was used to calculate the results of the initial stage of the reaction, either a nucleon-nucleon interaction or a pion-nucleon interaction. The details of the Monte Carlo calculation can be found in the papers published by Barashenkov et al.[17], Metropolis et al.[21] and Denisov et al.[3]. A statistical model of multiple particle production developed by Barashenkov can be found in [29].

Barashenkov and various colleagues[15-17,20] have performed Monte Carlo calculations using the internuclear cascade model. They simulated the interactions of high energy protons with the nuclei of nuclear emulsion. These calculations were performed for incident proton energies of 6.2, 9, 17, and 25 BeV. Angular distributions and the energy spectrum of the secondary particles created in the 9 BeV proton-nucleus interactions are given[16]. More detailed angular and energy distributions for these events along with the results of calculations of nuclear cross-sections are presented[17]. The angular distribution and the momentum distribution of secondaries from 25 BeV proton-nucleus interactions are found in reference[15]. Artykov et al.[20] present a complete summary of all the Monte Carlo calculations made on the proton-nucleus interactions. Table 1 illustrates part of the results they obtained for the case where the target is an average nucleus in the emulsion (Ga^{70}). Table 2 lists some of the results obtained for the interaction of 25 BeV protons with heavy emulsion nuclei (Ag^{108}

TABLE 1[20,30]

AVERAGE CHARACTERISTICS OF PARTICLES PRODUCED BY INTERACTIONS OF PROTONS WITH AN AVERAGE NUCLEAR EMULSION NUCLEUS (Ga^{70})

	6.2 BeV		9 BeV		17 BeV		25 BeV	
Characteristic	Cascade Model Theory	Experiment	Cascade Model Theory	Experiment	Cascade Model Theory	Experiment	Cascade Model Theory	Experiment
$\langle n_s \rangle$	2.80±.15 (old) 2.7 ±0.1 (new)	2.65±.10 2.7 ±0.2 (31.32)	3.4 ±.2 (old and new)	3.2 ±.2 (16)	5.5 ±.3 (old) 5.3 ±.3 (new)	5.89±.06 (34) T≈19.8 BeV	6.9 ±.4 (old) 6.2 ±.3 (new)	6.6 ±.1 (35) 5.5 ±.2 (36)
$\langle N_h \rangle$	8.3 ±0.4 (old) 7.8 ±0.4 (new)	9.7±0.3 8.8 (31,33)	8.3 ±.6 (old) 8.5 ±.4 (new)	8.3 ±.9 (16)	9.7 ±.6 (old) 9.4 ±.4 (new)	8.5 ±.5 (34) T≈19.8 BeV	8.9 ±.5 (old) 9.7 ±.5 (new)	6.7 ±.2 (35) 8.4 (36)
$\langle E \rangle$ BeV	0.70±.05 (old)	- - - -	0.85±.05 (old) 1.30±.6 (new)	1.0 ±0.2 (16)	1.3 ±.1 (old) 1.8 ±.1 (new)	- - - -	2.0 ±.1 (old) 2.4 ±.1 (new)	2.3 ±.2 (35)
$\langle p_T \rangle$ BeV/c	0.40±.02 (old) 0.42±.02 (new)	- - - -	0.40±.02 (old) 0.43±.02 (new)	0.37±.07 (16)	0.42±.02 (old) 0.46±.023 (new)	- - - -	0.42±.02 (old) 0.47±.025 (new)	- - - -

Legend: $\langle n_s \rangle$-Average number of light tracks

$\langle N_h \rangle$-Average number of (dark + gray) tracks

$\langle E \rangle$ -Average kinetic energy of shower particles

$\langle p_T \rangle$-Average transverse momentum of shower particles

T-Energy of primary proton

TABLE 2 (21), (65)

AVERAGE CHARACTERISTICS OF PARTICLES PRODUCED BY INTERACTION OF 25 BeV PROTONS WITH HEAVY EMULSION NUCLEI (Br^{80} and Ag^{108})

Characteristic	Cascade Model Theory	Experiment
$\langle n_s \rangle$	7.8 ± 0.2 (old) 7.9 ± 0.4 (new)	8.6 ± 0.8 (36)
$\langle N_h \rangle$	15.8± 0.8 (old) 15.2± 0.8 (new)	13 ± 0.3 (33) 15.4± 1.5 (38)
$\langle E \rangle$ BeV	1.8 ± 0.1 (old) - - - - -	2.1 ± 0.2 (39)
$\langle p_T \rangle$ BeV/c	0.5 ± 0.010 (old) 0.46± 0.023 (new)	0.48± 0.02 (39)

Notation is the same as that of Table 1.

and Br^{80}). The entries under the heading "Experiment" will be discussed later in this section.

In another paper(4), Artykov *et al*. present the results of a Monte Carlo calculation of the interactions of 17 BeV negative pions with emulsion nuclei using the cascade model. Table 3 shows some of the results obtained in their calculation. The experimental work listed will be discussed in a later part of this section.

In a more recent article, Artykov *et al*.(30) pre-

TABLE 3 (20)

AVERAGE CHARACTERISTICS OF PARTICLES PRODUCED IN INTERACTIONS OF 17 BeV NEGATIVE PIONS WITH AN AVERAGE HEAVY NUCLEUS OF EMULSION

Characteristic	Cascade Model Theory	Experiment
$\langle n_s \rangle$	7.1 ± 0.5	7.1 ± 0.2 (40) 6.0 ± 0.3 (41)
$\langle N_h \rangle$	4.0 ± 0.4	4.5 ± 0.4 (40)
$\langle p_T \rangle$ (BeV/c)	0.39 ± 0.04	0.59 ± 0.02 (40)

Notation is the same as that of Table 1.

sent the results of new calculations performed by the Monte Carlo method using the cascade model. The energies of the primary mesons and nucleons varied from a few BeV to $\sim 10^3$ BeV. There was a major difference between these cascade calculations and the work previously discussed[20]. The 1967 calculations did not assume that one intranuclear nucleon could interact simultaneously with several particles produced in an earlier stage of the cascade. In order to explain experimental results in the region of primary energies above ~100 BeV, it was necessary to consider such many particle reactions.

Agreement with experimental data was obtained in the $\gtrsim 100$ BeV region, but the average transverse momentum and the average kinetic energy exceed the observed values at lower primary energies. An effort was made to decrease these two quantities by changing the momentum distributions used in the calculations but this resulted in an unallowable increase of shower particle multiplicities. The values of average transverse momentum found by Artykov et al.[30] are given in Table 1. Since they are larger than the previous values obtained[20] and since the authors made no definite statement about their being more acceptable, both values are given at each primary energy.

In their discussion of the tube model theory, Belen'kji and Landau[11] calculated the dependence of the multiplicity of the secondary particles created in high energy nucleon-nucleon collisions on the energy of the primary nucleon. They obtained the result

$$n \sim E^{\frac{1}{4}}.$$

When they extended the hydrodynamical theory to particle-nucleus interactions, they found that the multiplicity of secondaries is also a function of the number of nucleons in the nucleus involved in the interaction. This result is

$$n \sim A^{0.19}.$$

Belen'kji and Milekhin[12] and Milekhin[13] made more extensive analytical calculations using the tube model and arrived at this same dependence of the multiplicity on the energy of the primary particle and the number of nucleons of the target nucleus. Milekhin[13] also obtained the distributions over the emission angles, the energies, and the transverse momenta of the secondary particles.

Many experimental investigations of high-energy particle nucleus interactions have been reported in the literature[3,4,14-19,35,40-55].

Friedlander[42] analyzed 9 BeV proton-nucleus interactions in emulsion and explained his experimental results in terms of the tube model. He calculated the average multiplicity of shower particles for two types of emulsion nuclei, light (C-N-O) and heavy (Ag-Br). Using only events which contained more than three shower particles, he obtained $\langle n_s \rangle = 5.24 \pm 0.14$ and $\langle n_s \rangle = 6.00 \pm 0.30$ for light and heavy target nuclei, respectively. He also claimed that the dependence of the average multiplicity of shower particles on the number of heavily and medium ionizing tracks was in good agreement with the tube model. He concluded that almost all the shower particles were emitted from a single mass-center which is in contradiction with the cascade model.

Barashenkov *et al.*[16] performed an independent analysis of data obtained in a different experiment of 9 BeV proton-nucleus interactions in emulsion. They found discrepancies between the observed shower particle multiplicities and those predicted by the tube model. On the basis of this and taking the angular distribution, the energy spectrum, and the transverse momenta of the secondary particles into account, they concluded that their results were better explained by the internuclear cascade model. Some of their results are given in Table 1.

Farley[43] introduced a new theory of nucleon-nucleus collisions to explain the data obtained from a group of nucleon-nucleus collisions where the energy of the primary proton varied from 6.6 BeV to 40000 BeV. It strongly resembled the tube model. Called an excited nucleon model, it describes the interaction in the following way: the incident nucleon collides with the nucleus and both are left in an excited state. The primary nucleon leaves the nucleus and then loses its energy in the form of secondary particles. The excited nucleus in turn breaks up into evaporation particles. No internuclear cascade takes place. This model has been used very seldom, if at all.

Bogachev et al.[44] analyzed a group of 9 BeV proton-nucleus interactions in emulsion. Measurements were made only on events where the number of shower particles was at least three. From the energy spectrum of the shower particles, they concluded that the majority of secondary pions were produced in secondary collisions within the nucleus. They found the multiplicity of shower tracks and the mean energy of the shower particles to be in agreement with results predicted by cascade theory. From the average value of energy used for meson production in these events, they concluded that the primary proton underwent approximately two collisions with an average emulsion nucleus.

Barashenkov et al.[17] compared their experimental data obtained from 9 BeV proton-nucleus events with Monte

Carlo calculations made using 9 BeV primary protons in emulsion and found that they were in good agreement with the cascade model. They claimed that Friedlander's[42] conclusion in favor of the tube model was based on the consideration of a narrow group of facts and that, actually, his results could be accounted for by the cascade model.

Barbaro-Galtieri et al.[35] reported on an analysis of 27 BeV proton-nucleus events in emulsion. A portion of their results can be seen in Table 1. They calculated the ratio r of the mean multiplicities for heavy and light emulsion nuclei and obtained

$$r = \frac{\langle n_s \rangle_H}{\langle n_s \rangle_L} = \frac{8.2 \pm 0.2}{5.0 \pm 0.2} = 1.6 \pm 0.3.$$

From the hydrodynamical theory, they calculated, following Belen'kji and Milekhin[12],

$$r = \frac{1.55(A_{AgBr}^{1/3} - 0.25)}{0.84(A_{CNO}^{1/3} + 1)}^{3/4} = 1.62$$

where A_{AgBr} = 94 (Average of Ag^{108} and Br^{80})

A_{CNO} = 14 (Average of C^{12}, N^{14}, O^{16}).

They pointed out that while the agreement between the data and the tube model was satisfactory, there was a large discrepancy between the experimental results and the value of r expected from the cascade theory (between 2 and 3). This latter value is attributed to Rozental' and Chernavskii[27]. The rest of the analysis of the 27 BeV proton-nucleus events such as the energy spectrum and angular distributions of the shower particles, is explained in terms of the tube model.

In a review of the work done on 9 BeV proton-nucleus interactions up to late 1961, Tolstov[18] notes that the majority of the results were shown to be in agreement with the cascade model but in contradiction with the predictions of the tube model. One exception was noted, however, namely the work of Friedlander[42]. Tolstov claimed that the conditions set by Feinberg[10] for introduction of the tube mechanism were not met. Along with this, it was pointed out that there were discrepancies in the analysis of the data, which, if corrected, would result in Friedlander's results actually being in agreement with the cascade model.

Matsumoto[46] analyzed a group of particle-nucleus interactions whose primary particles had energies ranging from 1.5 to 500 BeV. From his results he concluded that events with a large number of heavily ionizing tracks could not be interpreted as a single nucleon-nucleon collision inside the nucleus. He could find no evidence to reject the cascade model although this model was in disagreement with his transverse momentum data. However, he stated that all his data could be explained by the tube model.

In his study of meson production in 26.7 BeV/c proton-nucleus interactions in emulsion, Lim[36] could find little evidence to support the tube model. He interpreted his results in the following manner: the interactions were of two types--single collision events and multiple collision events. In the former type almost all of the shower particles were produced in a single nucleon-nucleon collision in the target nucleus. In the latter type the shower particles were the result of two or more successive collisions in the target nucleus. After their production in the initial nucleon-nucleon collision, the shower particles traverse the nucleus in a collimated beam, boring a tunnel through the nucleus and colliding only with the nucleons contained in this tunnel. Because of this only a small number of shower particles undergo secondary collisions before leaving the nucleus. In the events where two or more meson-producing collisions take place, the shower particles are emitted in wider angles causing the tunneling process to break down. This results in a larger number of secondary collisions in the target nucleus. Some of Lim's results are shown in Table 1.

Meyer et al.(49) investigated the interactions of 25 BeV protons with emulsion nuclei. They found the dependence of the mean number of shower particles on the number of nucleons in the nucleus to be

$$\langle n_s \rangle = 3.4A^{0.14\pm0.03}$$

which is in agreement with the tube model. However they pointed out that the cascade model also makes the same prediction so no decision could be reached as to which model was more consistent with the data.

Tolstov[14] criticizes the results of Friedlander[42] and Barbaro-Galtieri et al.[35]. He cites the results of Monte Carlo calculations of 9 BeV proton-nucleus interactions plus the experimental results of Barashenkov et al.[16] and Tolstov[18] as support for the cascade model since they were in general agreement. He examines several points in the two papers[35,42] which affect the conclusion on the validity of the tube model and claims that if the analysis had been performed in a more rigorous manner, the corrected results would have indeed been consistent with the cascade mechanism. He also takes issue with their calculations of the inelasticity of the interactions.

Barashenkov et al.[15,19] show that the experimental results from proton-nucleus interactions at 9 BeV and 25 BeV are in agreement with the predictions of the cascade theory obtained from Monte Carlo calculations.

Hoffman et al.[40] studied the interaction of 17 BeV/c negative pions with the heavy nuclei of emulsion which was exposed in a strong magnetic field. They obtained angular, momentum, and transverse momentum distributions for both the positive and the negative secondary particles. Some of their results can be seen in Table 3.

Jain et al.[50] analyzed more than 2000 interactions in nuclear emulsion which were initiated by pions and protons.

The primary particles and their energies were 5.4 BeV negative pions, 6.3 BeV/c protons, 16.3 BeV/c negative pions, and 28 BeV/c protons. The ratio of the mean multiplicities of shower particles for heavy and light nuclei was found to be in agreement with the tube model. However, the angular distributions obtained were interpreted in terms of secondary collisions of the shower particles within the nucleus which would be compatible with the cascade model.

Artykov et al.[4] took the data of Hoffmann et al.[40] for 17.2 BeV negative pion-heavy nucleus interactions in emulsion and compared the results with Monte Carlo calculations of 17 BeV pion-heavy nucleus interactions in emulsion using the cascade theory. Complete results were presented both in tabular form and also in the form of histograms--e.g. the angular, momentum, and transverse momentum distributions of the secondaries. Table 3 compares the experimental results with the cascade theory. They concluded that the cascade mechanism accounted for the observed experimental results.

Artykov et al.[20] summarized all the Monte Carlo calculations made on proton-nucleus interactions using the cascade model and compared them with the experimental results published up to that time[16,31-37]. They found all the experimental results for the energy range 1-30 BeV to be in good agreement with the cascade model. A portion of their work can be seen in Table 3.

Kohli *et al.*[41] investigated 17.2 BeV negative pion-nucleus interactions in emulsion. Their results seemed to indicate better agreement with the cascade model than with the predictions of the tube model. The observed mean multiplicities were close to the values predicted by the cascade model. The variation of the average multiplicity of shower particles with the number of nucleons in the target nucleus was found to be

$$\langle n_s \rangle = 3.4A^{0.13\pm0.02}$$

which disagrees with the tube model prediction of

$$\langle n_s \rangle = KA^{0.19}.$$

The angular distributions also were in agreement with the cascade model. Nevertheless, the authors were very careful about drawing any rigid conclusions from their results. Two reasons were cited for doing so. The first of these is the fact that the method which they used to separate events containing interactions with light and heavy nuclei was open to question. This problem will be treated in a later chapter. Secondly, the internuclear cascade is expected at these high energies to be confined to a narrow cone which has approximately the same dimensions as the tube in the tube model. In this energy region, the authors note, the parameters of the secondary particles could very likely be insensitive to the nature of the mechanism which produced them.

In another paper, Kohli *et al.*[51] reported on an investigation of the interactions of 17.2 BeV mesons with heavy emulsion nuclei. Their results were compared with the predictions of the cascade theory which were reported by Artykov et al.[4]. They found the experimental data to be in agreement only for the events having at least eight heavily and medium ionizing tracks. The theory did not agree with the experimental data when the overall sample of heavy nucleus events was considered.

Shen[52] compared the existing data on high energy proton-nucleus interactions with the cascade model and claimed that the cascade model could not satisfactorily explain the observed results. He then proposed a theoretical model which is similar to the tube model. This model is used to make predictions about the secondary particles produced in a nucleon-nucleus interaction. As a example he found the dependence of the average shower multiplicity on the energy of the primary nucleon and the number of nucleons in the target nucleus to be

$$\langle n_s \rangle = 0.95 E_p^{0.46} A^{0.15}, \quad 6 < E_p < 60 \text{ BeV}.$$

This new model is shown to agree with the data he used. He concludes that the tube mechanism with his modifications is the major process in nucleon-nucleus collisions at higher energies, gradually replacing the internuclear cascade as the incident particle energy increases above E_p = 15 BeV. Therefore he claims that the fact that the cascade model has agreed with experimental results in the energy range 10-30 BeV is not surprising. He also shows that his model is applicable to pion-nucleus interactions.

Rao et al.[53] have performed an analysis of proton-nucleus interactions in emulsion where the energies of the primary particles were 24 and 27 BeV/c. The observed multiplicities were shown to be in agreement with the tube model. They calculated the ratio of the average multiplicities from heavy and light nucleus events using the relation:

$$r = \frac{\langle n_s \rangle_{Ag-Br}}{\langle n_s \rangle_{C-N-O}} = \left(\frac{A_{Ag-Br}}{A_{C-N-O}}\right)^{0.19} = 1.44$$

This same relation was also used by Freidlander[42] and Lohrmann et al.[45].

In their analysis of the interactions of 21 BeV protons with heavy emulsion nuclei in a strong magnetic field, Azimov et al.[54] found that the kinematical characteristics of the positive and negative secondary pions were identical. They also found that the transverse momentum of the secondary pions was almost independent of emission angle except in the small-angle region. They also summarized the results of two other experiments: the first was a study of 13.8 BeV/c proton-heavy nucleus collisions by Gil et al.[94]; the second was an analysis of the interactions of 25 BeV/c protons with heavy nuclei performed by Garbowska et al.[39]. Table 4 presents a portion of this summary. General agreement was found between the experimental data and the theoretical cascade model calculations except for the average values of transverse momenta.

TABLE 4 (28,54)

AVERAGE CHARACTERISTICS OF SHOWER PARTICLES PRODUCED BY INTERACTIONS OF PROTONS WITH HEAVY EMULSION NUCLEI

Characteristic	13.8 BeV/c Experiment	13.8 BeV/c Cascade Model Theory	20.8 BeV/c Experiment	20.8 BeV/c Cascade Model Theory
$\langle n_s \rangle$	6.7 ±0.6	5.2 ±0.3	7.6 ±0.3	6.9 ±0.3
$\langle E \rangle$ BeV	1.2 ±0.2	1.0 ±0.1	1.2 ±0.1	1.5 ±0.2
$\langle p_T \rangle$ BeV/c	0.42±0.02	0.49±0.01	0.40±0.01	0.50±0.01
k_π (%)	43.9±5.0		37.9±5.4	

Notation is same as Table 1 except k_π = fraction of kinetic energy of the collision carried away by pions.

Transverse Momentum

The behavior of the transverse momenta of the secondary particles produced in high energy interactions has been of great interest in the last several years. Since the transverse momentum of a particle is invariant under a Lorentz transformation, this property is a very useful quantity in the study of high energy interactions. It is hoped that detailed knowledge about the transverse momenta of the secondary particles will give a better understanding of the interaction mechanism.

One of the problems in high energy physics has been the derivation, consistent with multiple particle production theories, of a function which will fit the experimentally measured transverse momentum distributions of the secondary particles.

Perhaps the earliest analytical expression used to describe the empirical transverse momentum distribution is due to Pinkau[56]. Known as the Boltzmann distribution (hereafter abbreviated BD), it has the form

$$(BD) \equiv f_1(p_T)dp_T = \frac{p_T}{\sigma^2}\exp\left[\frac{-p_T^2}{2\sigma^2}\right]dp_T$$

where p_T represents transverse momentum and σ is a parameter which is evaluated from the experimental data.

Imaeda[57] started with Fermi's[7] expression for the momentum distribution of the secondary particles and from this obtained the transverse momentum distributions known as the Planck distribution (PD) for secondary mesons and the Fermi distribution (FD) for secondary baryons

$$(PD) \equiv f_2(p_T)dp_T = \frac{y^2}{F_+(a)}\sum_{n=1}^{\infty}(+1)^{n+1}K_1(ny)dy$$

$$(FD) \equiv f_3(p_T)dp_T = \frac{y^2}{F_-(a)}\sum_{n=1}^{\infty}(-1)^{n+1}K_1(ny)dy$$

where

$$F_\pm(a) = a^2\sum_{n=1}^{\infty}(\pm 1)^{n+1}\frac{K_2(na)}{n},$$

$$y \equiv \frac{(M^2+p_T{}^2)^{\frac{1}{2}}}{kT},$$

and

$$a \equiv \frac{M}{kT}$$

$K_n(x)$ is the modified Bessel function of the second kind, k and T are the Boltzmann constant and temperature and the velocity of light c is unity in the units used in deriving these distributions.

Imaeda and Avidan[58] attribute the linear exponential distribution to Lohrmann and Bowler. No details of its derivation are given. Abbreviated (LD) it is given by

$$(LD) \equiv f_4(p_T)dp_T = \frac{p_T}{p_0^2} \exp\left[-\frac{p_T}{p_0}\right]dp_T .$$

Several attempts have been made to show that one or more of these distribution functions best describe the experimental data. Using the data from eight different experiments which had primary energies ranging from 1-300 BeV, Imaeda and Avidan[58] found that the (BD) did not fit the data well whereas the (LD) and the (PD) were equally good approximations to the experimental transverse momentum distribution. Jain et al.[106] analyzed transverse momentum distributions from 6.3 BeV proton-nucleon, 16.3 BeV/c pion-nucleon, and 28 BeV/c proton-nucleon interactions. They found that the (LD) was the best fit to each distribution.

Aly, Kaplon, and Shen[59] assumed that the secondary particles in high energy collisions have distributions which are axially symmetric and that p_x and p_y are statistically independent variables. Under these assumptions they claimed that the Boltzmann distribution was the only one which could describe the transverse momentum distribution. They fitted transverse momentum distributions obtained from four experiments whose primaries had energies ranging from 16 to 1000 BeV with Boltzmann distributions.

Friedlander[60] compared various numerical characteristics of the (LD) and the (BD). He evaluated the parameters p_0 and σ in the two distributions by means of unbiased maximum likelihood estimators for N measured values of p_T for the (LD):

$$p_0 = \frac{1}{2N}\sum_{i=1}^{N} p_{Ti} = \tfrac{1}{2}\langle p_T \rangle$$

and for the (BD):

$$\sigma = \left(\frac{1}{2N}\sum_{i=1}^{N} p_{Ti}^{\,2}\right)^{\frac{1}{2}}.$$

He found that the (LD) did not fit the available experimental data* for secondary baryons whereas the (BD) was a good fit. The chi-square goodness-of-fit test was used in this procedure. However, for the case of secondary mesons, Friedlander was only able to obtain a good fit to the experimental data with a superposition of two Boltzmann distributions. This has the form

$$f_5(p_T)\,dp_T = \frac{1-\alpha}{\sigma_1^2}\exp\left[\frac{-p_T^2}{2\sigma_1^2}\right] + \frac{\alpha}{\sigma_2^2}\exp\left[\frac{-p_T^2}{2\sigma_2^2}\right]dp_T$$

where α denotes the fractional contribution of the σ_2 component which is the dominant one at high values of trans-

*See Friedlander for an extensive bibliography of experiments[60] verse momentum.

Imaeda[57] has complied an extensive bibliography of research done on transverse momentum up to 1967. He has included interactions where the primary particles range in energy from <6 BeV up to cosmic ray energies. He used a new distribution derived by Hagedorn[61]

$$(KD) \equiv f_6(p_T)dp_T = \frac{y^2K_1(y)}{a^2K_2(a)}dy$$

where $K_1(x)$ and $K_2(x)$ are the modified Bessel functions of order one and two, respectively,

$$y \equiv \frac{(M^2+p_T{}^2)^{\frac{1}{2}}}{kT}, \quad a \equiv \frac{M}{kT}$$

M is the mass of the particle and k and T are the Boltzmann constant and the temperature. Natural units were used so $c = 1$. From his analysis Imaeda concluded that the experimental p_T distributions were well represented by the (FD) for secondary baryons with $kT = (0.110\text{-}0.125)$ BeV and by the (PD) for secondary mesons with $kT \sim 0.125$ BeV whereas the (BD) with $\sigma^2 = (0.1\text{-}0.2)(\text{BeV}/c)^2$ for baryons and the (LD) with $p_0 = 0.16$ BeV/c for pions also fit the experimental data. He disputed Friedlander's[60] claim that only the (BD) is compatible with the assumption of axial symmetry and asserts that the other p_T distributions are not incompatible with the axial symmetry assumption. He discussed the derivation of Aly, Kaplon and Shen[59] which led to the (BD) in detail and states that the assumption of the statistical independence of p_x and p_y does not necessarily hold for secondary particles. To support this statement he cites the work of Wayland and Bowen[61] which explicitly comments that Friedlander[60] and Aly et al.[59] erroneously claimed that the distribution function must have the following form because of axial symmetry:

$$F(p_T) = f(p_x)f(p_y).$$

According to Wayland and Bowen[61], such an assertion is too strong a condition to impose on the form of the distribution function. They claim that this is only true if p_x and p_y are statistically independent, which they say is not a necessary condition for axial symmetry.

Using their two temperature statistical model for multiple particle production, Wayland and Bowen[61] also arrive at the (PD) as the transverse momentum distribution in their theory.

Cocconi[62] in his discussion of the transverse momentum distribution of particles produced in high energy hadron collisions used the (LD) exclusively in his analysis.

As far as the two theoretical models of particle-nucleus interactions are concerned, the nature of the cascade model makes it very difficult to make predictions about the shape of the transverse momentum distribution of the secondary particles. Since the only method available at present for making analytical calculations with this model is the Monte Carlo method, the transverse momentum distribution will depend on the particular theoretical model of multiple particle production which is used in the calculation to generate the secondary particles.

Matsumoto[46] does comment that the cascade model probably does not predict a distribution of transverse momentum which is symmetric with respect to the plane perpendicular to the direction of the primary particle. He also remarks that the cascade theory may not account for similarities between p_T distributions from nucleon-nucleus and nucleon-nucleon interactions.

Milekhin[13] derives the transverse momentum distribution predicted by the tube model from Landau's[9] hydrodynamical theory of particle production. He obtains the (PD) for secondary mesons and the (FD) for secondary baryons.

Ijaz and Campbell[63] reported on an analysis of 7.0 BeV/c negative pion-proton interactions in a liquid hydrogen bubble chamber. They obtained a fit to their experimental data with the transverse momentum distribution function derived by Hagedorn[64] in his treatment of strong interaction theory based on statistical thermodynamics. This function has the form:

$$f_6(p_T)\,dp_T = c p_T^{3/2} \exp\left[\frac{-p_T}{T_0}\right]$$

where c is a normalization constant and T_0 is the highest possible temperature attainable in the interaction. However, it must be noted that this form of the distribution function was obtained under the asymptotic assumptions that $p_T \gg T_0$ and $p_T \gg m_\pi$[64]. This implies that the distribution function stated above should be valid for pions only in the region where p_T is larger than a few times the pion mass (using natural units).

Kajzar[65] has obtained a distribution function for transverse momentum which is based on a thermodynamic approximation to the statistical model of multiple meson production. This function is the same, up to a constant factor, as Hagedorn's distribution function[64] which was discussed in the previous paragraph. However, to obtain this relation, it is necessary to consider Hagedorn's distribution function in the form it has <u>before</u> the asymptotic assumptions are made. Since Hagedorn[64] shows that his distribution function is equivalent to the (PD) previously discussed, it is not necessary to consider either Kajzar's[65] or Hagedorn's[64] function as a separate part of this investigation.

In his analysis of the transverse momentum of secondary particles produced in high energy collisions of hadrons with nucleons, Cocconi[62] used data from experiments where the primary particles had momenta ranging from a few BeV/c up to cosmic ray momenta of $(10^4\text{-}10^5)$ BeV/c.

From this study he claimed verification of a property of the transverse momentum of the secondary particles which had been indicated previously in individual experiments--namely that the average transverse momentum is approximately constant. He also found that the value of the average transverse momentum is mass-dependent: it increases as the mass of the secondary particle considered increases. He gives some typical values to support this assertion:

for pions $\langle p_T \rangle = 0.30$ BeV/c

for protons $\langle p_T \rangle = 0.44$ BeV/c

for Sigma particles $\langle p_T \rangle = 0.51$ BeV/c

If the average transverse momentum of the secondary particles created in high energy hadron-nucleon interactions is truly constant, several implications follow. First of all, $\langle p_T \rangle$ should be independent of the energy of the incident particle causing the interaction. It also should exhibit no dependence on the number of secondary particles produced in the interaction. Thirdly, $\langle p_T \rangle$ should be independent of the angle of emission of the secondaries. Finally, the constancy of average transverse momentum would provide a method for estimating the momenta of secondary particles which due to certain circumstances would be otherwise undetermined.

The expression

$$p_{T_i} = p_i \sin \theta_i$$

defines the transverse momentum of the i^{th} secondary particle. Here p_i and θ_i represent the momentum and the angle of emission, respectively, of the particle. If the average transverse momentum is constant, this property provides a method for estimating the momentum of a particle whose momentum cannot be measured directly. This is done by assuming that the transverse momentum of the particle is equal to the average transverse momentum of all the particles with directly measured momenta. The momentum of the particle is then found from

$$p_i = \frac{\langle p_T \rangle}{\sin \theta_i} .$$

Although the transverse momenta of secondary particles produced in high energy particle-nucleus interactions have been studied to some extent, to date there has been very little work done to ascertain whether or not the average value of transverse momentum is independent of emission angle, multiplicity of secondary particles, and the energy of the primary particle. A notable exception to this situation can be found in the analysis of 21 BeV proton-heavy nucleus interactions by Azimov et al.[54] mentioned earlier. Besides finding $\langle p_T \rangle$ to be almost independent of emission angle, they also found evidence that it is independent of the number of strongly ionizing particles.

Table 5 presents a summary of some values of average transverse momentum obtained in the experiments which inves-

TABLE 5

VALUES OF AVERAGE TRANSVERSE MOMENTUM OF SECONDARY PIONS IN PARTICLE-NUCLEUS INTERACTIONS

Incident Particles	$\langle p_T \rangle$ (MeV/c) Predicted by Cascade Model	Experimental $\langle p_T \rangle$ (MeV/c)	Target Nucleus*	References
6.2 BeV	400±20 (old)	- - - - - -	Em	Artykov et al. (20,30)
Protons	420±20 (new)		Em	
9BeV	400±20 (old)	370±20	Em	Artykov et al. (20,30)
	435±25		LEm	
Protons	410±27		Al	
	415±28 (new)		Fe	Barashenkov et al. (16)
	430±20		Em	
	440±25		HEm	
17 BeV	420±20 (old)	- - - - - -	Em	Artykov et al. (20,30)
Protons	460±23		Em	
25 BeV	420±20 (old)	480±20	Em	Artykov et al. (20,30)
	500±10		HEm	
Protons	470±30		LEm	
	420±28		Al	Garbowska et al. (39)
	430±28 (new)		Fe	
	470±25		Em	
	460±23		HEm	
26.7 BeV Protons	- - - - - - -	325±60	Em	Lim (36)
4.5 BeVπ^-	- - - - - - -	290±50	Em	Aly et al. (66)
17 BeVπ^-	390±60	410±20 π^+		Artykov et al. (20)
	390±60	360±20 π^-	Em	Hoffman et al. (40)
	390±60	390±20 $\pi^\pm$		
17.2 BeVπ^-	- - - - - - -	362±52	LEm	Kohli et al. (41)
		372±23	HEm	
13.8 BeV/c Protons	490±10	400±10	HEm	Gil et al. (55)
20.8 BeV/c Protons	500±10	400±10	HEm	Azimov et al. (54)

*Legend: LEm--Lt. Emul. Nuc. (CNO); Em--Av. Emul. Nuc.; HEm--Heavy Emul. Nuc. (Ag-Br) tigated particle-nucleus interactions. Only the results for secondary pions are shown because they are the subject of interest in the investigation being reported.

Many investigations have been made of high energy nucleon-nucleon and pion-nucleon interactions, and the behavior of the transverse momentum of the secondary particles produced in these events has been extensively studied. For bibliographies of the work which has been published, several excellent reviews are available; for example--those of Ohba and Kobayashi[67], Rozental' and Chernavskii[27], and Pinkau [26], to name a few.

Results which were obtained by Malhotra[68] from an analysis of 16 BeV/c pion-nucleon interactions and those obtained by Spergel et al.[69] from their study of very high energy ($>10^{10}$eV) nucleon-nucleon interactions indicate that the average transverse momentum of secondary pions produced in collisions of these two types of events is independent of the energy of the incident particle. Malhotra[68] also found evidence that the average transverse momentum of the secondary pions is independent of the number of charged particles produced in the interaction. Other investigators[68-70] have found indications that the average transverse momentum of secondary particles in high energy interactions is independent of the direction of emission of the particles. Table 6 shows some of the experimental results on average transverse momentum which have been obtained in high energy pion-

TABLE 6

PUBLISHED RESULTS ON AVERAGE TRANSVERSE MOMENTUM OF SECONDARY PIONS FROM π-N INTERACTIONS

Detector	Energy of Primary Pion (BeV)	Type of Interaction	$\langle p_T \rangle$ (MeV/c)	Reference
H_2 B.C.	4	π^--4Prongs	288±3	Aachen-Birmingham, Collab.(73)
Heavy Liq.B.C.	6.1	π^--Mult.Prod.	315	Bellini et al.(74)
Prop. B.C.	7	π^--Mult.Prod.	310±20	Petrzilka (75)
Emul.	7.3	π^--Mult.Prod.	270±20	Friedlander et al.(76)
Emul.	7.3	π^--Mult.Prod.	270±20	Bozoki et al.(77)
H_2 B.C.	10	π^--4 Prongs	348±5	Biswas et al.(78)
Emul.	17.2	π^--Mult.Prod.	344±26	Kohli (79)
H_2 B.C.	16	π^--Mult.Prod.	360±10	Goldsack et al.(80)
Emul.	8	π^--Mult.Prod.	290±29	Dubey & Kohli (81)
Heavy Liq.B.C.	17	π^--Mult.Prod.	414	Huson & Fretter(82)
Emul.	4.4	π^--Mult.Prod.	300±23	Malhotra (68)
Heavy Liq.B.C.	5.9	π^--204 Prong	303±13	Bellini et al.(83)
Emul.	6.7	π^--Mult.Prod.	310±20	Belyukov et al.(84)
Emul.	7.5	π^--Mult.Prod.	286±18	Grote et al.(85)
Heavy Liq.B.C.	18	π^--2&4 Prong	360±18	Bellini et al.(83)
B.C.	18	π^--Mult.Prod.	425(π^+) 397(π^-)	Ferrero et al. (86)
H_2 B.C.	11.4	π^--4 Prong	339	Ferbel & Taft(87)
Prop-Fr. B.C.	17.96	π^--Mult.Prod.	365±21	Barkow et al.(104)
Prop. B.C.	6.65	π^--Mult.Prod.	337±16	Grote et al.(85)

nucleon interaction analyses.

One of the purposes of this investigation is to examine the transverse momentum of secondary pions produced in pion-nucleus interactions and to compare the results with results which have been obtained from studies of high energy particle-nucleon interactions. Since these two types of interactions differ distinctly from a physical viewpoint, one would expect that they yield distinctly different results.

Multipion Resonances

In a pion-nucleus interaction which results in the creation of a number of secondary particles, two or more of the final state particles may be the products from the decay of an intermediate particle or resonant state. These resonances are short lived particles with a characteristic lifetime of about 10^{-23} sec.[88]. Due to their extremely short lifetime, it is impossible to observe resonances directly. However, their identification and the contribution of a resonance to a physical process are made possible by the fact that a kinematical correlation exists among the decay products of a resonant state. This correlation arises because the conservation of 4-momentum must apply to the decay of the resonance into final state particles. The sum of the energies of the final state particles which are the decay products of a resonance must be equal to the energy of the resonance. In addition, the sum of the momenta of the decay products must equal the momentum of the resonance which produced them.

Starting with the relativistic expression for the total energy of a particle

$$E^2 = (\vec{p})^2+m^2$$

this expression can be generalized to a system of n particles and solved for the mass. One obtains

$$M^2_{12...n} = (\sum_{i=1}^{n} E_i)^2-(\sum_{i=1}^{n} \vec{p}_i)^2$$

The quantity $M_{12...n}$ is called the invariant mass of the system of n particles. For the case in which the n particles are the decay products of a resonance, $M_{12...n}$ is the mass of that resonance. If the interaction process does not proceed via the formation of a resonant state, the resulting distribution of n-particle mass is the phase space distribution for the n uncorrelated particle states(89). In the case where resonance formation does occur in the interaction process, the invariant mass distribution will exhibit a peak at the value of the mass of the resonance. This peak will occur superposed on the phase space curve.

Since the secondary pions produced in the pion-nucleus events investigated in this work were the only particles on which momentum measurements were performed, the particle correlations were limited to two types: two-pion and three-pion correlations. The results will be presented in the chapter on analysis of data.

CHAPTER III

EXPERIMENTAL PROCEDURE

Experiment

The experimental data for this investigation was obtained from a stack of fifty-five pellicles composed of Ilford K-5 nuclear emulsion. These pellicles form one-third of the π^- emulsion stack from the University of California at Berkeley. The dimensions of each pellicle are 15 cm. by 7.5 cm. and the pellicle thickness before processing was approximately 600 microns.

This stack of nuclear emulsion was exposed to a 16.2 BeV negative particle beam at CERN in Geneva, Switzerland. The content of the particle beam was $\geq$90% negative pions. The remainder of the beam consisted mainly of muons but included kaons and antiprotons. The beam was incident in the pellicles along the 15 cm. direction.

Before the stack was developed at Berkeley, a grid consisting of 1mm. squares was optically exposed on the bottom of each pellicle. Every square contains a pair of co-ordinate numbers and therefore the grid serves as a reference in describing the location of events within a pellicle. The position of the grid is almost the same for each of the pellicles which makes it possible to follow particle tracks from one pellicle to the next. The grid exposure creates only a minimum amount of obscuration since just the bottom layer of emulsion grains was blackened.

Before processing, the emulsion pellicles were mounted on glass plates.

Equipment

A selection of microscopes and optical equipment was available for use in this investigation. The optical quality of this equipment varied to some extent. Therefore an attempt was made to use a suitable optical system for the particular measurement or operation being performed. For general purpose measurements and scattering measurements, two microscopes were employed each of which consists of commercial Leitz Wetzlar optical equipment and a travelling stage. These travelling stages were designed and built to specifications in the machine shop of the University of Oklahoma department of physics. The optical systems of these two microscopes include Leitz Ortholux binocular microscope heads. The stages of the microscopes are capable of motion in two perpendicular directions in a plane which is perpendicular to the optic axis. Since the emulsion plate-holder on each microscope is rotatable, any track in the emulsion can be aligned with either direction of stage travel. This feature makes many measurements simpler to perform.

The travelling stages of these two microscopes were modified in an attempt to eliminate stage noise (the deviation of the motion of the stage from a straight line) in one direction. As a result of this modification, one microscope has such a low level of stage noise that it is possible to use it to determine the momenta of particles in the BeV range by the method of multiple Coulomb scattering.

Distances along the two directions of stage motion are measured accurately with precision micrometer dials which are attached to the travelling stages. These micrometers are calibrated in microns.

Micrometers calibrated in microns are attached to the fine focusing mechanisms of the microscopes enabling vertical displacements to be measured directly.

A Leitz Wetzlar Ortholux binocular microscope with a travelling stage of somewhat different design is also available. This stage travels only in one direction perpendicular to the optic axis, however, and in most respects, it is inferior to the stages on the two microscopes described in the preceding paragraphs. Nevertheless, this microscope does possess excellent rigidity and it also has a superior fine focusing mechanism. Therefore this microscope was used for all critical measurements in the vertical direction.

Scanning was performed on a Spencer binocular microscope mounted on an ordinary dovetail stage. This stage was connected through a drive mechanism to an electric motor which allowed uniform motion in one direction. This drive mechanism was designed to allow the scanning speed to be varied. The range of scanning speeds obtainable with this drive mechanism varied from 1 mm. to 1 cm. per minute.

Each of the microscopes was mounted on its own individual table. These installations were tested thoroughly for effects due to vibrations and were found to be relatively isolated from the environment of the basement of the physics building.

The laboratory room in which the emulsion plates are kept and measurements are made is maintained at approximately 70°F and 60% relative humidity. These conditions were provided by a combination air-conditioner and dehumidifier working in tandem with a separate evaporative cooler being used as a humidifier. A regular window unit air conditioner serves as a back-up system in case of a failure in the main system.

All optical measurements were performed using a blue filtered light source. The blue light provides visual comfort and its short wavelength insures better resolution of small objects.

Critical measurements were performed using Leitz Wetzlar eyepieces and objectives with the microcsopes. The three types of eyepieces used were the Leitz periplan GF 10X, 16X, and 25X. A variety of objectives was available for use. Those which were used more frequently were the Leitz 10X, numerical aperture 0.25, which was used for general location work; the Leitz 53X oil immersion, numerical aperture 0.95, 1000 micron working distance; Koristka 55X oil immersion, numerical aperture 0.90, working distance 3500 microns; Leitz 100X oil immersion fluorite apochromat, numerical aperture 1.32, 370 microns working distance; Leitz plano 100X oil immersion apochromat, numerical aperture 1.32, 370 microns working distance; Koristka 100X oil immersion, numerical aperture 1.25, 530 microns working distance.

Upon comparing the three 100X objectives, it was found that the Koristka 100X objective has a very noticeable curvature of field whereas the Leitz 100X fluorite and plano objectives have almost no curvature of field at all. Consequently, these two Leitz objectives were used in combination with the 10X eyepieces when the most critical measurements were made. Since the Leitz Wetzlar microscopes used for measurements have an inherent body-tube magnification of 1.25X this optical system has a total magnification of 1250X, which is close to the limit for usable magnification of optical microscopes. The Leitz 53X objective was used in combination with 10X eyepieces whenever less critical measurements were performed. Compens 15X eyepieces were used in combination with a Koristka 55X objective for most of the scanning work. However, some scanning was performed using the Leitz 53X objective with 16X eyepieces.

A Leitz Wetzlar screw-type eyepiece micrometer was used for measuring small distances when extreme accuracy was desired, such as in scattering. The measuring portion of this 12.5X micrometer consists of a moveable cross hair which travels along a scale with twelve equal divisions. A hand-operated drum controls the motion of this cross hair. One complete turn of the drum moves the cross hair through one division on the scale. The inherent setting accuracy of the micrometer cross hair is ±0.1 drum division or ±0.001 scale division. An eyepiece reticle was used for measuring less critical distances in a fixed field of view. This reticle was calibrated using one of the micrometer dials attached to the travelling stages of the microscopes.

In order to measure angles in the plane of the emulsion, an eyepiece goniometer was used. This goniometer was constructed in the physics department machine shop from a design used by Barkas' group[90,91] at the Lawrence Radiation Laboratory in Berkeley, California. It consists of a rotating portion graduated in degrees and a fixed vernier scale which allows measurement to the nearest tenth of a degree of arc. The regular microscope eyepiece tube is replaced by the goniometer and the eyepiece fits into the rotating portion. This allows the eyepeice and cross hair to be rotated to make the measurements.

Scanning

Since part of the information which was desired consisted of the cross sections for certain types of interactions, a large number of events of each type being studied was required. Therefore a scanning method was employed which insured that large numbers of events would be located in such a way that the mean free path could be easily calculated. In this experiment this was accomplished by careful and systematic scanning along the tracks of many beam pions. The scanner carefully recorded the position of each beam track in the emulsion preparatory to scanning the track for interactions. This was done in order to prevent duplication in scanning and to enable any beam track to be relocated at a later time. These tracks were then followed by the scanner until the particle making the track either interacted or left the emulsion pellicle. Most of the tracks which did not interact traversed the entire length of the emulsion. When an interaction was observed, its position and nature were carefully recorded. The rate at which the scanning was done was initially 14 cm. of track per hour, but this was later increased to 22 cm. per hour. The magnification used for scanning was 825X since the Spencer scanning microscope has an inherent tube magnification of unity.

The beam tracks in the emulsion used in this experiment have an average divergence of ±5 minutes of arc over the width of the emulsion pellicles. The divergence of the beam over the entire emulsion at the entrance edge is approximately ±8 minutes of arc(92). Only those tracks which had a divergence of less than 1^{o} from the average beam direction were scanned.

Selection of Events

In order to insure that the events to be investigated were actually pion-nucleus interactions, it was necessary that some type of selection criterion be extablished. The events found were composed of several different kinds of tracks using a subjective track classification scheme according to the estimated grain density. These were light, or minimum ionizing tracks with $g \lesssim 1.5\ g_{min}$; gray, or medium ionizing tracks with $1.5\ g_{min} \lesssim g \lesssim 5.0\ g_{min}$; and dark or heavily ionizing tracks with $g \gtrsim 5.0\ g_{min}$. Here g_{min} represents the minimum value of the grain density. In general, the light tracks were assumed to be due to pions and the dark and gray tracks were assumed to be proton tracks. It is important to remember that neutral particles leave no tracks in nuclear emulsion. Therefore it is possible to observe and therefore to directly measure the kinematical properties of charged particles only.

Some events which are classified as pion-nucleus interactions can actually be treated as pion-nucleon interactions. Therefore, to avoid confusion in later discussions, a distinction should be made between the terms "pion-nucleus interaction" and "pion-nucleon interaction". The events which were of interest in this investigation consisted of the interactions of the beam pions with all of the different nuclei in the emulsion except hydrogen. These interactions could have different results: a) a large momentum transfer to the target nucleus accompanied by multiple pion production, b) either a partial or complete break-up of the target nucleus accompanied by multiple pion production. Interactions of type (a) contain either one dark track or no dark tracks and a dark blob is observed at the point of interaction. Those of type (b) contain two or more heavy tracks. The presence of one or more Auger electrons is an indication that a heavy emulsion nucleus was involved in the interaction. Events which possessed at least one of these characteristics will hereafter be referred to as pion-nucleus interactions.

Among the events found were some which contained either one dark track or no dark tracks, no dark blob at the point of interaction, and no Auger electrons. Although these are also pion-nucleus events, they involve the interaction of a beam pion with a hydrogen nucleus (proton) or with a single nucleon of a heavier nucleus. In the analysis of the latter class of events, the rest of the nucleons in the nucleus are neglected and the interaction is treated as a pion-nucleon interaction. All of these events will be referred to as pion-nucleon interactions.

It is possible to determine a lower limit on the size of the nucleus involved in the interaction from the number of heavy tracks (N_h)* contained in an event under the above assumption that the heavy tracks are due to protons.

Using these guidelines, the group of pion-nucleus events chosen for this investigation possessed total numbers of heavy tracks which ranged from zero to thirty-two. This indicated that the set of events analyzed contained interactions of pions with all the various types of nuclei (except hydrogen, of course) found in the emulsion: light (carbon, nitrogen, and oxygen), and heavy (silver and bromine). These events were chosen completely at random with no discrimination as far as the number of light tracks, dark tracks, or gray tracks in any one event was concerned. Several methods for more precise classification of the events will be discussed in detail in Chapter IV.

Angle Measurements

The information which had to be obtained for a detailed examination of the events consisted of the emission angle and the momentum for each particle track.

*N_h=Number of (dark + gray) tracks

Emission Angle

The angle between two particle tracks in the nuclear emulsion is given by

$$\cos\theta = \sin\phi_1 \sin\phi_2 + \cos\phi_1 \cos\phi_2 \cos(\delta_1 - \delta_2)$$

where ϕ_1, δ_1 and ϕ_2, δ_2 denote the projected angle and the dip angle of the first and second particle tracks, respectively. The projected angle ϕ is the projection of the space angle between two tracks onto a plane which is perpendicular to the line of sight. By the dip angle δ is meant the projection of the space angle onto a plane passing through the track of interest and perpendicular to the plane of the emulsion.

If the forward direction of the incident beam pion is selected as the x-axis of a three dimensional co-ordinate system, the above equation simplifies to

$$\cos\theta = \cos\phi \cos\delta$$

This gives the angle of emission θ of the secondary particle with respect to the forward direction of the incident pion in terms of the projected angle ϕ and dip angle δ of the secondary.

Projected Angle--The measurement of projected angles was performed with the goniometer previously described. The accuracy of this instrument is ±0.1 degree of arc. Several measurements of the projected angle were made and averaged for the value of ϕ used in all calculations.

Dip Angle--In order to determine the dip angle of a track, its tangent was measured. The tangent is the ratio of the true change in depth of a track segment to the length of the segment projected onto the plane of the emulsion. The micrometer dial attached to the fine focusing mechanism of the Ortholux microscope was used to measure the change in depth. Repeated focusing on the same point in the emulsion resulted in a determined micrometer accuracy of ±0.2 microns. Before the measurements were performed, the track segment to be measured was centered in the microscope eyepiece. The method used to measure the change in depth consisted of focusing first on one end of the track segment and then on the other end. Taking the difference between the two micrometer readings yielded the measured change in depth of the track. The calibrated eyepiece reticle was used to obtain the length of the track segment. Since the emulsion undergoes a certain amount of shrinkage during the development process, the measured change in depth must be corrected accordingly. This is accomplished by multiplying the measured change in depth by a shrinkage factor. The shrinkage factor for this stack of emulsion is 2.37. Several measurements were made on each dip angle, and the average value was used for tan δ.

Determination of Momentum

The momenta of the minimum ionizing tracks (assumed to be due to pions) were determined using scattering methods. These methods are based on the fact that charged particles passing through matter are scattered repeatedly through small angles by the Coulomb fields of the atoms in the matter. The average value of the scattering angle is dependent upon the charge and the velocity of the particle for a given medium through which the particle travels[90]. However in present emulsion techniques, the scattering angle is seldom measured directly. Instead a method known as the co-ordinate method is used. The following discussion is a brief description of the procedure used in the co-ordinate method of multiple scattering.

First the track to be measured is aligned with the direction of microscope stage motion which has the greatest distance of travel. This direction is taken to be the abscissa, x. The alignment should be accurate enough so that, if possible, the track will remain in view within the eyepiece over the entire interval to be measured without changing the y co-ordinate of the microscope stage. A length t, which is parallel to x, is selected as a base cell length. Using the eyepiece micrometer, the ordinate y_0 of the track at an arbitrary point along the abscissa, x=0, is measured. This point was chosen close to the event containing the track being measured. The plate is then displaced along the x axis a distance t, and the value, y_1, of the ordinate is recorded. This procedure is repeated until a set of ordinates, y_i, has been obtained. The recorded measurements represent the distances of the track from a hypothetical straight line which extends in a direction generally parallel to the track, at equal intervals of length t.

Next, the second differences

$$D_k = (y_{k+2}-y_{k+1})-(y_{k+1}-y_k)$$

are calculated. The average absolute value of D_k corrected for measurement noises is then calculated using the method described later in this section. This takes into consideration the fact that the y_i's are not the distances of the track from a true straight line. This average absolute value of D_k is called D_t and it is related to the mean angle $\bar{\alpha}$ between successive chords to the track by

$$D_t = \frac{\bar{\alpha}\ t}{57.3}$$

where $\bar{\alpha}$ is expressed in degrees and 57.3 is the conversion factor from degrees to radians.

Barkas[90] obtains the relation between the momentum of the particle and $\bar{\alpha}$:

$$p\beta = \frac{K_c z}{\bar{\alpha}}\left(\frac{t}{100}\right)^{\frac{1}{2}} = \frac{K_c z t^{3/2}}{573\ D_t}$$

where p is the momentum of the particle, β is its velocity in units of c, the speed of light, z is its charge in units of e. K_c is the dimensionless scattering factor, t is the cell length in microns, and 573 is a factor giving units of

MeV to $p\beta$ when D_t is measured in microns.

The most difficult problem in multiple scattering is the determination of the quantity D_t from the set of measured y_i's. This calculation is called noise elimination. There are several different types of error involved in each measurement, y_i made on the track: microscope stage noise, setting noise, grain noise, and distortion of the emulsion. It is practically impossible to achieve noise elimination from the direct determination of all the different noise levels. As an alternative to the direct determination of all noise levels, the following method of noise elimination was used.

All large angle nuclear scatterings were eliminated by discarding any $|D_k|$ which was greater than four times the average of the other $|D_k|$'s. This cut-off value is standard for such calculations. Considering that the statistical average of the second differences must be zero in the absence of any noise, the average of the second differences was subtracted from all second differences. This was done as a first approximate correction for simple track curvature. Next products of the second differences, D_k^2, $D_k D_{k+1} \ldots$, $D_k D_{k+N-1}$ (N=number of second differences) and their weighted averages were calculated. The weighing factor used was proportional to the square of the number of each product of second differences. The $\ell^{\underline{th}}$ product of second differences is given by

$$\langle D_k D_{k+\ell} \rangle = \frac{N-\ell}{N^2} \sum_{k=1}^{N-\ell} D_k D_{k+\ell}.$$

From Barkas'[90] treatment of noise elimination and the modification made by Burwell[94], Samimi[93] obtained the following mean square noise-corrected second difference Δ_t^2:

$$\Delta_t^2 = 2/3 \left[\langle D_k^2 \rangle + 2 \sum_{\ell=1}^{J-2} \left(1 - \frac{\ell^2}{J^2}\right) \langle D_k D_{k+\ell} \rangle \right] \Big/ \left(1 - \frac{1}{3J^2}\right)$$

where J is any large integer and $J \leq N+1$. The noise-eliminated absolute second difference was assumed to have a Gaussian distribution. Then D_t was calculated from Δ_t^2 from the relation

$$\Delta_t^2 = \frac{\pi}{2} D_t^2.$$

Although the set of y_i ordinates was measured at a base cell length t, pβ can also be calculated for cell lengths of M times t where $M = 1, 2, 3, \ldots, M_{max}$. Second differences were calculated at a cell length of M·t from

$$D_k^M = y_k - 2y_{k+M} + y_{k+2M}.$$

Using this relation the data yields M sets of second differences calculated at a cell length of M·t. M different values of pβ were obtained which were then averaged to give one value of pβ for that cell length. This method of calculating pβ from multiple cell lengths has two advantages: first it allows a more realistic choice of the optimum cell length and second, the M different pβ's must have only a statistical variation among them. In all the multiple cell length calculations, the maximum value of M was chosen such that $M_{max} \leq (N/10)+1$. The entire calculation was repeated for two different values of J in the equation for Δ_t^2 once with $J=N+1$ and once with $J=\frac{1}{2}(N+1)$.

The value of $p\beta$ which had the smallest relative error was chosen as the final answer from all the different $p\beta$'s which were calculated for each track from a set of measured y_i's. Since the errors in Δ_t^2 and $p\beta$ included a measure of the noise level in the measurement, the consistency of the data, and the statistical error, this was a reasonable choice.

The scattering measurements in this experiment were made using two different base cell lengths. The momenta of most of the secondary pions were measured using a base cell length of 250 microns. A cell length of 200 microns was used in the measurements performed on the remainder of the pions. It was found that the results given by the multiple scattering method are very inaccurate when the number of measured ordinates y_i in a single set is less than 10. For this reason, it was impossible to determine the momentum of any pion track whose length in an emulsion pellicle was less than 2.0 mm.. An upper limit of 100 measured y_i's was set on the scattering measurements performed on a single pion track. The number of ordinates which were measured varied for each pion track.

Errors

The equation for Δ_t^2 gives this quantity as the sum of averages of products of second difference $\langle D_k D_{k+\ell}\rangle$. Since each of these is averaged over many terms, it has an inherent variance associated with it. $\langle D_k D_{k+\ell}\rangle$ terms are related to the measurement noise, therefore they are a measure of the error which the measurement noise contributes to Δ_t^2. From[93] the variance in Δ^2 is given by

$$\sigma_{\Delta^2} = 2/3\left[\sigma_0^2+2\sum_{\ell=1}^{J-2}\left(1-\frac{\ell^2}{J^2}\right)\sigma_\ell^2\right]\Big/\left(1-\frac{1}{3J^2}\right).$$

In the derivation of this expression the quantities $\langle D_k D_{k+\ell}\rangle$ were treated as being statistically independent. σ_ℓ^2 represents the variance in $\langle D_k D_{k+\ell}\rangle$. Taking the error in Δ_t^2 to be the square root of its variance and using two other expressions for Δ_t^2 obtained by Samimi[93] in a detailed discussion of multiple scattering calculations, the error in each calculation of $p\beta$ is found to be

$$\Delta p\beta = \tfrac{1}{2}\frac{p\beta\sqrt{\sigma_{\Delta^2}^2}}{\Delta_t^2}.$$

Using this relation the error in the final answer is then calculated. Considering that this answer is the average of the M different $p\beta$'s calculated at the $M^{\underline{th}}$ multiple cell length, one obtains

$$\Delta\overline{p\beta} = \tfrac{1}{2}\sqrt{\sum_{i=1}^{M}\left(\frac{p\beta_i}{\Delta_i^2}\right)^2\sigma_{\Delta^2}^2/(M-1)}.$$

The error in the measurement of the projected angle ϕ was determined by repeated measurement of a representative group of projected angles and the calculation of the probable error for each angle in the group. It was found that the error was smallest for the projected angles of light tracks and largest for the projected angles of short, thick, dark tracks. The error in projected angle for light tracks was determined to be ±0.1 degree.

In order to determine the error in the measurement of the dip angle δ, repeated measurements were made of the change in depth of a typical set of tracks. The average error found by this method, ±0.2 microns, was then used to determine the error in the dip angle δ from

$$\Delta\delta = \frac{\Delta z}{z} \frac{\cos^3 \delta}{\sin \delta} .$$

The error in the angle of emission θ was determined from

$$\Delta\theta = \frac{\partial\theta}{\partial\phi}(\Delta\phi)^2 + \frac{\partial\theta}{\partial\delta}(\Delta\delta)^2 \ ^{\frac{1}{2}}$$

$$= \csc \Theta\{(\sin \phi \cos \delta\Delta\phi)^2 +)\cos \phi \sin \delta\Delta\delta)^2\}^{\frac{1}{2}}$$

The internal error in the average transverse momentum was calculated from the error in the emission angle and momentum of the measured pions:

$$\{\Delta\langle p_T\rangle\}_{\text{Int.}} = \frac{1}{N}\sum_{i=1}^{N}\{(\sin \theta_i)^2(\Delta p_i)^2 + (p_i \cos \theta_i)^2(\Delta\theta_i)^2\}^{\frac{1}{2}}.$$

The statistical error in the average transverse momentum was determined from the standard deviation σ and was given by

$$\{\Delta\langle p_T\rangle\}_{\text{Stat.}} = \frac{\left[\langle p_T^2\rangle-\langle p_T\rangle^2\right]^{\frac{1}{2}}}{N}.$$

In these two formulae, N is the number of values of transverse momentum used to calculate $\langle p_T\rangle$.

CHAPTER IV

ANALYSIS OF DATA

Data

A total of 1831.4 meters of track was scanned following the procedure discussed in the preceding chapter. The estimated muon content of the beam was ~7%[70]. In a controlled test conducted with an average scanner, it was found that some of the beam tracks were scanned twice. After correction for muon contamination and scanning duplicity, the track length scanned became 1493.0 meters. 3840 events were found which could be classified, according to the criteria discussed in Chapter III, as either pion-nucleus or pion-nucleon interactions. Since a pion-nucleon interaction actually involves an emulsion nucleus (although, except for the case of hydrogen, the nucleus is merely a spectator to the interaction), this group of events must also be considered in the determination of the mean free path for pion-nucleus interactions. Because of this necessity to include both types of events in cross section calculations, no distinction will be made between them in the next section of this chapter. The mean free path for these pion-nucleus interactions was 38.8 cm..

Out of the total of 3840 events, 472 were determined to be either the interaction of a beam pion with a hydrogen nucleus or with a loosely bound nucleon of a heavier emulsion nucleus. Beginning with the section about the distribution of events, this group of events will be referred to as the 16.2 BeV pion-nucleon interactions. The remaining 3368 will be denoted as the 16.2 pion-nucleus interactions. From these pion-nucleus interactions, a group of 298 events was randomly selected for analysis in this investigation. The group of events selected contained a total of 4003 tracks, of which 1609 were lightly ionizing tracks (assumed to be due to charged pions) and 2394 were heavily or medium ionizing tracks (due to protons, α-particles, deutrons, low energy pions, and strange particles). The average number of tracks per event was 13.4 ± 0.8, the average number of pion tracks per event was 5.4 ± 0.3, and the average number of heavy (dark + gray) tracks per event was 8.0 ± 0.8. Figure 1 shows the distribution of the number of pion tracks per event. The corresponding distribution for the number of heavy tracks per event is shown in Figure 2. Out of the total of 1609 pion tracks, it was possible to measure the momenta of 736 pions. However, the angle of emission was determined for all pion tracks.

Figure 3 presents a comparison of the angular distribution of the 736 pions with measured momenta with that of all the pions. From this distribution, it can be seen that

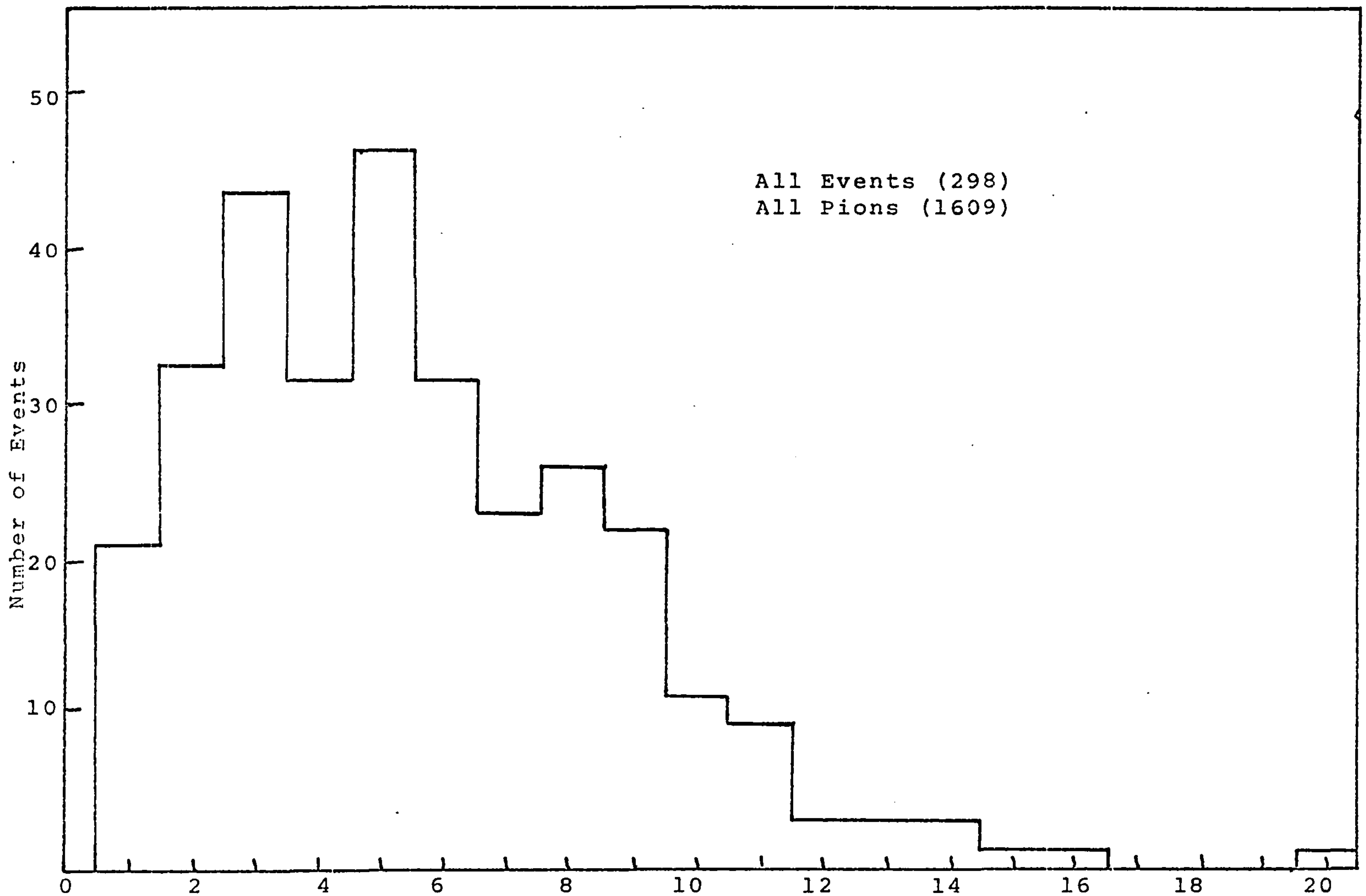

Fig. 1 Distribution of Pion Tracks According to Number of Charged Pions per Event for 16.2 BeV π-Nucleus Interactions

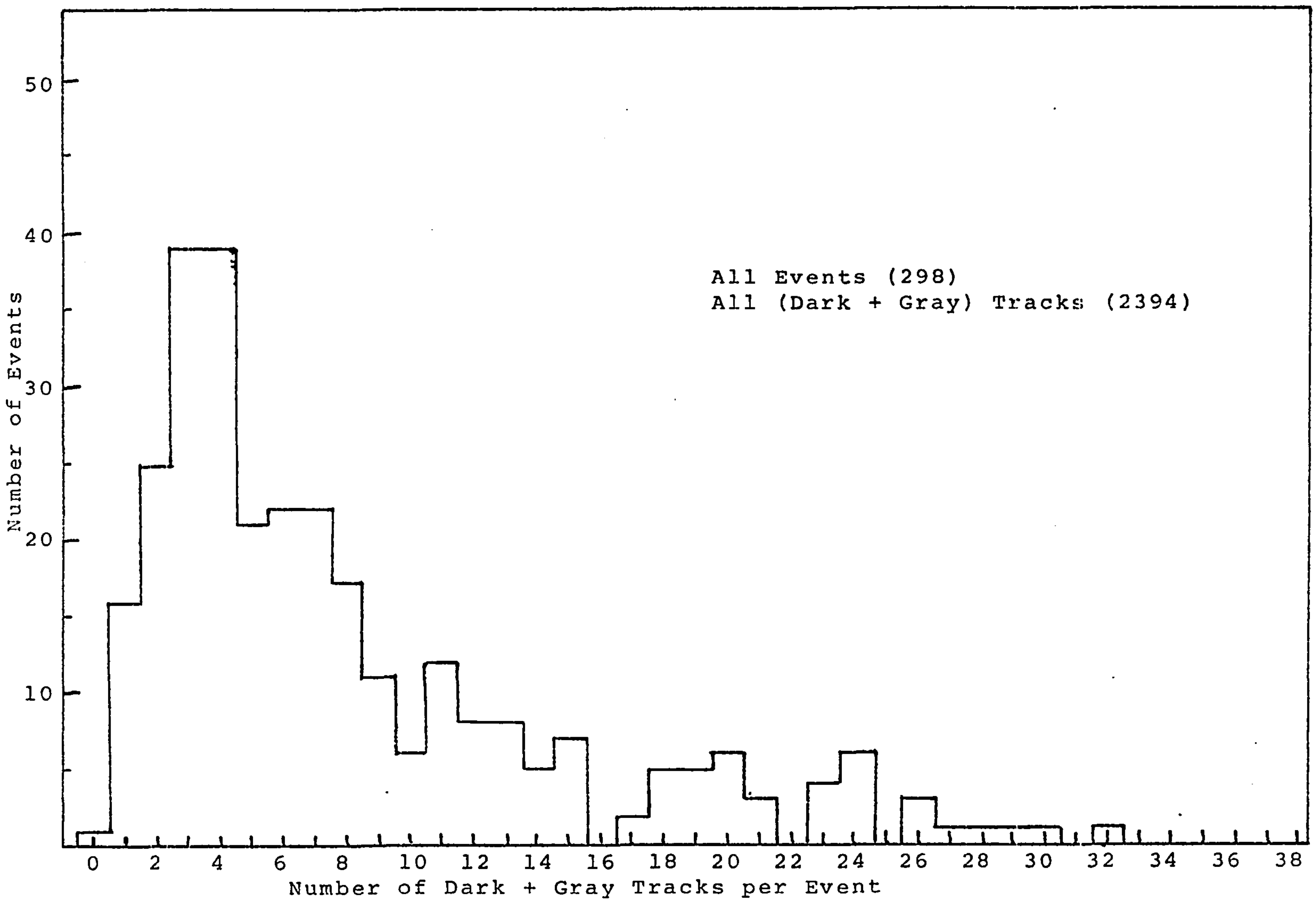

Fig. 2 Distribution of Heavy Tracks According to Number of Heavy Tracks per Event for 16.2 BeV π-Nucleus Interactions

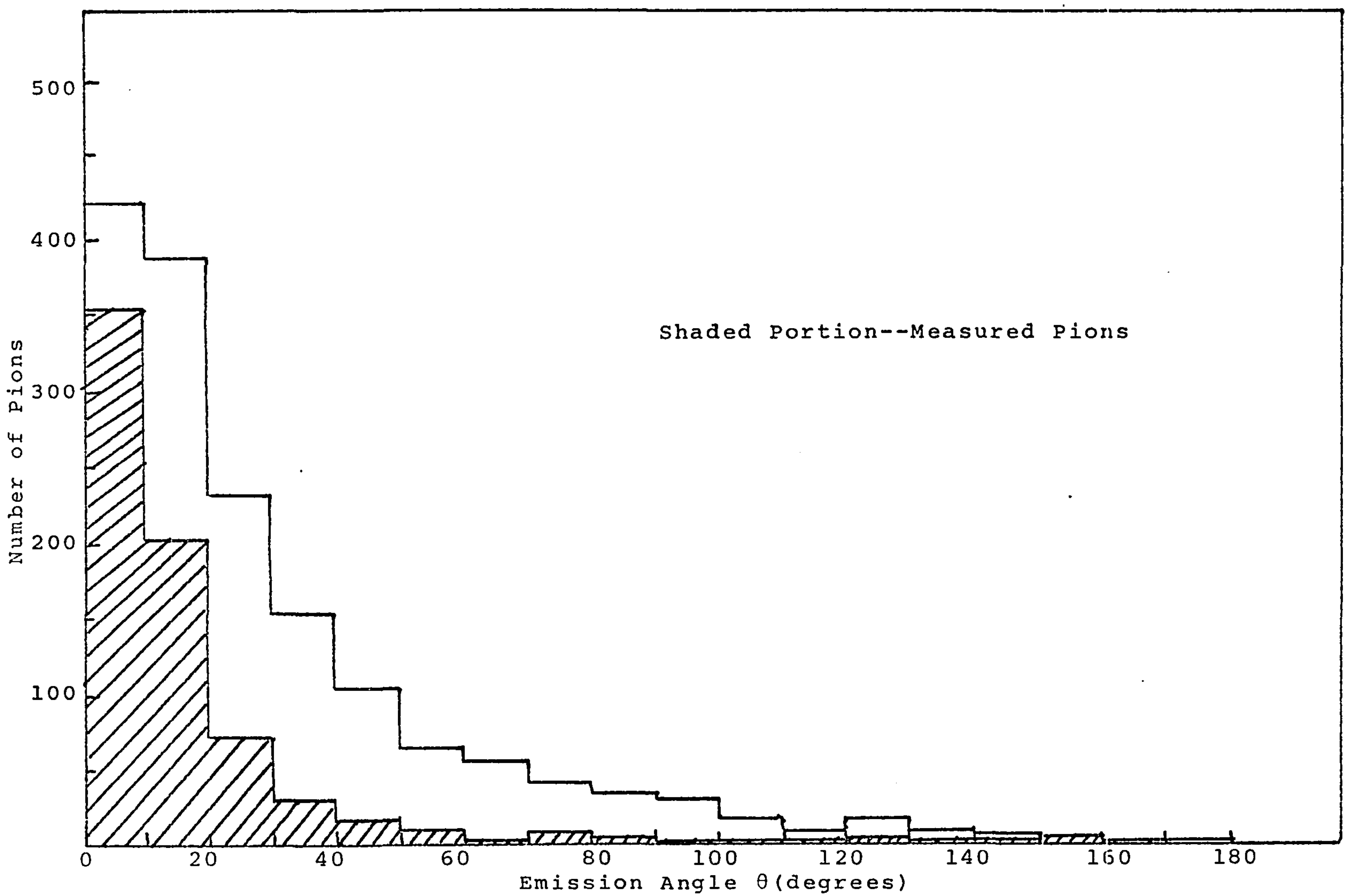

Fig. 3 Angular Distribution of Secondary Pions-16.2 BeV π-Nucleus Interactions

the momenta of most of the pions which were emitted at angles less than 20° were measured (69%). On the other hand, the momenta of relatively few (22%) of the pions with emission angles greater than 20° were measured. This implies that the set of pion tracks analyzed in this investigation may not be one which is wholly representative of secondary pions produced in pion-nucleus interactions.

Cross Sections

As was mentioned previously, Ilford K-5 nuclear emulsion is composed of hydrogen (H), light (C-N-O), and heavy (Ag-Br) nuclei. In order to determine a cross section for pion-nucleus interactions, it is necessary to know the density of nuclei of each kind in the emulsion. Table 7 shows the composition of standard Ilford K-5 emulsion as given by Barkas[90]. It also shows the number of nuclei of each

TABLE 7

COMPOSITION OF STANDARD ILFORD K-5 EMULSION (1)

Element	Concentration (gm/cm^3)	A_i (atomic wt.)	N_i ($\times 10^{20}$ $atoms/cm^3$)
Ag	1.8088	107.88	101.01
Br	1.3319	79.916	100.41
I	0.0119	126.93	0.565
C	0.2757	12.0000	138.30
H	0.0538	1.0080	321.56
O	0.2522	16.0000	94.97
N	0.0737	14.008	31.68
S	0.0072	32.06	1.353

element per unit volume (N_i). This was determined from the density of each element in the emulsion (ρ_i), its atomic weight (A_i) and Avagadro's number (N_0):

$$N_i = \frac{\rho i}{A_i} N_0 \text{ nuclei/cm}^3.$$

For cross-section calculations, the scanning efficiency has to be estimated in some acceptable manner. The primary objective of the scanning was the location and identification of electromagnetic interactions involving the beam pions. These events are often difficult to locate because of the fact that they contain, in the case of pair production, a maximum of three tracks and all tracks are lightly ionizing. Considering that pion-nucleus interactions generally contain at least one dark or medium ionizing track, it was reasonably safe to assume that the scanning efficiency for the detection of pion-nucleus interactions was 100%.

As stated in the previous section, the mean free path was found to be 38.8 cm.. The mean free path for pion-nucleus interactions can also be determined from the relation

$$\lambda = \frac{1}{N\sigma}$$

where λ represents the mean free path and

$$N\sigma = \sum_{i=1}^{m} N_i \sigma_i$$

N_i and σ_i being the number of nuclei of the $i^{\underline{th}}$ element per unit volume and the cross section for the interactions of pions with a nucleus of the $i^{\underline{th}}$ element in the emulsion, respectively.

Now, assuming that the cross section for each element is approximated by its geometrical cross-section, one has

$$\sigma_i = \pi R_i^2$$

where R_i denotes the nuclear radius. Putting the expression for the nuclear radius,

$$R_i = r_0 A_i^{1/3} \qquad (A_i\text{=number of nucleons in nucleus, } r_0\text{=constant}),$$

back into the equation for the mean free path, one obtains for r_0

$$r_0 = \frac{1}{\sqrt{\pi\lambda \sum_{i=1}^{m} N_i A_i^{2/3}}}$$

Using λ = 38.3 cm. and the information given in Table 7, the value

$$r_0 = 1.17\text{x}10^{-13}\text{cm.}$$

was obtained. This value falls within the range of values of r_0 which have been determined from experiments of various kinds. These values of r_0 range from $(1.07\pm0.02)\text{x}10^{-23}$ cm. obtained from scattering electrons off nuclei[95] to 1.5x 10^{-13} cm. determined from measuring the lifetime of α-decaying nuclei[95].

The geometrical cross-section for pion-nucleon interactions was then calculated using the value of r_0 just determined. This is

$$(\sigma_{\pi\text{-}N})_{Geom.} = \pi R_H^{\ 2} = \pi r_0^{\ 2} A_H^{\ 2/3} = \pi r_0^2$$

where R_H is the nuclear radius of hydrogen. This resulted in

$$(\sigma_{\pi\text{-}N})_{Geom.} = 42.7 \text{ mb.}$$

As average cross-section per nucleon was then calculated from the mean free path for pion-nucleus interactions (λ) and the number of nucleons per unit volume (n) in the emulsion from the relation

$$(\sigma_{\pi\text{-}N})_{Ave.} = \frac{1}{n\lambda}$$

where $n = \sum_{i=1}^{m} N_i A_i$, N_i being the number of nuclei of each element per unit volume and A_i the number of nucleons in the nucleus of each element in the emulsion. In this manner, a cross-section

$$(\sigma_{\pi\text{-}N})_{Ave.} = 13.2 \text{ mb.}$$

was obtained.

The two cross-sections $(\sigma_{\pi\text{-}N})_{Geom.}$ and $(\sigma_{\pi\text{-}N})_{Ave.}$ were compared with values of the π-N cross-section determined experimentally for pion-nucleon interactions at energies close to 16 BeV. The results are given in Table 8. The apparent "blocking" or "screening" effect of the nucleons in the nucleus can be seen here. On the average, about one-half of the nucleons in a nucleus are "blocked" out by other nucleons which results in a corresponding reduction of the "average" cross-section per nucleon from the value it would have if the nucleons were in the free state. Although the

TABLE 8

COMPARISON OF CROSS-SECTIONS AT PRIMARY ENERGIES NEAR 16.2 BeV

Interaction	Cross-Section (mb)	Reference
16.2 BeV/c	$(\sigma_{\pi-N})_{Geom.} = 42.5$	This experiment
π^--Nucleus	$(\sigma_{\pi-N})_{Ave.} = 11.1$	
16.2 BeV/c π^--N	$\sigma_{Tot} = 24.2 \pm 2.3$	Samimi(93)
16 BeV/c π^--p	$\sigma_{Tot} = 25.4 \pm 1.6$	Goldsack et al.(80)
17 BeV/c π^--p	$\sigma_{Tot} = 27$	Huson and Fretter(82)

geometrical cross-section is almost twice as large as the experimental value, this is not a surprising result. It indicates that the nucleon exhibits a certain amount of transparency when involved in an interaction with a high-energy pion.

Distributions of Events According to Number of Pions

Table 9 shows the distribution of events according to the number of secondary pions in each event. This is compared with the corresponding distribution from the analysis of the 16.2 BeV negative pion-nucleon interactions(93). As can be seen, the total number of secondary pions in the two different sets of events is almost the same and the distributions of the pions are quite similar.

TABLE 9

DISTRIBUTION OF EVENTS ACCORDING TO
NUMBER OF SECONDARY PIONS

	16.2 BeV π^--Nucleus Interactions			16.2 BeV π^--Nucleon Interactions		
No.of Pions	No.of Events	Tot.# of Pions	#Dk.+ Gy. Tks.	No. of Events	Tot.# of Pions	#Dk. Tks.
1	21	21	78	126	126	41
2	32	64	162	43	86	15
3	43	129	255	121	363	33
4	31	124	195	63	252	9
5	45	225	352	42	210	17
6	31	186	262	34	204	6
7	22	154	193	9	63	5
8	25	200	259	18	144	0
9	21	189	210	7	63	3
10	10	100	150	3	30	0
11	8	88	119	3	33	1
12	2	24	13			
13	2	26	49			
14	2	28	35			
15	1	15	15			
16	1	16	20			
17						
18						
19						
20	1	20	27			
Total	298	1609	2394	469	1574	132

According to Type of Nucleus

A reliable method for determining which type of emulsion nucleus, (C-N-O) or (Ag-Br), takes part in a particle-nucleus interaction has been a source of disagreement for high energy experimentalists for quite some time. Although several methods for separating the two types have been proposed, it is still quite difficult to achieve an unambiguous separation. Almost all of the separation schemes which have been proposed are based on the number of heavy tracks (N_h) observed in the individual events.

Friedlander[42] and Barbaro-Galtieri[35] used the following criteria in their investigations of high energy proton-nucleus interactions in emulsion: events with $N_h \geq 7$ involved heavy nuclei exclusively whereas events with $1 < N_h \leq 4$ involved mostly light nuclei. Events with $N_h = 5,6$ were excluded from consideration because they contained a mixture of heavy and light nuclei and there was no reliable method available for separating the two kinds.

In their study of proton-nucleus interactions, Jain _et al._[50] actually employed three methods of separation. The first one ascribed events with $N_h \geq 7$ as involving only heavy emulsion nuclei, whereas those events with $N_h < 7$ were mostly interactions involving light nuclei. In order to obtain agreement with the tube model in their analysis, a second method was used. This assumes events with $N_h \leq 5$ to be due to light nuclei and those with $N_h > 7$ to be due to heavy nuclei. They also used a third separation scheme--dividing the events into two classes, those with $N_h \leq 5$ and those with $N_h > 5$.

In an earlier paper, Lohrmann et al.[45] had used this same method of selection in their study of high energy particle-nucleus interactions from 6.2-3500 BeV. Events with $N_h \leq 5$ were classified as light nucleus interactions and events with $N_h > 5$ were classified as heavy nucleus interactions.

Kohli et al.[41] used the criteria of Lohrmann et al.[47] in their investigation of 17.2 BeV pion-nucleus interactions. It is based upon the existence of a Coulomb barrier in cases involving heavy nuclei--where the nucleus is not strongly excited. This barrier prevents the emission of low energy particles from these nuclei. Thus, they used the following criteria: events with $1 < N_h \leq 6$ and having at least one track <65μ in length belong to the (C-N-O) group. Events with $N_h \leq 6$ and with no track <65μ long belong to the (Ag-Br) group along with all events having $N_h \geq 7$.

According to Rao et al.[53], there is even disagreement about using the Coulomb barrier as a criterion. They based their method of selection on the characteristics of the recoil nuclei in the proton-nucleus interactions they studied. Events with tracks between one and ten microns in length (attributed to recoil nuclei) which are observed in the forward direction and having $N_h \leq 8$ they classify as light nuclei. Those events with $N_h > 8$ and those with $N_h \leq 8$ but with recoil nucleus tracks emitted in the backward direction, were classified as heavy nucleus events.

Bogachev *et al.*[44] assumed that events with $N_h \leq 8$ were due to light nuclei and those with $N_h > 8$ were due to heavy nuclei. Variations of this same criterion were employed by Bogdanowicz *et al.*[38] and Barashenkov *et al.*[16] in their studies of proton-nucleus interactions at different primary energies.

Ciurlo *et al.*[70], in their analysis of the interactions of 16.2 BeV/c pions in nuclear emulsion, classified events with $1 < N_h \leq 6$ as light (C-N-O) nucleus events and those with $N_h \geq 7$ as heavy (Ag-Br) nucleus events.

Since no selection criterion has been universally accepted, the pion-nucleus events used in this investigation were separated solely on the basis of the number of heavy tracks in each event. However, several different separation schemes were used and these were labelled Methods I through VI. Table 10 shows the six methods used in the analysis. Characteristics of each group of events were determined and it was discovered that all six methods gave approximately the same results. The angular distributions, the transverse momentum distributions, and the average transverse momentum for each method used were almost the same for each group of events, (C-N-O) and (Ag-Br). Only one difference was noticeable, that being in the average multiplicities of

TABLE 10

VARIOUS SELECTION CRITERIA USED FOR LIGHT AND HEAVY NUCLEI

Selection Method #	Light Nuclei (C-N-O)	Heavy Nuclei (Ag-Br)
I	$1 < N_h \leq 4$	$N_h \geq 7$
II	$N_h \leq 7$	$N_h > 7$
III	$N_h \leq 5$	$N_h > 7$
IV	$1 < N_h \leq 6$	$N_h \geq 7$
V	$N_h \leq 8$	$N_h > 8$
VI	$N_h \leq 5$	$N_h > 5$

the secondary pions. This difference is not unexplainable, however, and will be discussed further in the next chapter. Because of the similarities of the results obtained using each of the six selection criteria, it was decided to choose one method which was representative of these six and to show only the results obtained using the chosen criterion. Method III, which was used by Jain et al.[50] was selected as the representative criterion. In this classification scheme, events with $N_h \leq 5$ involve light (C-N-O) nuclei and those with $N_h > 7$ involve heavy (Ag-Br) nuclei. Events which have $N_h = 6$ or $N_h = 7$ are excluded from consideration.

Multiplicities

The average multiplicities of charged secondary pions and heavy tracks, already stated as $\langle n_s \rangle = 5.4 \pm 0.3$ and

$\langle N_h \rangle = 8.0 \pm 0.8$, are compared in Table 11 with results obtained from other particle-nucleus interaction studies and also with the predictions of the cascade model. The average multiplicities for this experiment, the 16.2 BeV pion-nucleus interactions, agree with the results obtained by Kohli et al.[41] for 17.2 BeV pion-nucleus interactions. However they are slightly higher than the average multiplicities observed by Jain et al.[50] in 16.3 BeV/c pion-nucleus interactions. There is also agreement between the multiplicities obtained in this analysis and experimental results and cascade model predictions for 17 BeV proton-nucleus interactions. However, one should be very careful in evaluating the significance of this agreement. It does not necessarily follow that a pion-nucleus interaction should yield the same results as a proton-nucleus interaction. In the case of pion-nucleon and proton-nucleon interactions, the results are sometimes significantly different for interactions occurring at the same primary energy[96,97].

In order to compare the pion multiplicity from the 16.2 BeV pion-nucleus interactions with the tube model, the relation given by Lohrmann et al.[47] was used:

$$\langle n_s \rangle = kA^{0.19}E^{0.25}$$

Here A is the number of nucleons in the target nucleus, E is the energy in BeV of the primary particle, and k is a proportionality constant. Before this relation could be

TABLE 11

PARTICLE-NUCLEUS INTERACTIONS
AVERAGE MULTIPLICITIES

Interaction	Experiment or Theory	$<n_s>$	$<N_h>$	Ref. No.
16.2 BeV/c π^--Nucleus	Experiment	5.40±0.31	8.03±0.80	This experiment
16.3 BeV/c π-Nucleus	Experiment	4.49±0.11	6.88±0.12	(50)
17 BeV/c π-Heavy Nucleus	Experiment	7.1 ±0.2	15.5±0.3	(40)
17.2 BeV π^--Nucleus	Experiment	5.65±0.10	- - - - -	(41)
17 BeV π^--Heavy Nucleus	Cascade Model	7.1 ±0.5	4.0 ±0.4	(4)
6.2 BeV p-Nucleus	Experiment	2.65±0.10	9.7 ±0.3	(31)
	Experiment	2.7 ±0.2	- - - - -	(32)
	Experiment		8.8	(33)
	Cascade Model	2.8 ±0.15	8.3 ±0.4	(20)
	Cascade Model	2.7 ±0.1	7.8 ±0.4	(30)
9 BeV p-Nucleus	Experiment	3.2 ±0.2	7.8 ±0.8	(16)
	Experiment	5.68±0.14	- - - - -	(42)
	Experiment	- - - - -	8.3 ±0.9	(33)
	Cascade Model	3.4 ±0.2	8.3 ±0.6	(20)
	Cascade Model	3.4 ±0.2	8.5 ±0.4	(30)
17 BeV p-Nucleus	Experiment	- - - - -	8.3 ±0.9	(33)
	Experiment	5.89±0.6	8.5 ±0.1	(30)
	Cascade Model	5.5 ±0.3	9.7 ±0.6	(20)
	Cascade Model	5.3 ±0.3	9.4 ±0.4	(30)
25 BeV p-Nucleus	Experiment	6.4 ±0.5	6.7 ±0.2	(30)
	Cascade Model	6.9 ±0.4	8.9 ±0.5	(20)
	Cascade Model	6.2 ±0.3	9.7 ±0.5	(30)
26.7 Bev/c p-Nuc.	Experiment	5.5 ±0.2	6.7 ±0.2	(36)
27 BeV p-Nucleus	Experiment	6.6 ±0.1	7.2 ±0.2	(35)

TABLE 11 (Cont.)

Interaction	Experiment or Theory	$<n_s>$	$<N_h>$	Ref. No.
28 BeV/c p-Nuc.	Experiment	6.3 ±0.1	7.2 ±0.2	(50)
16.2 BeV/c π^--Nucleus	Tube Model	3.7 ±7.4		(11,17,41,47)
27 BeV p-Nucleus	Experiment	6.4 ±0.1	7.7 ±0.1	(98)
19.8 BeV/c p-Nucleus	Experiment	5.63±0.06	7.42±0.08	(34)

used, however, an estimate of the value of the proportionality constant k was needed. From several experiments (17,41,47) and from Belen'kji and Landau's[11] theoretical discussion of the tube model, the value of k was found to vary approximately from 1.0 to 2.0. Using these two limits on the value of k, the number of nucleons (25) of an average emulsion nucleus, and the primary energy, 16.2 BeV, the multiplicity predicted by the tube model could be anywhere within the range 3.7-7.4. This wide range assured that the observed pion multiplicity from the 16.2 BeV pion-nucleus interactions would lie between the limits calculated. As a result no significance can be attached to the outcome of the comparison.

Table 12 presents a comparison of the pion multiplicity from the 16.2 BeV pion-nucleus interactions with multiplicities observed in pion-nucleon interactions in the same region of primary energy. As can be seen, the multiplicity of the pions from the 16.2 BeV pion-nucleus interactions is significantly higher than the other multiplicities. A comparison was also made with the multiplicities from 18 π^--p and π^--n experiments listed in the extensive review of multiplicities in inelastic high-energy interactions by Barashenkov <u>et al</u>.[96]. These multiplicities ranged from 1.13±0.1 for 1.09 BeV π^--n collisions to 3.05±0.17 for interactions of 17 BeV π^- with neutrons. Again, the pion multiplicity from the 16.2 BeV pion-nucleus in-

TABLE 12

COMPARISON OF PION MULTIPLICITIES

Interaction	Detector	$\langle n_s \rangle$	Reference
16.2 BeV/c π-Nucleus	Emulsion	5.4 ±0.3	This experiment
16.2 BeV/c π^--Nucleon	Emulsion	3.5 ±0.2	(93)
6.1 BeV/c π^--Nucleon	Heavy Liquid Bubble Cham.	3.63±0.15	(74)
7.0 BeV/c π^--Nucleon	Propane Bubble Cham.	3.4 ±0.15	(75)
7.3 BeV/c π^--Nucleon	Emulsion	4.1 ±0.1	(76)
16 BeV/c π^--p	H_2 Bubble Cham.	3.77±0.25	(80)
16.3 BeV/c π^--Nucleon	Emulsion	4.77±0.12	(99)

teractions is significantly higher.

Figure 4 shows the distribution of $\langle n_s \rangle$ versus N_h for the data obtained in this experiment. $\langle n_s \rangle$ increases almost uniformly, within error, with N_h. No step occurs in the plot to indicate a separation between light and heavy nuclei. This contradicts the prediction of Friedlander[42] but is in agreement with the results given by Jain et al.[50]. According to Matsumoto[46], this dependence of $\langle n_s \rangle$ on the value of N_h should rule out the possibility that the target is effectively a single nucleon in the nucleus.

Figure 5 shows the relation between $\langle N_h \rangle$ and n_s for the pion-nucleus events. $\langle N_h \rangle$ increases faster with increasing n_s than the corresponding dependence of $\langle n_s \rangle$ on N_h seen in Figure 4. The results of Jain et al.[50] indi-

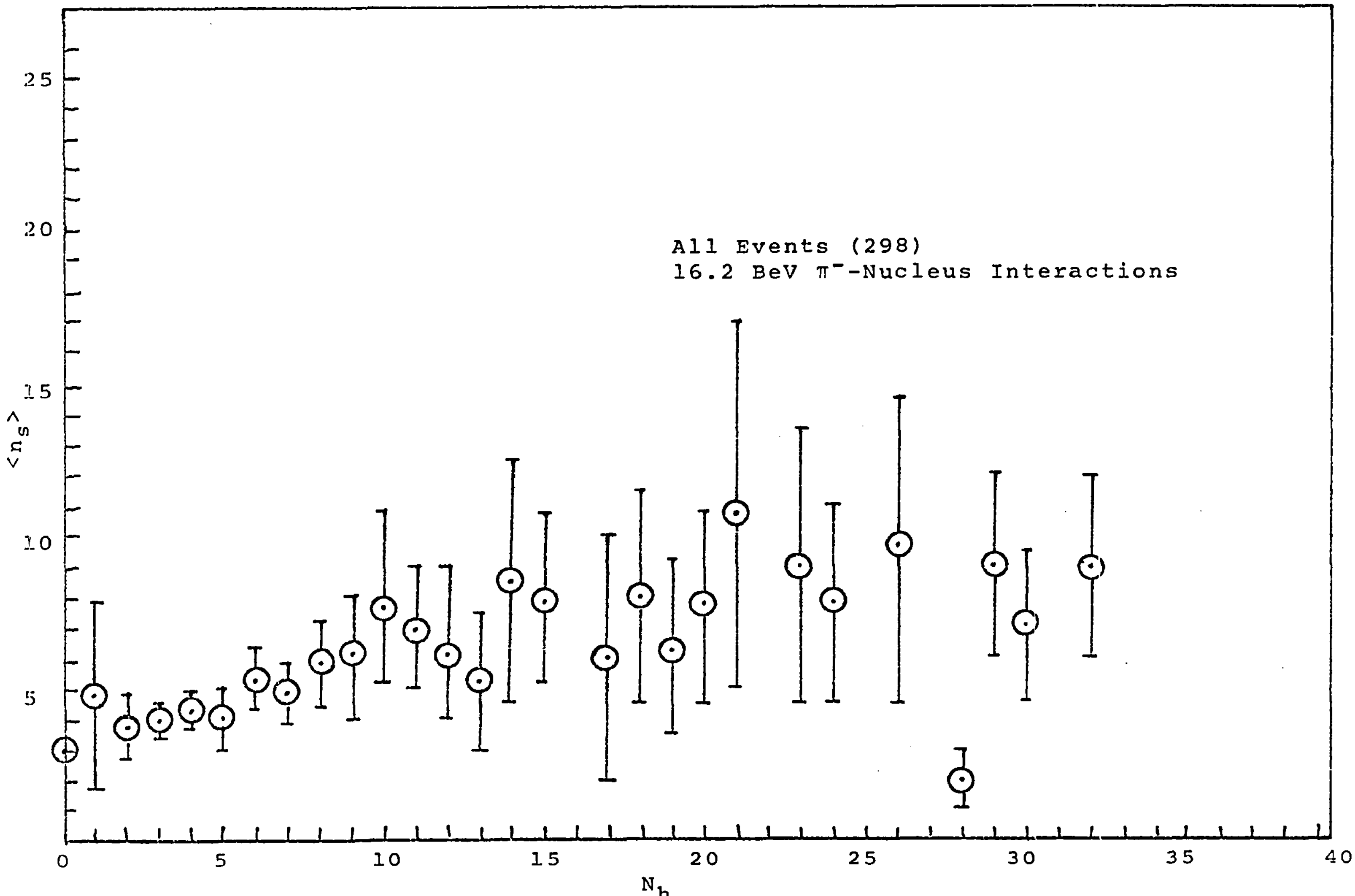

Fig. 4 Average Number of Pion Tracks vs. Number of Heavy Tracks per Event for 16.2 BeV π-Nucleus Interactions

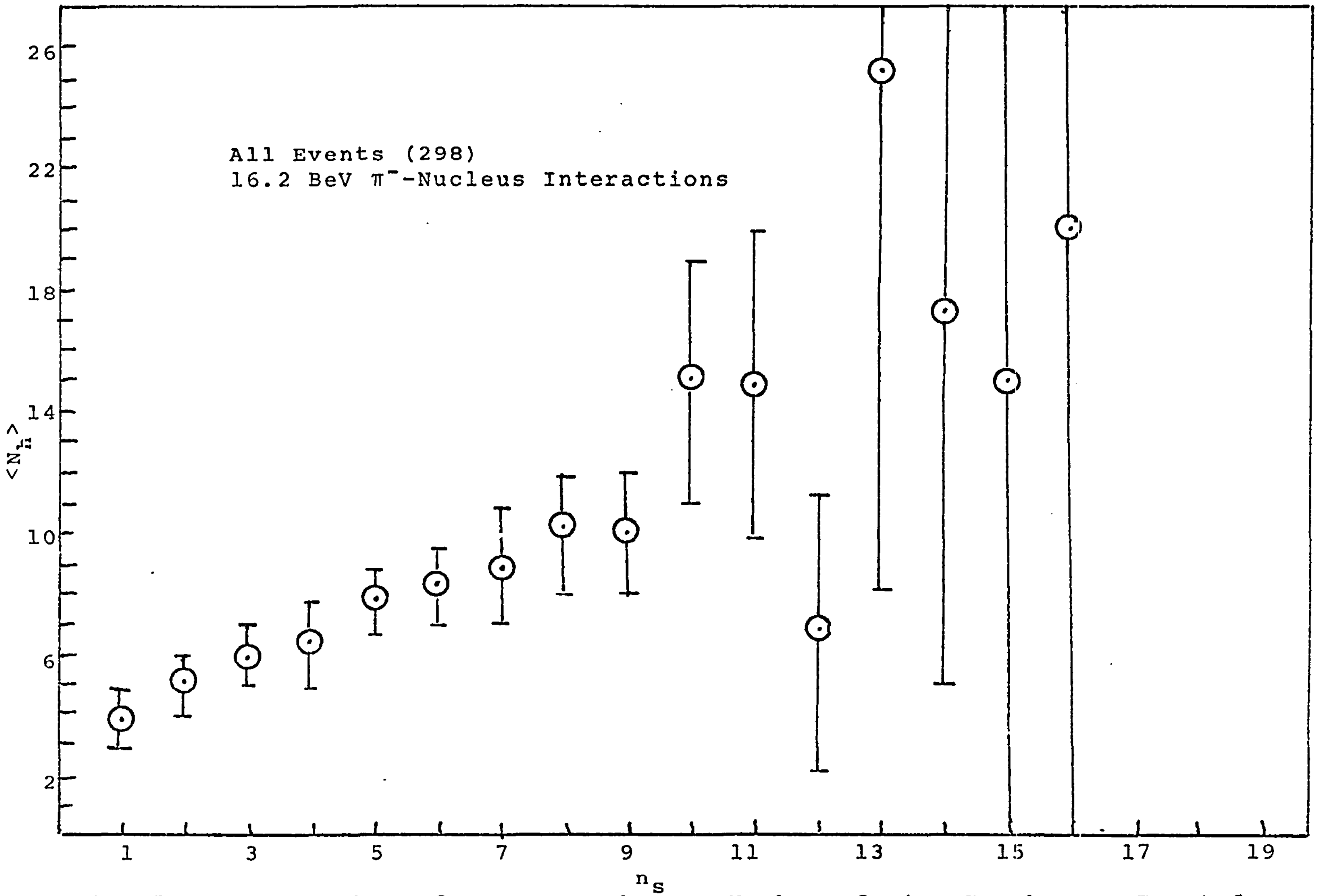

Fig. 5 Average Number of Heavy Tracks vs. Number of Pion Tracks per Event for 16.2 BeV π-Nucleus Interactions

cated that $<N_h>$ approached an approximately constant value for larger values of n_s. Due to the large statistical error in $<N_h>$ shown in Figure 5 for $n_s>12$, the behavior of $<N_h>$ in the region of large n_s is quite uncertain for this experiment.

Shen[52] shows a linear increase of $<N_h>$ with n_s but a slower increase of $<n_s>$ with N_h. He cites the suggestion of Going[98] to explain the difference in dependence--that the shower particles are almost all produced in a single interaction. He claims that if the cascade mechanism were responsible for the production of the shower particles, then n_s and N_h should be more closely related to each other. This would imply that no significant difference should be observed in the dependence of $<N_h>$ on n_s and of $<n_s>$ on N_h. Since $<n_s>$ does exhibit a slower increase with N_h than $<N_h>$ does with n_s, this would agree with Shen's contention, at least at lower multiplicities (<10).

In an effort to determine the relationship between the dependence of $<N_h>$ on n_s and that of $<n_s>$ on N_h, the following calculation was made. Since both n_s and N_h have overall averages, one can write

$$<n_s> = K<N_h>+\delta$$

where K and δ are constants and the averages are taken over all the events. Thus, the above expression can be written as

$$\frac{1}{N_e}\sum_{i=1}^{N_e}(n_s)_i = \frac{K}{N_e}\sum_{i=1}^{N_e}(N_h)_i+\delta$$

where $(n_s)_i$ and $(N_h)_i$ are the number of light tracks and the number of heavy tracks, respectively, in the $i^{\underline{th}}$ event, and N_e is the total number of events. Now let the events be ordered according to the number of light tracks per event. Let L_j = number of events in the group corresponding to j light tracks per event. Multiplying through by N_e, the above equation can be rewritten in terms of L_j,

$$\sum_{j=1}^{N_d} jL_j = K\sum_{j=1}^{N_d} L_j\langle N_h\rangle_{n_s=j}+\delta\sum_{j=1}^{N_d} L_j$$

where N_d is the number of distinct groups of events classified according to the number of light tracks. $\langle N_h\rangle_{n_s=j}$ represents the average number of heavy tracks in the group of events which has j light tracks per event. Rearranging the terms, one obtains

$$\sum_{j=1}^{N_d} L_j(j-K\langle N_h\rangle_{n_s=j}-\delta) = 0. \qquad (1)$$

Before the quantity in parentheses can be set equal to zero term by term, it is necessary to assume that each of these terms has the same sign. One then obtains

$$j-\delta = K\langle N_h\rangle_{n_s=j}.$$

Solving this for $\langle N_h\rangle$ and using the fact that j is the number of light tracks in a group, the result is

$$\langle N_h\rangle_{n_s} = \frac{1}{K}\,n_s-\frac{\delta}{K}\,. \qquad (2)$$

This gives the dependence of $\langle N_h \rangle$ on the number of light tracks n_s which is shown in Figure 5.

In an analagous manner, ordering the events according to the number of heavy tracks per event, the result

$$\langle n_s \rangle_{N_h} = K N_h + \delta \tag{3}$$

is obtained. This gives the dependence of $\langle n_s \rangle$ on the number of heavy tracks N_h, which is shown in Figure 4.

Since the same constant K, which can be evaluated from the initial expression, occurs in both of the derived relations, (2) and (3), this implies that the two graphs, Figure 4 and 5, should be related if the assumptions made above are valid. The slope of the graph in Figure 4 is 0.25 and that of Figure 5 is 1.1. Since these two quantities are not reciprocals of each other, the validity of the assumptions made in the derivation are therefore brought into question. From the data it was determined that the sign of the quantity in parentheses in relation (1) is not the same for all of the terms in the series. Therefore this quantity cannot be set equal to zero term by term. Because of this limitation, if a relationship does exist between the two graphs, it cannot be determined in a straightforward manner.

Figure 6 shows the pion multiplicity distribution for (C-N-O) and (Ag-Br) events. These histograms were compared with previous results[35,36,42,50]. Considering only the

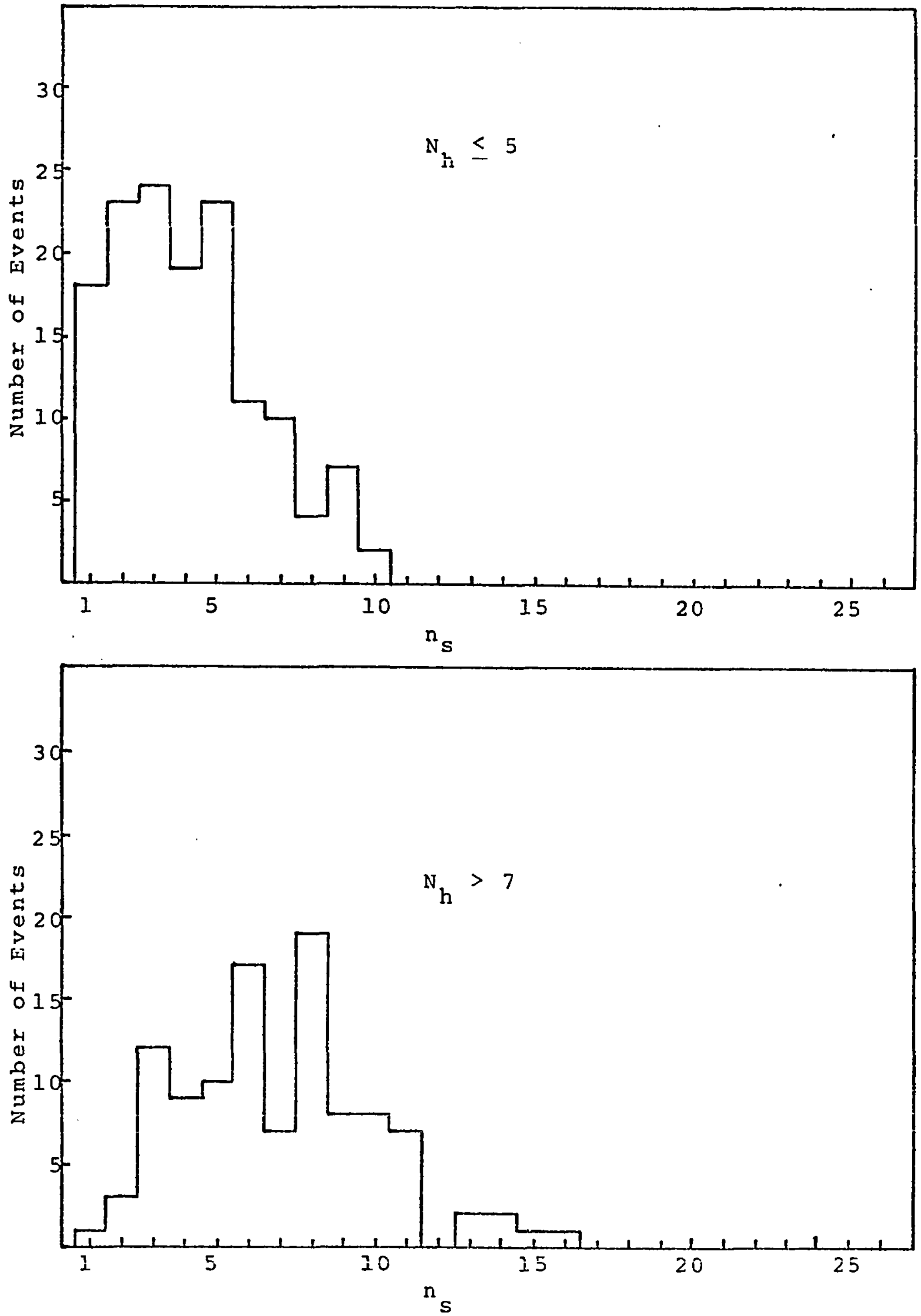

Fig. 6 Distribution of Secondary Pions from 16.2 BeV π-Nucleus Interactions

light nucleus interaction histogram, it was found that the secondary peak reported by Lim[36] is absent in the other results, including the 16.2 BeV pion-nucleus interactions. Lim[36] gives two possible interpretations for these peaks in his multiplicity distribution. Either the main peak in the distribution is the result of single-collision events (e.g. a pion-nucleon collision) and the secondary peaks are the result of more than one collision in the same target nucleus, or the secondary peaks could have resulted from the tube mechanism.

The average pion multiplicities for light and heavy nucleus events were calculated. Tables 13 and 14 show the results for this experiment along with other results for comparison. The values calculated for each of the six selection criteria are presented here because the average multiplicity was the only characteristic in which the six criteria differed significantly. The theoretical value given for the tube model at 16.2 BeV was calculated as before, from the relation given in (47) and the results of (17,41,47). As before, such wide ranges of multiplicities insure that the observed values will lie between the limits. The methods with larger values of $\langle n_s \rangle$ (II,IV,V, and VI) agree reasonably well with the predictions of the cascade model for proton-nucleus interactions at 25 BeV.

Considering Table 14, it is evident that Methods II,

TABLE 13

AVERAGE PION MULTIPLICITIES FROM THE INTERACTION OF PARTICLES WITH LIGHT EMULSION NUCLEI

Primary Particle	$\langle n_s \rangle$	Reference
16.2 BeV/c π^-	1.3 -6.6	Tube Model (9,14)
Method I	3.98±0.20	
Method II	4.34±0.15	This experiment
Method III	4.11±0.17	
Method IV	4.22±0.17	
Method V	4.47±0.15	
Method VI	4.34±0.15	
16.2 BeV π^-	4.78±0.26	(9)
9 BeV p	5.24±0.14	(6)
	3.0 ±0.2	(14)
	2.9	Cascade Model (33)
	2.8	Cascade Model (34)
	3.9 ±0.2	Cascade Model (22)
25 BeV p	4.6 ±0.3	Cascade Model (22)
	4.9	Cascade Model (9)
	6.4	Tube Model (9)
	5.15±0.23	(35)
27 BeV p	5.0 ±0.2	(7)
25 BeV/c p	4.8 ±0.2	(11)
25 BeV p	5.1 ±0.3	(36)

III, and, within the indicated error, V are in good agreement with the cascade model. Since the groups classified as events involving light nuclei are probably contaminated by the inclusion of some events which involve heavy nuclei, this would indicate that the multiplicities calculated for the light nuclei groups may be too large. However, all the values of $\langle n_s \rangle$ for the light nucleus groups are lower than the value of $\langle n_s \rangle$ given by Kohli et al.[41] in a study of 17.2 BeV pion-nucleus interactions. A possible explanation

TABLE 14

AVERAGE PION MULTIPLICITIES FROM THE INTERACTION OF PARTICLES WITH HEAVY EMULSION NUCLEI

Primary Particle	$\langle n_s \rangle$	Reference
16.2 BeV/c π^-	4.8 -9.5	Tube Model (17,41,47)
Method I	6.73±0.22	
Method II	7.10±0.25	This experiment
Method III	7.10±0.25	
Method IV	6.73±0.22	
Method V	7.36±0.28	
Method VI	6.53±0.20	
17.2 BeV π^-	5.89±0.30	(41)
17 BeV π^-	7.1 ±0.2	(40)
	7.1 ±0.5	Cascade Model (4)
9 BeV p	6.00±0.30	(42)
	3.5 ±0.30	(16)
	4.1	Cascade Model (17)
	3.7	Cascade Model (18)
	3.8 ±0.2	Cascade Model (30)
15 BeV p	7.9 ±0.4	Cascade Model (30)
	7.8 ±0.2	Cascade Model (20)
	8.6 ±0.8	(38)
	6.8	Cascade Model (41)
	8.0	Tube Model (41)
	6.8 ±0.4	(15)
27 BeV p	8.2 ±0.2	(35)
25 BeV/c p	6.3 ±0.1	(53)
25 BeV p	6.4 ±0.1	(49)

for this difference is their admission that the selection criteria which they used for (C-N-O) events may have as much as 50% error connected with it.

Figure 7 shows the dependence of the average number of heavy tracks on the number of secondary pions for both light and heavy nuclei. For the case of (C-N-O) nuclei, $\langle N_h \rangle$ is independent of the number of secondary pions pro-

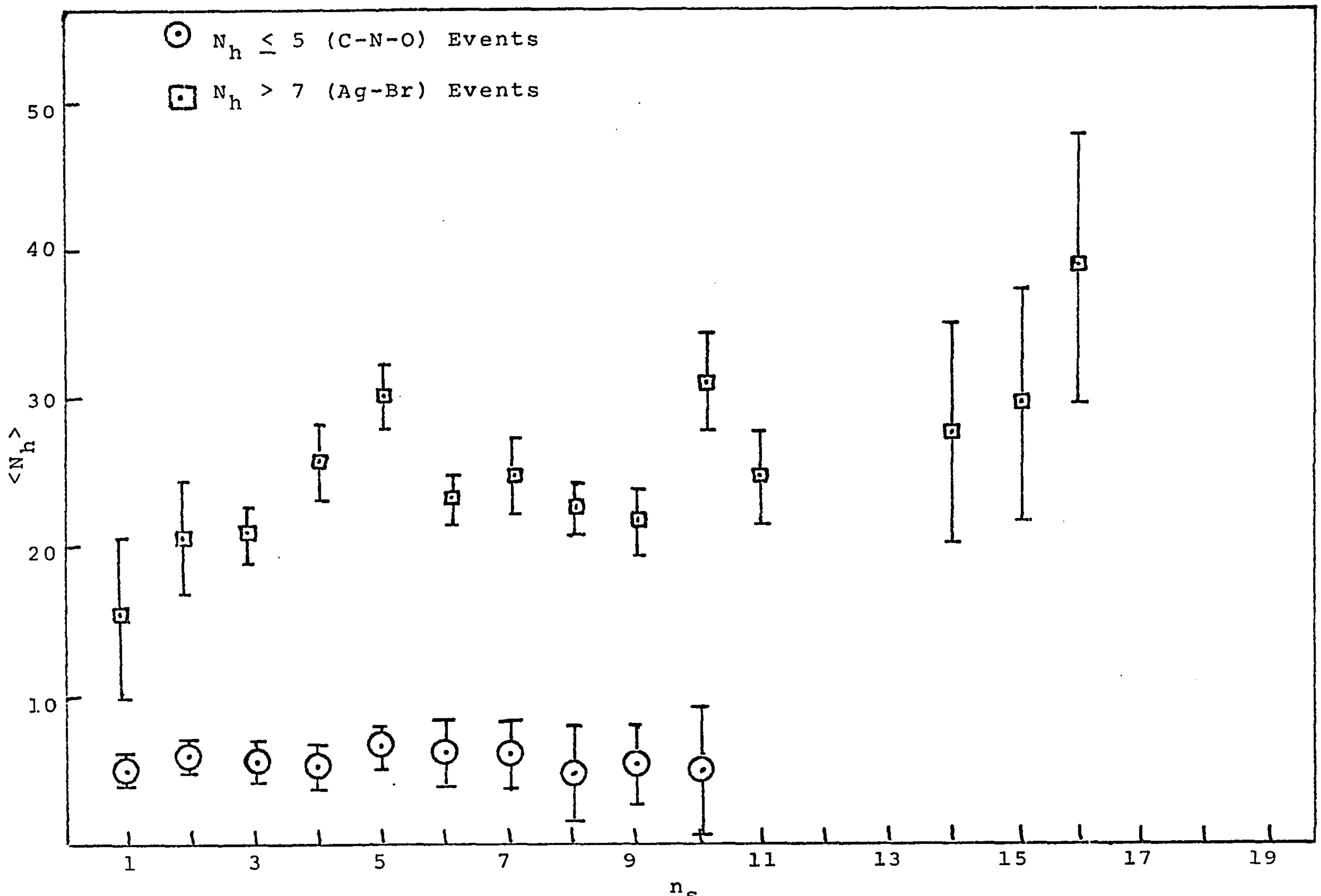

Fig. 7 $\langle N_h \rangle$ vs. n_s for (C-N-O) and (Ag-Br) Events duced in an interaction. In the case of heavy nuclei (Ag-Br) the results seem to indicate a tendency for $<N_h>$ to increase as n_s increases. This agrees with the results shown by Meyer et al.[49], Kohli et al.[41], and Artykov et al.[20]. Kohli et al.[41] and Meyer et al.[49] explain the observed results in the following way: if one assumes that the atomic masses of (C-N-O) are small (12-16), then N_h should have a constant value no matter what n_s may be. These light nuclei can completely disintegrate when only a small amount of energy has been transferred to them in a collision. Therefore, when the target is a light nucleus (C-N-O), the effect of multi-nucleon interactions is of no importance. The rise in $<N_h>$ with n_s observed in the case of heavy nuclei may be caused by an increase of secondary interactions due to an inter-nuclear cascade produced in the heavy nucleus. Because of their large atomic weight (the average is 94 for Ag-Br), there is an increase in the value of N_h (which is a measure of the excitation) with the increase in the number of collisions taking part in the nucleus (measured by n_s).

The rather erratic behavior of $<N_h>$ with n_s in the case of the (Ag-Br) nuclei in Figure 7 cannot be immediately explained. The (Ag-Br) events are supposedly almost entirely free of any light nucleus events. On the other hand, the (C-N-O) group exhibits an almost constant value of $<N_h>$ yet this group must surely contain some (Ag-Br) events. This indicates that the number of (Ag-Br) events which have been included in the (C-N-O) group is small enough so that their contribution does not affect the value of $<N_h>$.

The ratio of the mean multiplicity of shower particles from the (Ag-Br) events to that found in the (C-N-O) events was calculated. Table 15 shows the results and a comparison of the results with other work. From the values

TABLE 15

VALUE OF RATIO $<n_s>_{Ag-Br}/<n_s>_{C-N-O}$

Experiment or Theory	r	Reference
16.2 BeV/c π^--Nucleus		
Method I	1.69	This experiment
Method II	1.63	
Method III	1.73	
Method IV	1.57	
Method V	1.65	
Method VI	1.69	
27 BeV p-Nucleus	1.6 ± 0.3	(35)
6.3 BeV/c p-Nucleus	1.2 ($N_h \le 7 . N_h > 7$) 1.6 ($N_h \le 5 . N_h > 7$)	(50)
9 BeV p-Nucleus	1.15±0.06	(42)
Tube Model	1.62	(11,12)
Cascade Model	2-3	(42,27)
9 BeV p-Nucleus Cascade Model	1.17	(16)
9 BeV p-Nucleus Cascade Model	0.97	(30)
25 BeV p-Nucleus	1.71	(30)
Tube Model	1.44	(42,47,49)

of $\langle n_s \rangle$ obtained by Barashenkov et al.[16] and Artykov et al.[30] from their Monte Carlo calculations of 9 BeV proton-nucleus interactions using the cascade model, values of r were calculated which are radically different from the prediction made by Rozental and Chernavskii[27] discussed previously. The value of r determined from the latest Monte Carlo calculations on 25 BeV proton-nucleus collisions[30] is in good agreement with the results of Methods I, II, III, and IV. However, the tube model prediction agrees with all of the results except those of Method IV. The other values obtained from the cascade model are much smaller than the experimental results.

The dependence of the mean shower particle multiplicity upon the atomic weight of the target nucleus was also investigated. Table 16 compares the experimental results

TABLE 16

DEPENDENCE OF AVERAGE SHOWER MULTIPLICITIES ON NUMBER OF NUCLEONS IN NUCLEUS

Experiment	$\langle n_s \rangle = CA^B$	Reference
16.2 BeV π^--Nucleus	$4.2\ A^{0.12}$	This experiment
17.2 BeV π^--Nucleus	$3.4\ A^{0.13}$	(41)
24 BeV p-Nucleus	$3.4\ A^{0.14}$	(49)
Cascade Model	$CA^{0.18-.19}$	(17,23)
Tube Model	$CA^{0.19}$	(47,11,12)
Modified Tube Model	$CA^{0.15}$	(52)

with the theoretical predictions. The results obtained from the 16.2 BeV pion-nucleus interactions are in good agreement with the results of Kohli et al.[41] and Meyer et al.[49] but there is general disagreement between the results at 16.2 BeV and the theoretical predictions.

Angular Distributions

From Figure 3, it can be seen that the angular distribution of all the secondary pions in the laboratory system is anisotropic, with a broad peak in the forward direction. This distribution is in reasonably good agreement with the corresponding distribution obtained from a Monte Carlo calculation of the interactions of 9 BeV protons with average emulsion nuclei[17] using the cascade model.

Figure 8 shows the angular distributions for (C-N-O) and (Ag-Br) events. These were compared with previous experimental and theoretical results. The distributions from the 16.2 BeV pion-nucleus interactions were in agreement with the experimental results of 17.2 BeV pion-nucleus interactions[41] and 26.7 BeV/c proton-nucleus interactions[36]. They also agreed with the Monte Carlo calculations made using the cascade model of 17 BeV pion-nucleus[4], 9 BeV proton-nucleus[17] and 25 BeV proton-nucleus[30,19] interactions. The angular distributions for the (Ag-Br) events are broader than those for the (C-N-O) events. Lim[36] and Jain[50] both attribute the broadening to secondary inter-

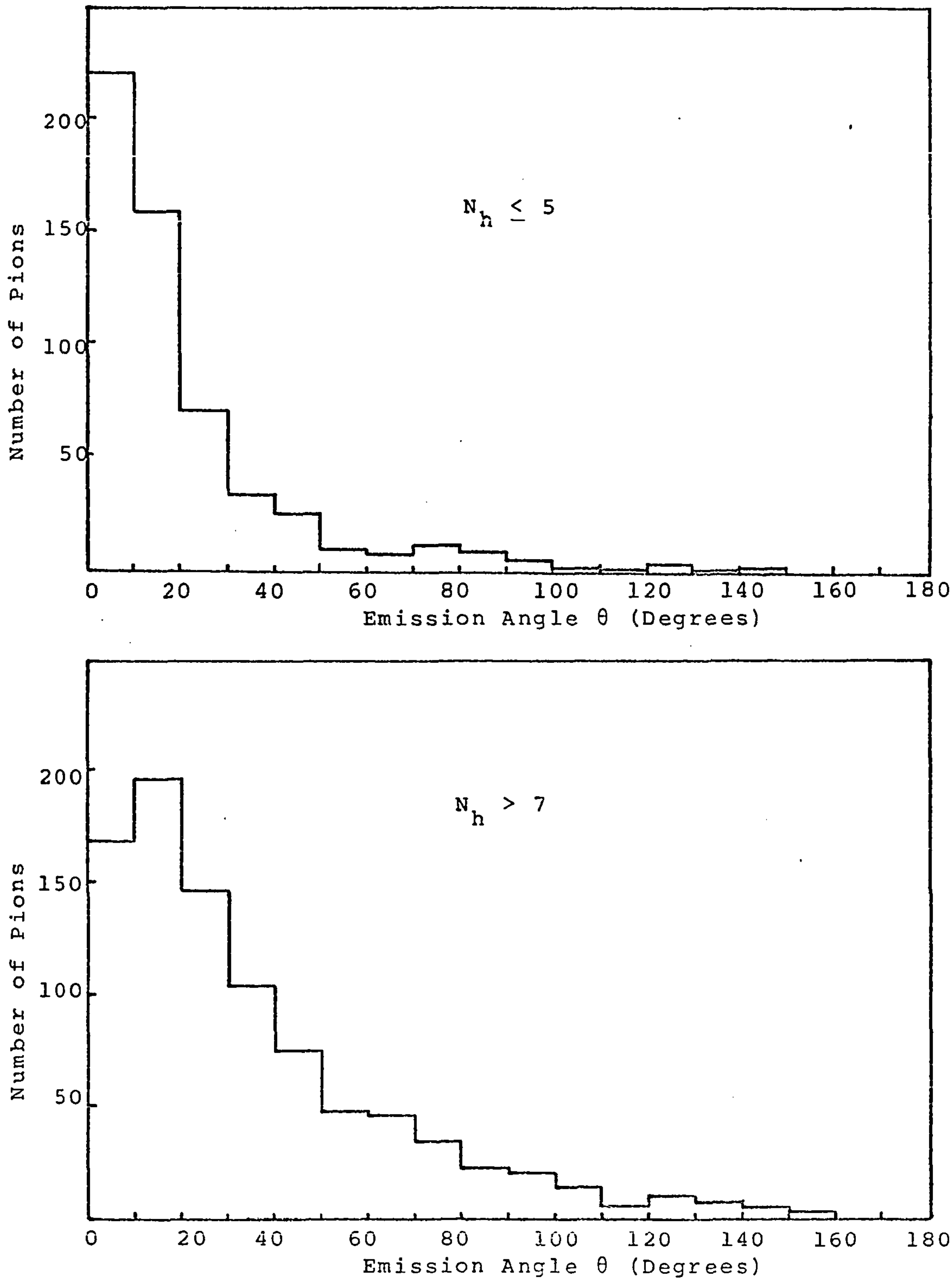

Fig. 8 Angular Distribution of Secondary Pions from 16.2 BeV π-Nucleus Interactions

actions of the shower particles with the nucleons of the target nucleus. Lim(36) states that not all of these shower particles are produced in the first interaction of the primary particle with a nucleon. Jain(50) says that the secondary interactions have two effects: first, they cause the excitation of the nucleus and second, they cause scattering of the secondary particles as they emerge which results in a wider angular distribution.

Transverse Momentum

Figure 9 shows the distribution of transverse momentum for the secondary pions with measured momenta. The most probable value occurs between 100 MeV/c and 200 MeV/c and the distribution has a long tail extending to between 1500 and 2000 MeV/c. These results agree with the transverse momentum distributions found by Lim(36) for 26.7 BeV/c proton-nucleus collisions and by Matsumoto(46) in a survey of high energy nucleon-nucleus interactions. However, the cascade model prediction of the transverse momentum distribution for the shower particles produced in 25 BeV proton-nucleus collisions calculated by Artykov et al.(20) shows a most probable value in the interval (300-400) MeV/c as do the experimental results of Garbowska et al.(39) for the same interaction.

The transverse momentum distribution for the secondary pions from the pion-nucleus interactions at 16.2 BeV

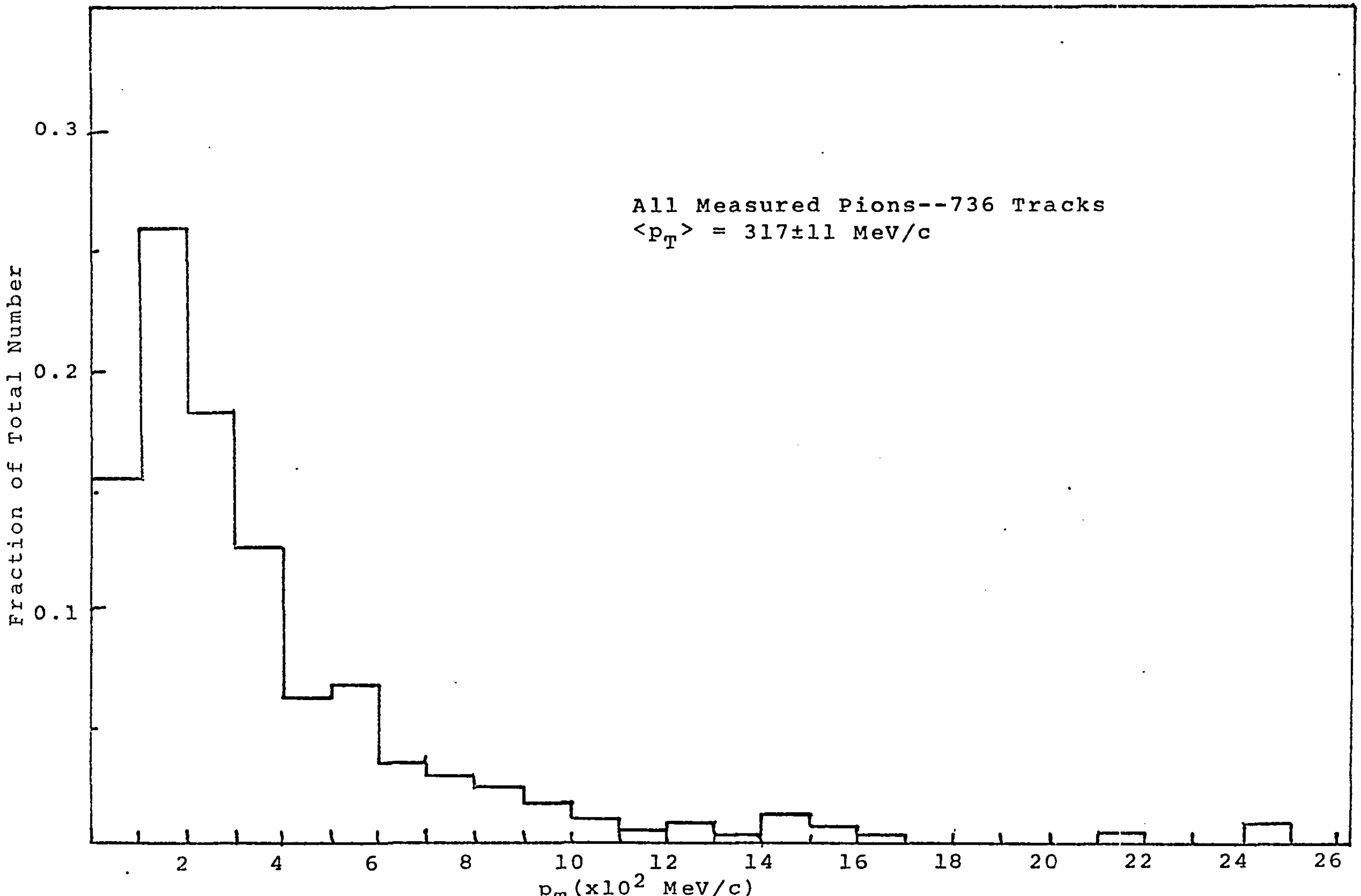

Fig. 9 p_T Distribution for 16.2 BeV π-Nucleus Interactions was also compared with distributions obtained from investigations of pion-nucleon interactions. There was very good agreement with the results of an analysis of pion-nucleon interactions at 16.2 BeV[93]. When compared with other results[77,80,82], reasonably good agreement was found with the results at 16 BeV/c[80] but the p_T distribution at 7.3 BeV/c[77] and 17 BeV/c[82] had peaks which occurred for $p_T >$ 200 MeV/c instead of between (100-200) MeV/c as was observed in the pion-nucleus interactions.

An attempt was made to fit the transverse momentum histogram in Figure 9 with the theoretical p_T distributions discussed in Chapter II. The χ^2 goodness-of-fit test[100] was employed to determine how well each distribution fit the experimental data. Chi-square was determined from the relation:

$$\chi^2 = \sum_{i=1}^{N} \frac{(X_e - X_o)^2}{X_e}$$

where X_e = number of values of p_T in the $i^{\underline{th}}$ interval predicted from the theoretical distribution and X_o = number of values of p_T observed in the $i^{\underline{th}}$ interval. The p_T distribution was divided into N intervals, with the only criterion imposed on each interval being that it had to contain at least a certain number of points X_e. Calculations of χ^2 were made with each $X_e \geq 5$ amd also with $X_e \geq 20$. The two calculations yielded essentially the same results. The number of degrees of freedom ν is given by

$$\nu = N-r$$

where r is the number of independent parameters which are estimated from the data. Table 17 presents a summary of the results of the application of the goodness-of-fit test to the raw p_T data obtained from the pion-nucleus interactions at 16.2 BeV. As indicated in the table, two different methods were used to extimate the parameters p_0 and σ found in the (LD) and (BD), respectively. The first estimates of p_0 and σ used were those given by Friedlander[60] and discussed in Chapter II. The second estimate of p_0 was obtained from the most probable value, $\tilde{p}_T$, of p_T. The second estimate of the parameter σ in the (BD) was given by the experimental standard deviation

$$\sigma = \{<p_T{}^2>-<p_T>^2\}^{\frac{1}{2}}.$$

The results presented here correspond to the minimum value of χ^2 obtained from a series of calculations using each of the p_T distribution functions. As can be seen from the table, none of the p_T distribution functions fit the raw data. The (LD) gives the best value of χ^2, but the fit is extremely poor.

An attempt was also made to fit the p_T distribution functions to the p_T data obtained from the 16.2 BeV pion-nucleon analysis. The goodness-of-fit test was applied to each distribution and the results obtained for the best value of x^2 are given in Table 18. The results were similar

TABLE 17

RESULTS OF GOODNESS-OF-FIT TEST FOR RAW p_T DATA
16.2 BeV PION-NUCLEUS INTERACTIONS

$f_i(p_T)dp_T$	Value of Parameter	Number of Degrees of Freedom	χ^2	Probability that a Random Sample Gives a Worse Fit (%)
$\frac{p_T}{\sigma^2}\exp\left[-\frac{p_T^2}{2\sigma^2}\right]dp_T$ (BD)	$\sigma^2=\frac{1}{2}\langle p_T^2\rangle$	9	186.6	0.0
	$\sigma^2=\langle p_T^2\rangle-\langle p_T\rangle$	9	409.5	0.0
$\frac{y^2}{F_t(a)}\sum_{n=1}^{\infty}(+1)^{n+1}K_1(ny)$ (PD)	kT = 135 BeV	11	82.9	0.0
$\frac{p_T}{p_0^2}\exp\left[-\frac{p_T}{p_0}\right]dp_T$ (LD)	$p_0 = \frac{1}{2}\langle p_T\rangle$	18*	53.4	0.0
	$p_0 = \tilde{p}_T=160$ MeV/c	9	40.4	0.0
$\frac{1-\alpha}{\sigma_1^2}\exp\left[-\frac{p_T^2}{2\sigma_1^2}\right]+\frac{\alpha}{\sigma_2^2}$	$\sigma_1^2 = 353983.0$	18*	2806	0.0
	$\sigma_2^2 = 725665.0$			
$\exp\left[-\frac{p_T^2}{2\sigma_2^2}\right]dp_T$	$\alpha = 0.116$			
$Cp_T^{3/2}\exp\left[-\frac{p_T}{T_0}\right]$	$\frac{1}{T_0} = \frac{5}{2\langle p_T\rangle}$	9	323.7	0.0
	$c = \frac{4}{3\pi}T_0^{-5/2}$			
$\frac{y^2K_1(y)}{a^2K_2(a)}dy$ (KD)	kT = 125 MeV/c	9	105.9	0.0

*Used p_T intervals of 50 MeV/c. All other calculations used 100 MeV/c intervals.

TABLE 18

RESULTS OF GOODNESS-OF-FIT TEST FOR RAW p_T DATA
16.2 BeV PION-NUCLEON INTERACTIONS (93)

$f_i(p_T)dp_T$	Value of Parameter	Number of Degrees of Freedom	χ^2	Probability that a Random Sample Gives a Worse Fit (%)
$\frac{p_T}{\sigma^2}\exp\left[-\frac{p_T^2}{2\sigma^2}\right]dp_T$ (BD)	$\sigma^2 = \frac{1}{2}\langle p_T^2\rangle$	8	456.3	0.0
	$\sigma^2 = \langle p_T^2\rangle - \langle p_T\rangle^2$	8	491.6	0.0
$\frac{y^2}{F_+(a)}\sum_{n=1}^{\infty}(+1)^{n+1}K_1(ny)dy$ (PD)	$kT = 125$ MeV	18*	111.6	0.0
$\frac{p_T}{p_0^2}\exp\left[-\frac{p_T}{p_0}\right]dp_T$ (LD)	$p_0 = \frac{1}{2}\langle p_T\rangle$	11	49.7	0.0
	$p_0 = \tilde{p}_T = 148$ MeV/c	10	48.2	0.0
$\frac{1-\alpha}{\sigma_1^2}\exp\left[-\frac{p_T^2}{2\sigma_1^2}\right]+$	$\sigma_1^2 = 240292.0$			
	$\sigma_2^2 = 492599.0$	9	293.8	0.0
$\frac{\alpha}{2\sigma_2^2}\exp\left[-\frac{p_T^2}{2\sigma_2^2}\right]dp_T$	$\alpha = 0.121$			
$Cp_T^{3/2}\exp\left[-\frac{p_T}{p_0}\right]$	$\frac{1}{T_0} = \frac{5}{2\langle p_T\rangle}$	9	149.0	0.0
	$c = \frac{4}{3\ \pi}T_0^{-5/2}$			
$\frac{y^2K_1(y)}{a^2K_2(a)}dy$ (KD)	$kT = 125$ MeV	11	137.4	0.0

*Used p_T intervals of 50 MeV/c. All other calculations used 100 MeV/c intervals.

to the fit to the pion-nucleus p_T data. All distributions gave a poor fit to the raw p_T data with the linear distribution giving the lowest value of χ^2.

In an effort to obtain a better fit to the p_T histograms from 16.2 BeV pion-nucleus and pion-nucleon interactions, a different approach was tried. Since the higher values of p_T had large experimental errors associated with them (as much as 40-50%), the p_T histogram was cut off at p_T=1200 MeV and the goodness-of-fit test applied again. This time the statistical error in the observed frequency in each p_T interval was considered in the calculation to give the maximum possible value of χ^2. This error is given by

$$\Delta X_0 = \sqrt{X_0}.$$

The results obtained using the pion-nucleus p_T data are shown in Table 19. This time the two linear distributions appear to fit the modified data better than the other distributions. The (LD) which has p_0 evaluated in terms of $\langle p_T \rangle$ gives a better fit to the modified data than the other (LD).

The p_T data from the 16.2 BeV pion-nucleon interactions was also cut off at 1200 MeV/c and the same goodness-of-fit test applied to the modified histogram. Table 20 shows the results of these calculations. Here none of the distributions fit the data well even when the statistical error in X_0 is considered. The two linear distributions gave the

TABLE 19

RESULTS OF GOODNESS OF FIT TEST 16.2 BeV π-Nucleus Events

$f_i(p_T)dp_T$	Value of Parameter	Number of Degrees of Freedom	χ^2	Probability that a Random Sample Gives a Worse Fit (%)
$\frac{p_T}{\sigma^2}\exp\{-\frac{p_T^2}{2\sigma^2}\}dp_T$ (BD)	$\sigma^2=\frac{1}{2}\langle p_T^2\rangle$	9	97.40	0.0
	$\sigma^2=\langle p_T^2\rangle-\langle p_T\rangle^2$	17	268.40	0.0
$\frac{y^2}{F_+(a)}\sum_{n=1}^{\infty}(+1)^{n+1}K_1(ny)dy$ (PD)	kT=135 MeV	10	26.75	0.1
$\frac{p_T}{p_0^2}\exp\{-\frac{p_T}{p_0}\}dp_T$ (LD)	$p_0=\frac{1}{2}\langle p_T\rangle$	8	2.92	89.1
	$p_0=\tilde{p}_T=147$MeV/c	8	3.54	82.9
$\{(\frac{1-\alpha}{\sigma_1^2})\exp\{-\frac{p_T^2}{2\sigma_1^2}\}+(\frac{\alpha}{\sigma_2^2})\exp\{-\frac{p_T^2}{2\sigma_2^2}\}\}$ $\times dp_T$	$\sigma_1^2=51000$ $\sigma_2^2=725665$ $\alpha=0.0523$	8	85.25	0.0
$\frac{y^2K_1(y)}{a^2K_2(a)}dy$ (KD)	kT=125 MeV	9	30.69	0.0
$cp_T^{3/2}\exp\{-\frac{p_T}{T_0}\}$	$\frac{1}{T_0}=\frac{5}{2\langle p_T\rangle}=8.68\times10^{-3}$ $c=\frac{4b^{5/2}}{3\sqrt{\pi}}=7.01\times10^{-6}$	11	153.3	0.0

TABLE 20

RESULTS OF GOODNESS OF FIT TEST 16.2 BeV π-NUCLEON EVENTS

$f_i(p_T)dp_T$	Value of Parameter	Number of Degrees of Freedom	χ^2	Probability That a Random Sample Gives a Worse Fit (%)
$\frac{p_T}{\sigma^2}\exp\{-\frac{p_T^2}{2\sigma^2}\}dp_T$ (BD)	$\sigma^2=\frac{1}{2}\langle p_T^2\rangle$	9	85.14	0.0
	$\sigma^2=\langle p_T^2\rangle-\langle p_T\rangle^2$	5	208.85	0.0
$\frac{y^2}{F_+(a)}\sum_{n=1}^{\infty}(+1)^{n+1}K_1(ny)dy$ (PD)	kT=135 MeV	10	27.46	0.0
$\frac{p_T}{p_0^2}\exp\{-\frac{p_T}{p_0}\}dp_T$ (LD)	$p_0=\frac{1}{2}\langle p_T\rangle$	8	9.36	24.2
	$p_0=\tilde{p}_T=143\text{MeV/c}$	9	9.54	29.4
$\{(\frac{1-\alpha}{\sigma_1^2})\exp\{-\frac{p_T^2}{2\sigma_1^2}\}+(\frac{\alpha}{\sigma_2^2})\exp\{-\frac{p_T^2}{2\sigma_2^2}\}\}dp_T$	$\sigma_1^2=62500$	7	56.87	0.0
	$\sigma_2^2=492599$			
	$\alpha=0.0426$			
$\frac{y^2K_1(y)}{a^2K_2(a)}dy$ (KD)	kT=125 MeV	10	27.69	0.0
$cp_T^{3/2}\exp\{-\frac{p_T}{T_0}\}$	$\frac{1}{T_0}=\frac{5}{2\langle p_T\rangle}$	7	56.87	0.0
	$c=\frac{4}{3\sqrt{\pi}}T_0^{-5/2}$			

"best" fits, although poor ones at that. One possible explanation for this failure to obtain a good fit lies in the calculation of momentum from multiple scattering measurements. If a majority of the values of $p\beta$ have been either over-or underestimated from the calculations, this would bias the p_T data in favor of certain intervals of p_T resulting in large contributions to the value of χ^2.

Other calculations were also made using the p_T data in an attempt to obtain a good fit with one or more of the distribution functions. None of the others were as successful as the ones discussed here. Among these was a calculation of χ^2 taking into account the experimental error in each value of p_T. This was done by assigning each track an equal area in the histogram, and spreading this area uniformly from $(p_T-\Delta p_T)$ to $(p_T+\Delta p_T)$. The only effect that this calculation had on the histogram was to make it somewhat smoother. The goodness-of-fit test gave no better results with the smoothed distribution. Figure 10 shows the smoothed distribution and the regular distribution.

In Figure 11 the different distribution functions are shown fitted to the p_T histogram for the pion-nucleus interactions. The smooth curves represent the best fits of each distribution function to the data as determined from the goondess-of-fit test.

Figure 12 shows the p_T distributions for the groups of light and heavy nucleus events. These distributions were

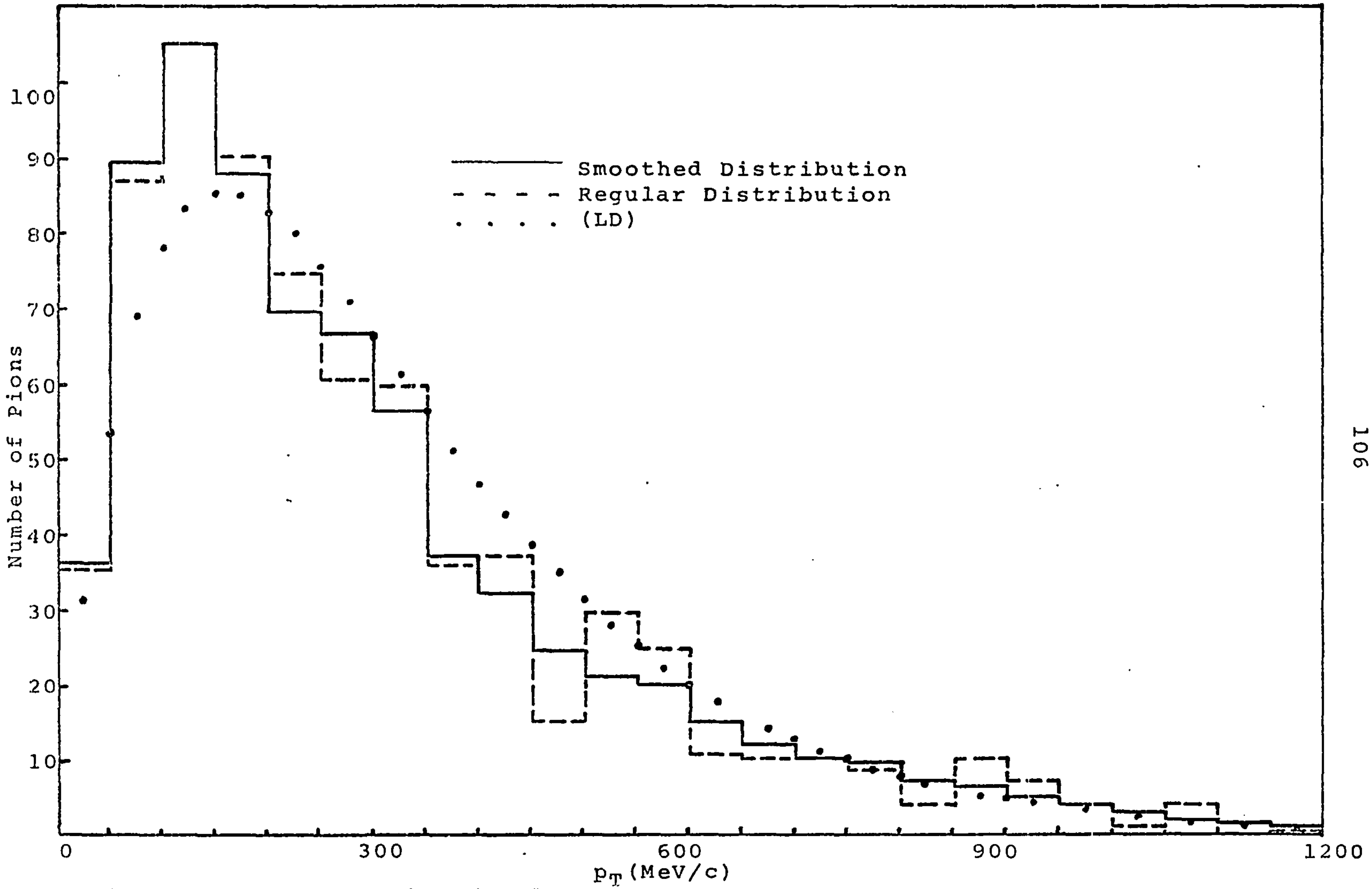

Fig. 10 p_T Distribution for 16.2 BeV π-Nucleus Interactions Obtained Considering Error in Each Value of p_T

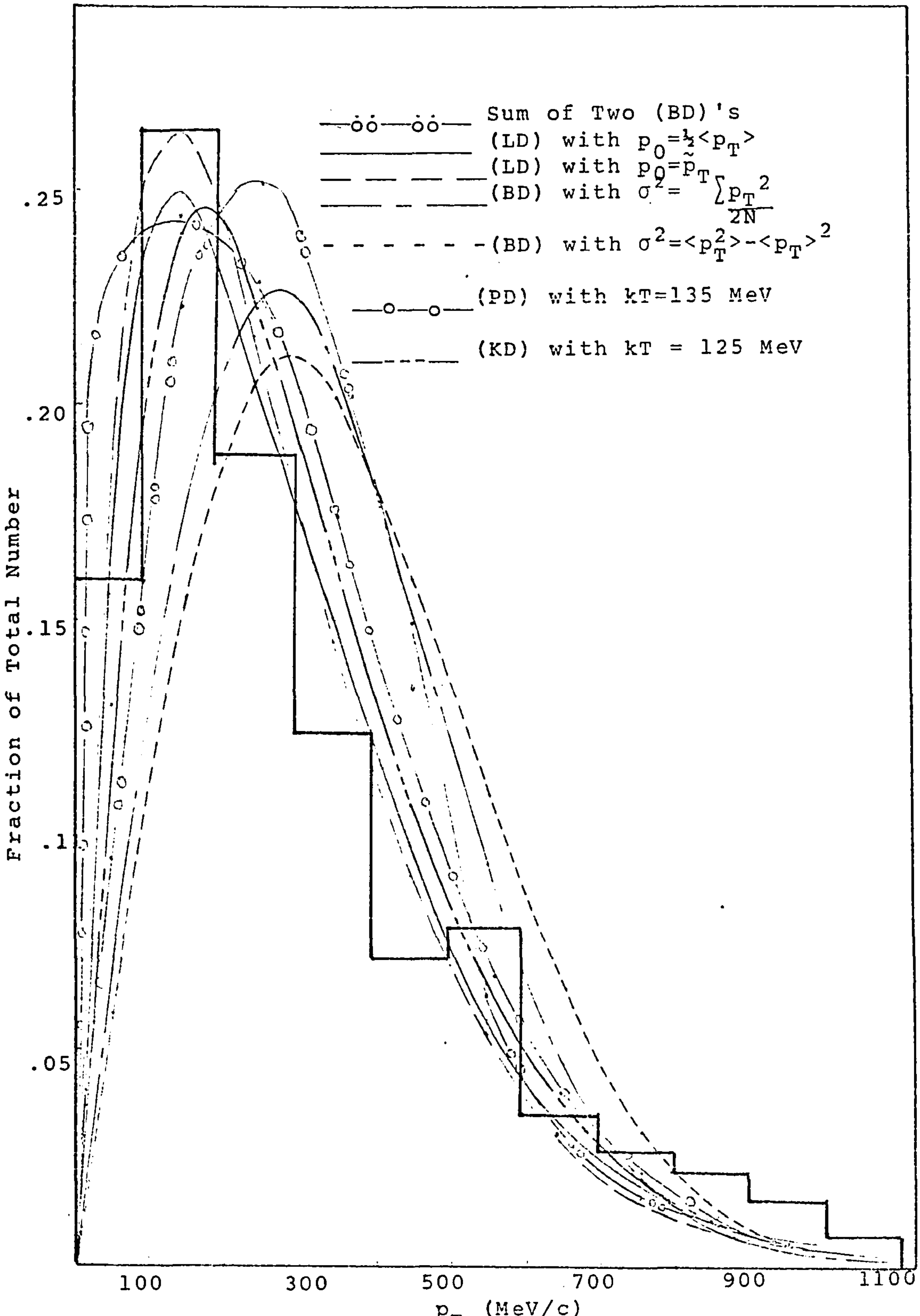

Fig. 11 p_T Distribution with Best Fit p_T Curves for Each Distribution Function

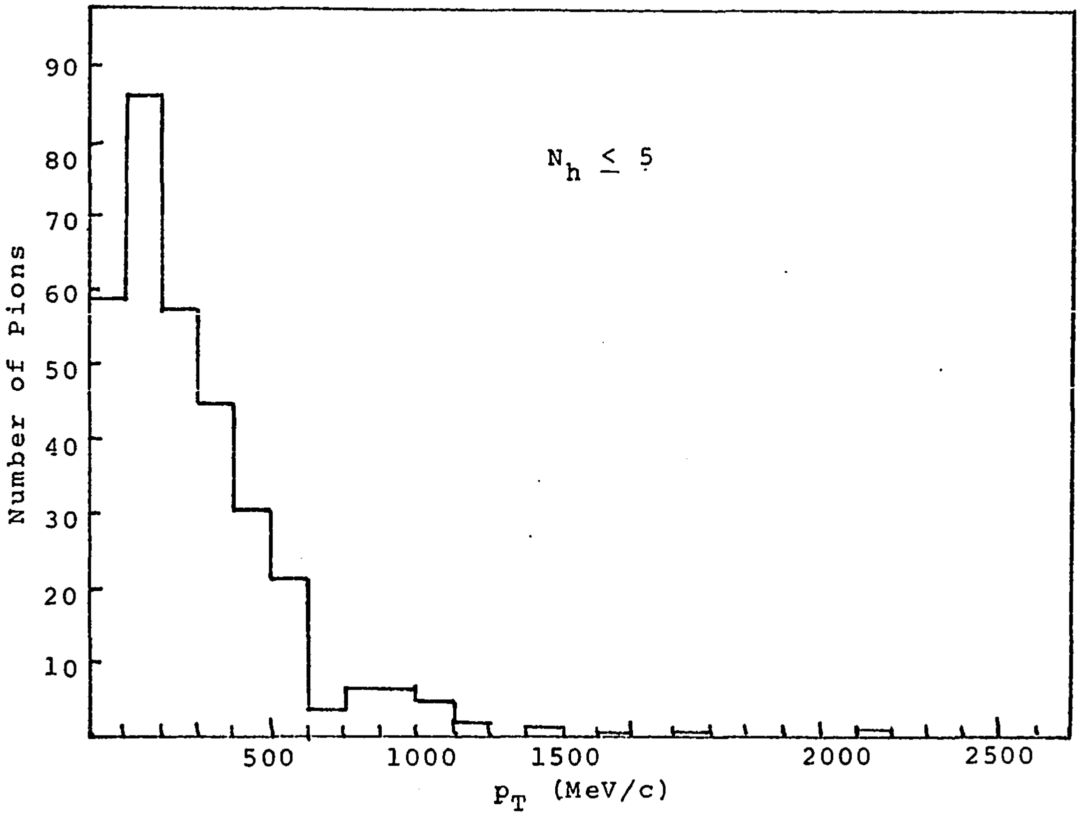

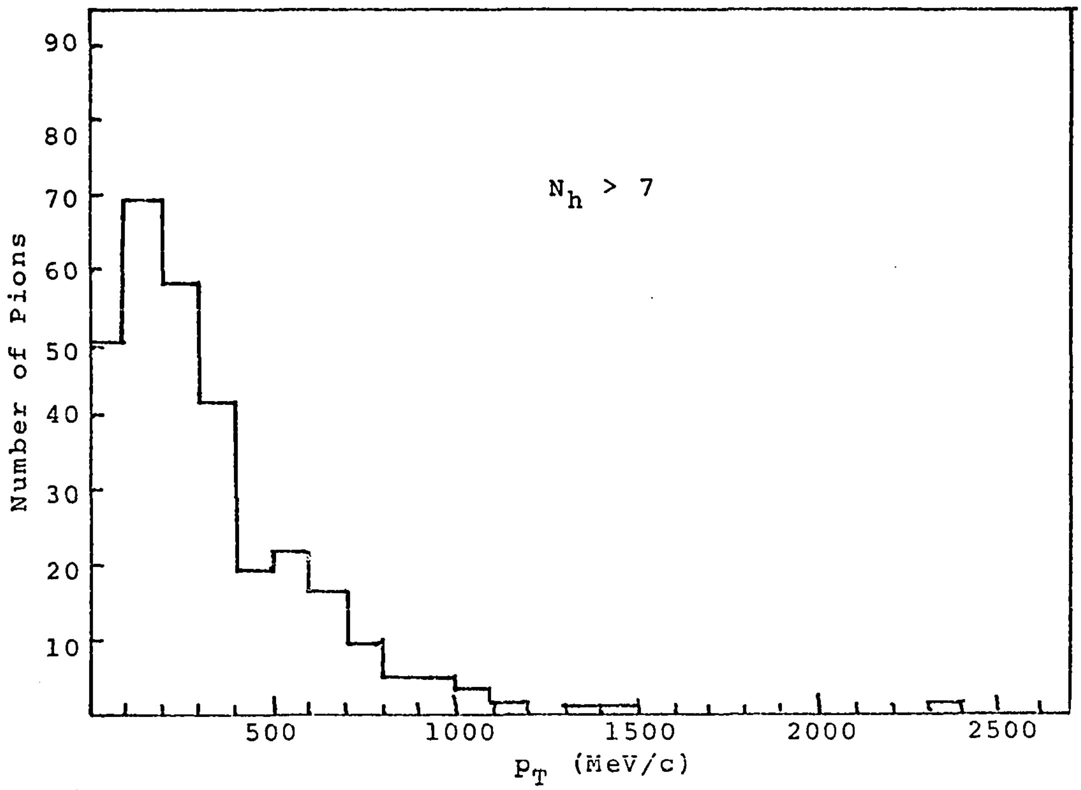

Fig. 12 p_T Distribution for Secondary Pions from 16.2 BeV π-Nucleus Interactions compared with those obtained from other experiments. The distribution from the (C-N-O) events was in good agreement with the results obtained by Kohli *et al.*[41]. However, Kohli's data shows a most probable value of p_T between (200-300) MeV/c in the distribution for (Ag-Br) which disagrees with the value (100-200) MeV/c shown in Figure 12. Disagreement with the cascade model distribution and the experimental data of Artykov *et al.*[20] from 9 BeV proton-nucleus collisions also was found. However, there was good agreement with the cascade model distribution obtained by Artykov *et al.*[4] and the experimental distribution obtained by Hoffman *et al.*[40] from 17 BeV pion-heavy-nucleus interactions. The distributions of Matsumoto[46] also compared favorably with the 16.2 BeV pion-nucleus data.

The secondary pions with measured momenta were divided into groups according to their angle of emission. Figures 13 and 14 show the distributions of transverse momentum for each angular group. It should be noted that the most probable value of p_T does not occur in the interval (100-200) MeV/c only in the case of the two groups with the smallest number of measured pion tracks.

The average transverse momentum of all the secondary pions with measured momenta was determined to be 317±5 MeV/c. The statistical error in $\langle p_T \rangle$ obtained using the relation given in Chapter III was ±10 MeV/c. Taking these two errors to be independent, a value of 317±11 is obtained. Table 21

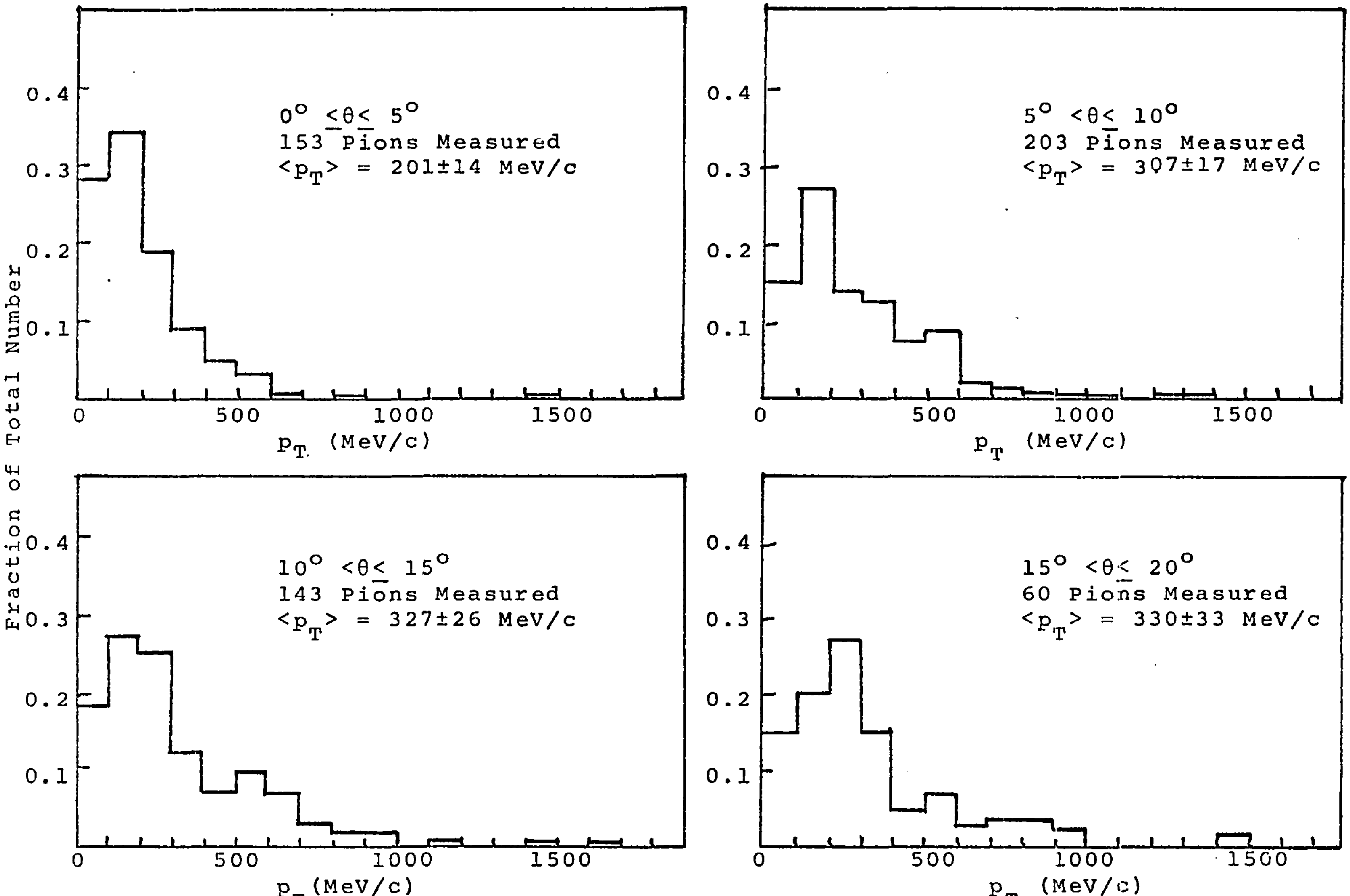

Fig. 13 p_T Distribution for Secondary Pions with Measured $p\beta$

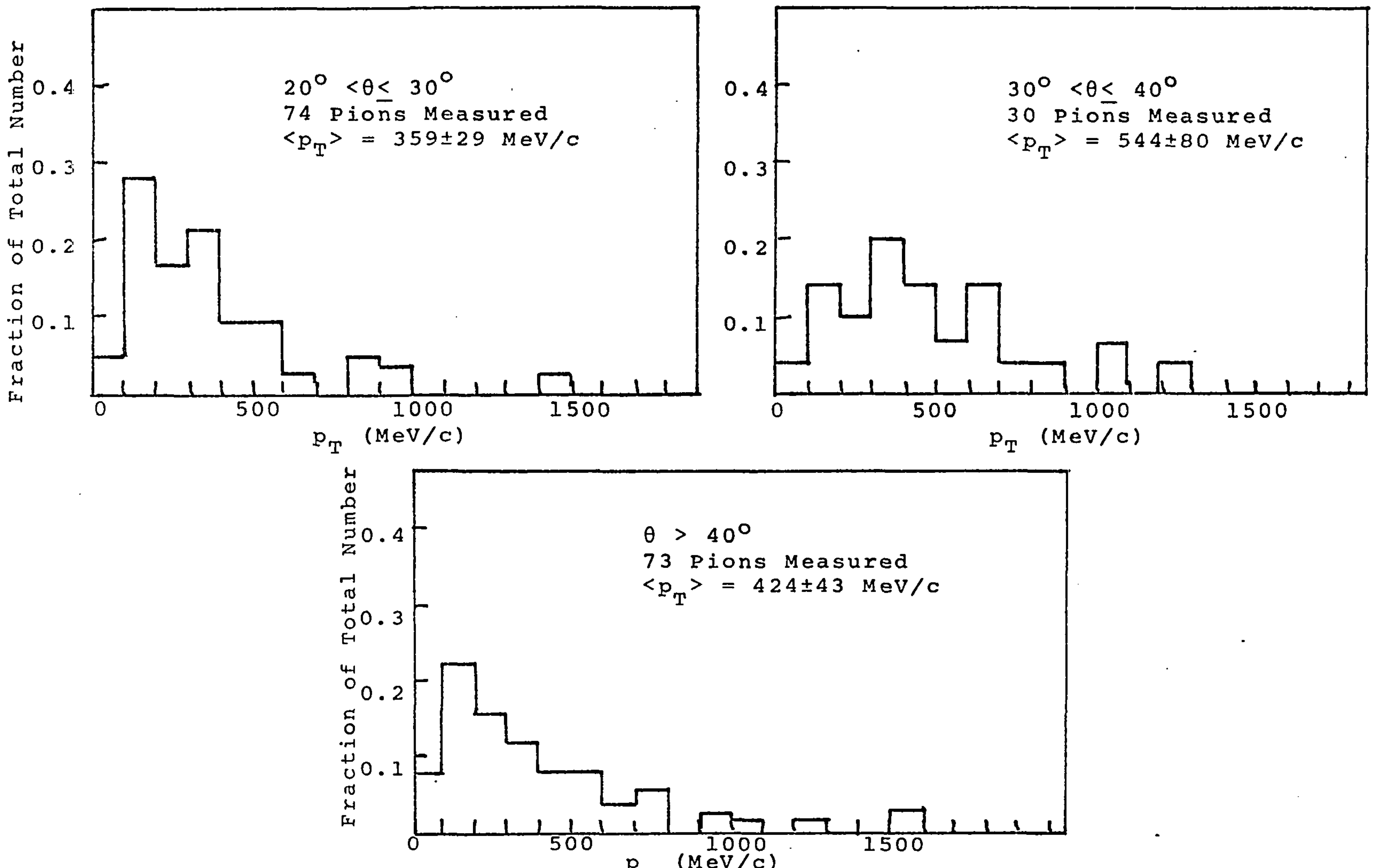

Fig. 14 p_T Distribution for Secondary Pions with Measured $p\beta$

TABLE 21

AVERAGE TRANSVERSE MOMENTUM OF SECONDARY PIONS PRODUCED IN INTERACTIONS OF HIGH ENERGY PARTICLES WITH AVERAGE EMULSION NUCLEI

Primary Particle	$<p_T>$ (MeV/c)	Reference
16.2 BeV π^-	317±11	This experiment
4.5 BeV π^-	290±50	(66)
6.2 BeV p	400±20	Cascade Model (20)
9 BeV p	370±70	(16)
9 BeV p	400±20	Cascade Model (20)
9 BeV p	430±20	Cascade Model (30)
17 BeV p	420±20	Cascade Model (20)
17 BeV p	460±23	Cascade Model (30)
25 BeV p	420±20	Cascade Model (20)
25 BeV p	470±25	Cascade Model (30)

compares this value with values of average transverse momentum obtained from other studies of particle-nucleus interactions. The value of $<p_T>$ from the 16.2 BeV pion-nucleus interactions is in good agreement with previous experimental results, but all of the cascade model predictions are significantly higher. No calculation of $<p_T>$ using the tube model was available for comparison.

$<p_T>$ was also determined for the groups of (C-N-O) and (Ag-Br) events and the results compared with previous results. This is shown in Tables 22 and 23. There is good

TABLE 22

AVERAGE TRANSVERSE MOMENTUM OF SECONDARY PIONS PRODUCED IN INTERACTIONS OF HIGH ENERGY PARTICLES WITH LIGHT (C-N-O) EMULSION NUCLEI

Primary Particle	$\langle p_T \rangle$ (MeV/c)	Reference
16.2 BeV π^-	305±15	This experiment
17.2 BeV π^-	362±52	(41)
9 BeV p	435±25	Cascade Model (30)
25 BeV p	470±30	Cascade Model (30)

TABLE 23

AVERAGE TRANSVERSE MOMENTUM OF SECONDARY PIONS PRODUCED IN INTERACTIONS OF HIGH ENERGY PARTICLES WITH HEAVY (Ag-Br) EMULSION NUCLEI

Primary Particle	$\langle p_T \rangle$ (MeV/c)	Reference
16.2 BeV π^-	340±15	This experiment
17.2 BeV π^-	372±23	(41)
17.2 BeV π^-	390±40	Cascade Model (4)
17 BeV π^-	390±20	(4,40)
9 BeV p	440±25	Cascade Model (30)
25 BeV p	480±20	(39)
25 BeV p	500±10	Cascade Model (20)
25 BeV p	460±23	Cascade Model (30)

agreement between the results from the 16.2 BeV pion-nucleus interactions and those obtained from an experimental study of 17.2 BeV pion-nucleus interactions[41]. Within error, the cascade model calculations for 17.2 BeV π^--nucleus interactions also agree with the results of this analysis. However, the rest of the experimental and theoretical values are all significantly higher. The differences between the value of $<p_T>$ for the secondary pions from the 16.2 BeV pion-nucleus interactions and the values of $<p_T>$ from the several proton-nucleus interaction analyses could be explained by a dependence of $<p_T>$ on the mass of the primary particle. As was mentioned earlier, one should not expect the characteristics of pion-nucleus and proton-nucleus interactions to be the same. The interaction mechanisms may be entirely different for the two types of interactions.

The value of $<p_T>$ obtained for the secondary pions from the 16.2 BeV pion-nucleus interactions was compared with the corresponding $<p_T>$ from the analysis of 16.2 BeV pion-nucleon collisions[93]. With ±6 MeV/c interval error and a statistical error of ±13 MeV/c, one gets 288±14 MeV/c for the pion-nucleon interactions. Table 6 of Chapter II gives some representative values of $<p_T>$ which have been found from other studies of pion-nucleon interactions. The value of $<p_T>$ from the pion-nucleus events lies approximately in the middle of the range of values of $<p_T>$ from the pion-nucleon interactions.

Figure 15 shows the dependence of $<p_T>$ on the number of secondary pions per event in the 16.2 BeV pion-nucleus

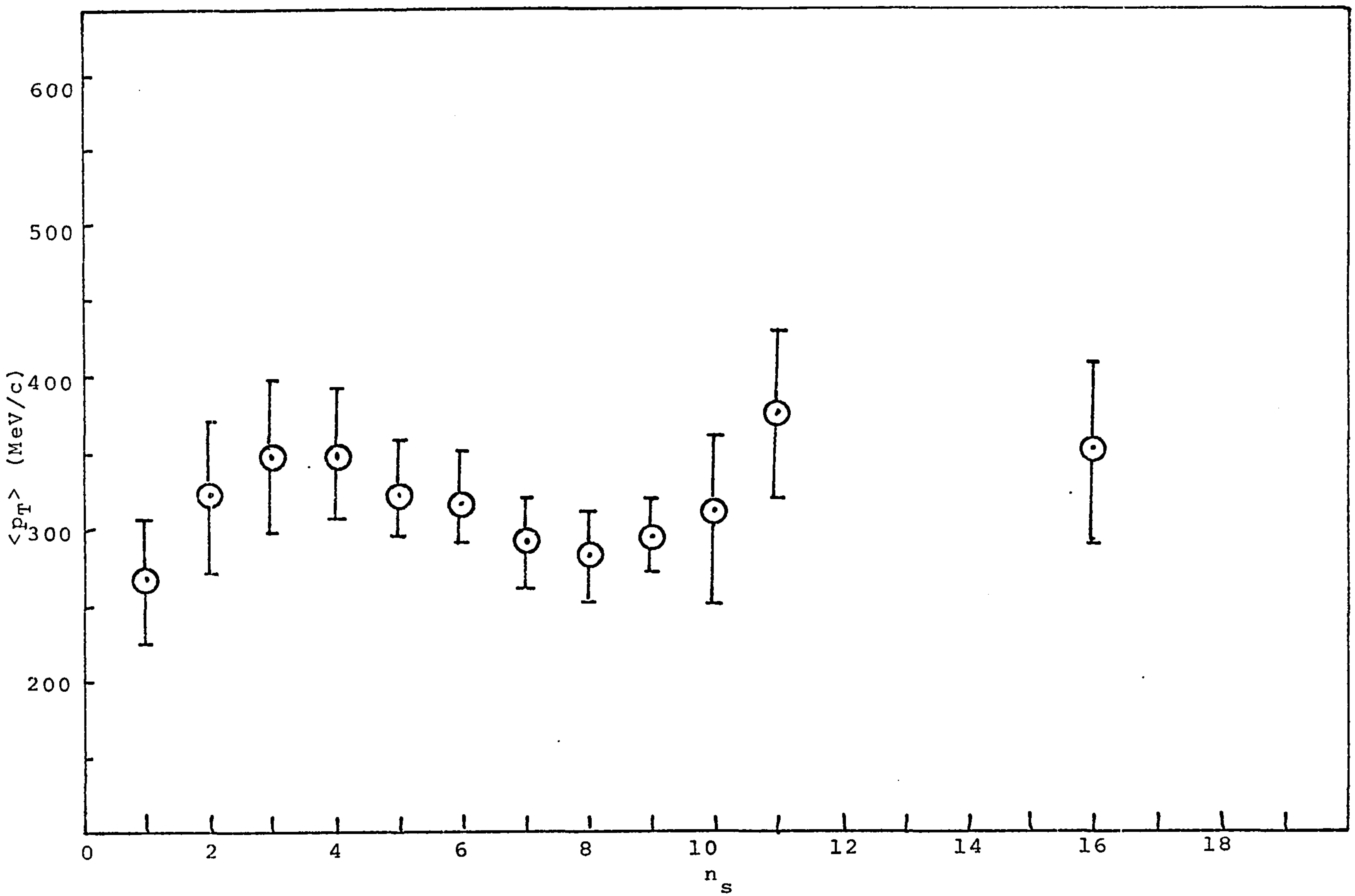

Fig. 15 $\langle p_T \rangle$ As a Function of n_s for 16.2 BeV π-Nucleus Interactions

interactions. This plot shows an almost uniformly oscillating behavior of $<p_T>$ with increasing n_s. This behavior has not been observed before. Previous results have shown indications that $<p_T>$ is independent of n_s. No reason is apparent for this strange behavior of $<p_T>$.

Figure 16 shows the dependence on the emission angle of $<p_T>$ for all the measured pions from the pion-nucleus events. It should be noted that the high value of $<p_T>$ obtained for the angular interval 30^o-40^o was determined using the measured momenta of only 30 pions. This is less than half the number used to calculate $<p_T>$ for the interval with the second smallest number of measured pions. Disregarding the four tracks with the highest values of p_T in the 30^o-40^o interval, the value of $<p_T>$ is reduced to 406±81 MeV/c. From this graph, $<p_T>$ increases rapidly with θ until θ reaches a value between 10^o-15^o. Beyond this region, the behavior of $<p_T>$ is somewhat uncertain, since poor statistics obscure the actual behavior.

The dependence of $<p_T>$ on θ for the (C-N-O) and the (Ag-Br) events is shown in Figure 17. Once again poor statistics prevent a determination of the behavior of $<p_T>$ for $\theta>30^o$ in the (Ag-Br) group. However, in the case of the (C-N-O) events, $<p_T>$ apparently increases with θ, although the rate of increase is small for $\theta>20^o$.

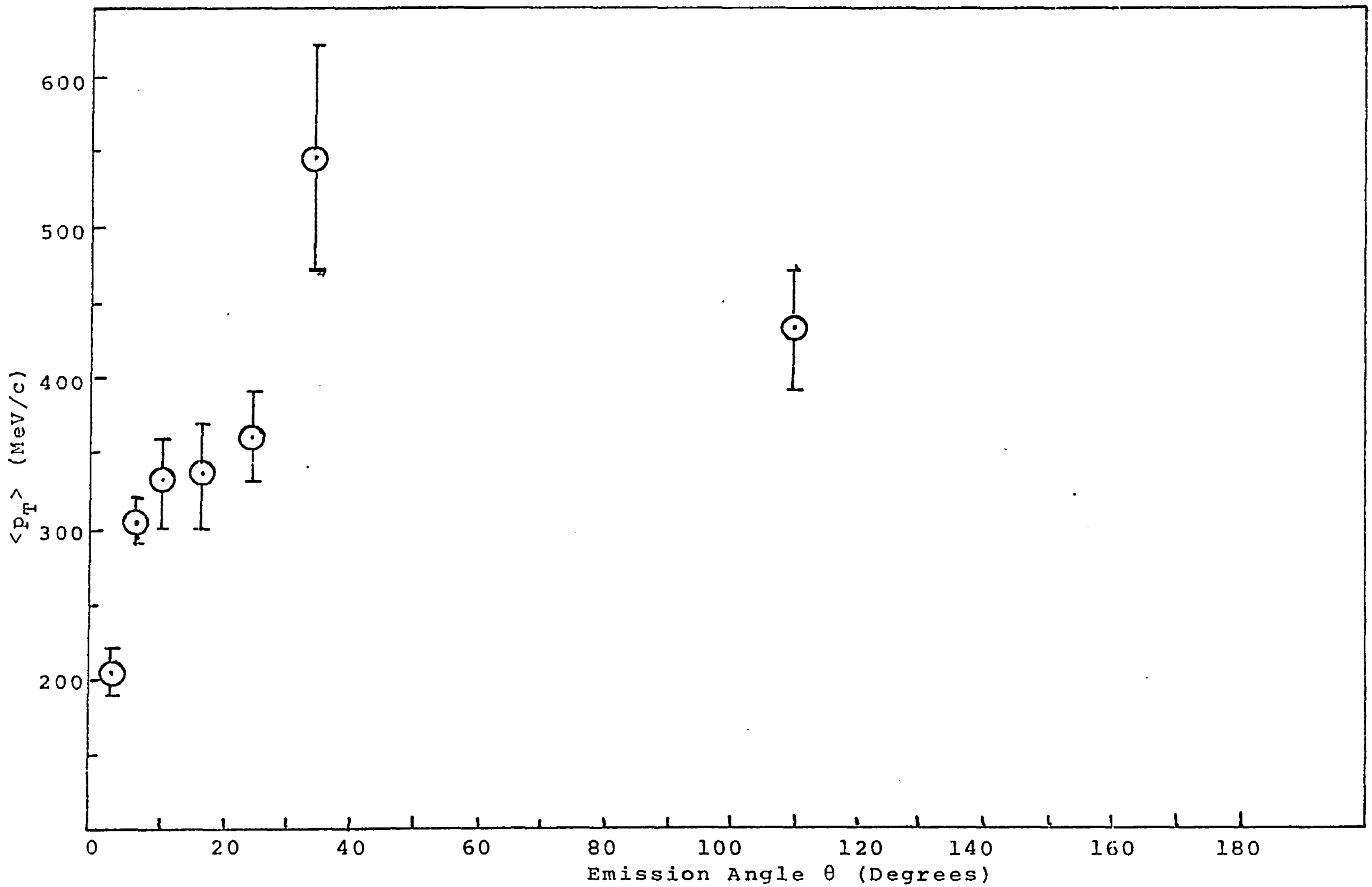

Fig. 16 $\langle p_T \rangle$ as a Function of Emission Angle θ for all Secondary Pions from 16.2 BeV π-Nucleus Interactions

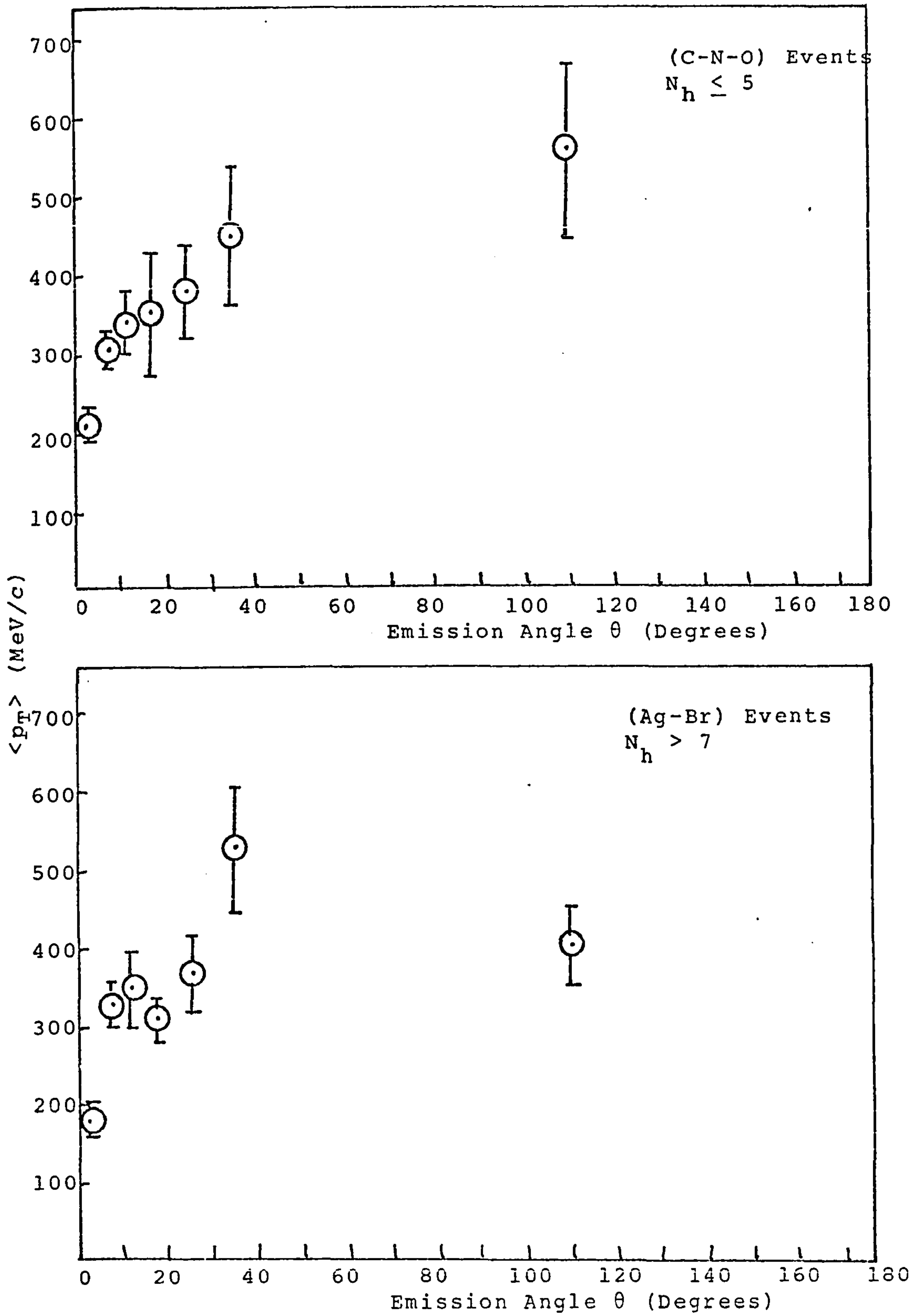

Fig. 17 $\langle p_T \rangle$ as a Function of θ for (C-N-O) and)Ag-Br) Events

Inelasticity

The fraction of the energy transferred in the laboratory system to secondary pions can be determined from the average multiplicity for charged pions and the average total energy of the pions. If $\langle n_s \rangle$ is the average charged pion multiplicity and $\langle W_\pi \rangle$ is the average total energy, the total energy transferred in pion production is given by

$$W_{tot} = 3/2 \langle n_s \rangle \langle W_\pi \rangle .$$

Here it has been assumed that one neutral pion is produced for every two charged pions, and that the neutral pions have the same energy distribution as the charged pions. The inelasticity for pion production can then be calculated from

$$K = \frac{W_{tot}}{E_0}$$

where E_0 is the energy of the primary pion.

The average total energy of the charged pions produced in the 16.2 BeV pion-nucleus interactions was determined to be 1.25 BeV. This resulted in an inelasticity $K = 0.62 \pm 0.02$ for pion production.

Similar calculations were also made using the data obtained from the analysis of 16.2 BeV pion-nucleon interactions(93). From an average total energy for charged secondary pions of 2.01 BeV, the value $K = 0.65 \pm 0.02$ was obtained.

The inelasticity for pion production calculated for 27 BeV proton-nucleus interactions(35) was 0.6. For 9 BeV proton-nucleus interactions the values 0.45±0.15[44], 0.33±0.09[101], and 0.33<K<0.44[16] were obtained. In analyzing 7.3 pion-nucleon interactions, Friedlander et al.[76] determined that K = 0.74±0.08.

Number of Collisions in Average Nucleus

The average multiplicities for charged pions and the average pion energies from both the 16.2 BeV pion-nucleus and pion-nucleon interactions were used to estimate the average number of collisions an incident pion undergoes in an emulsion nucleus. This calculation was performed in the following way: the initial collision was assumed to be a pion-nucleon collision at 16.2 BeV. The average multiplicity for all pions was determined from that for charged pions assuming that one neutral pion was produced for every two charged pions. Each pion produced was assumed to have an energy equal to the average energy observed for the charged pions. Next one of these secondary pions, which could possibly be the incident pion from the initial interaction, was assumed to collide with another nucleon of the nucleus. From the average charged pion multiplicities observed in pion-nucleon interactions given in the review by Barashenkov et al.[96], charge independence, and conservation of energy, the average energy of the secondary pions produced in the second collision was determined. These results were then combined with the results of the first collision to give a new pion multiplicity and average pion energy. This procedure was repeated until either the number of particles exceeded the average pion multiplicity or the pion energy exceeded the average pion energy from the 16.2 BeV pion-nucleus interactions. It was determined that on the average, an incident pion undergoes approximately two collisions in an emulsion nucleus.

Search for Multipion Resonances

All possible combinations of the measured secondary pions from each of the pion-nucleus events which contained at least two measured pion tracks were taken to calculate invariant masses. The invariant masses were calculated for two different groups: two-pions and three-pions. The resulting distributions are shown in Figures 18 and 19. These distributions involve events which have a total number of secondary particles ranging from two to about fifty. Since phase space curves are not available at the present time for final states of more than six particles (due to the complexity of the calculations involved[93]), no curves have been shown on the histograms in these figures. According to Samimi[102] in a discussion of phase-space calculations for n-particle final states, the distribution in phase space should be smooth with a maximum occurring at a low value of invariant mass. This should lie at a position which is of the order to a few times the minimum value of the invariant mass. Additional peaks which may appear in

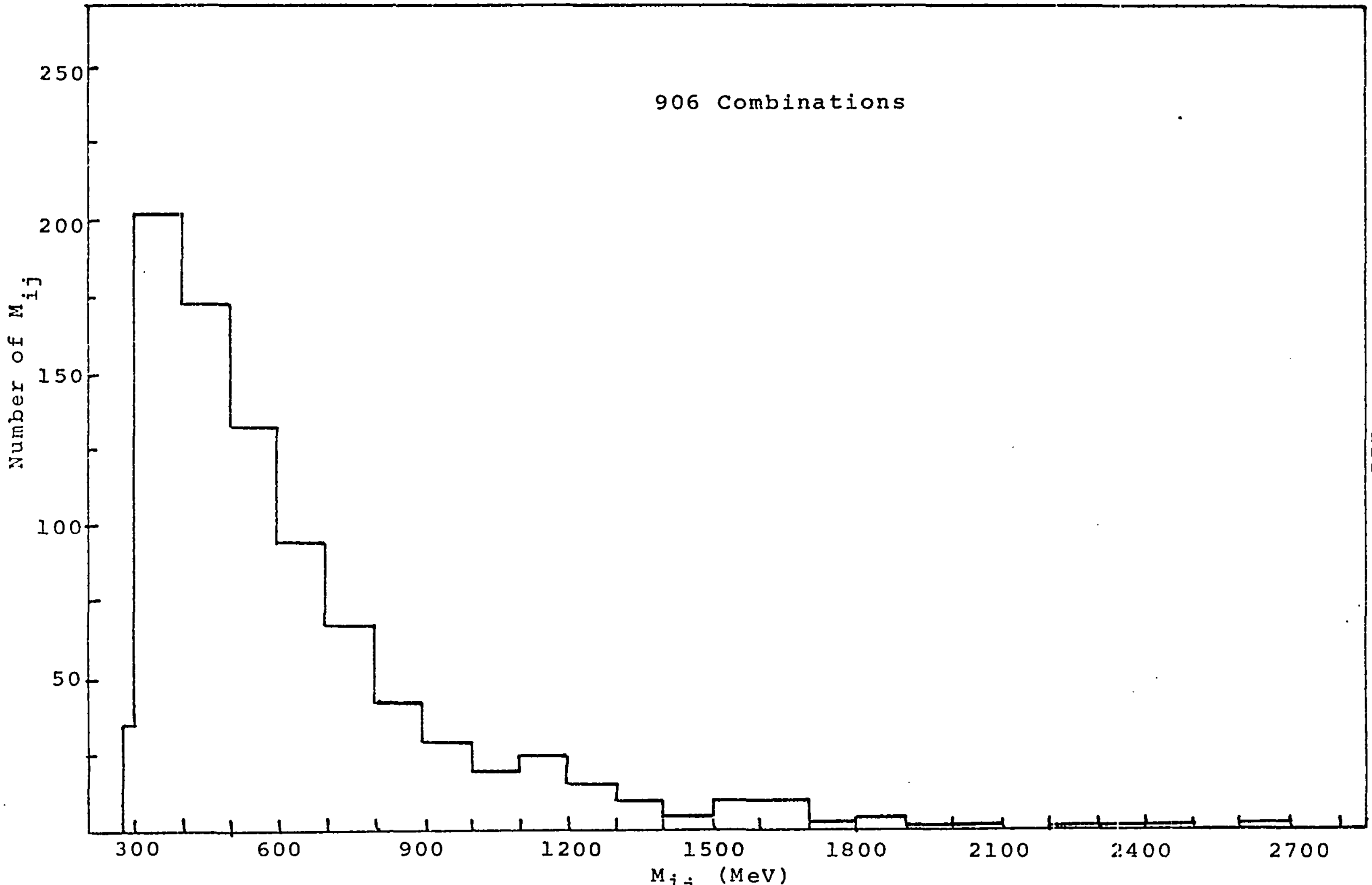

Fig. 18 π-π Correlation Histogram for 16.2 BeV π-Nucleus

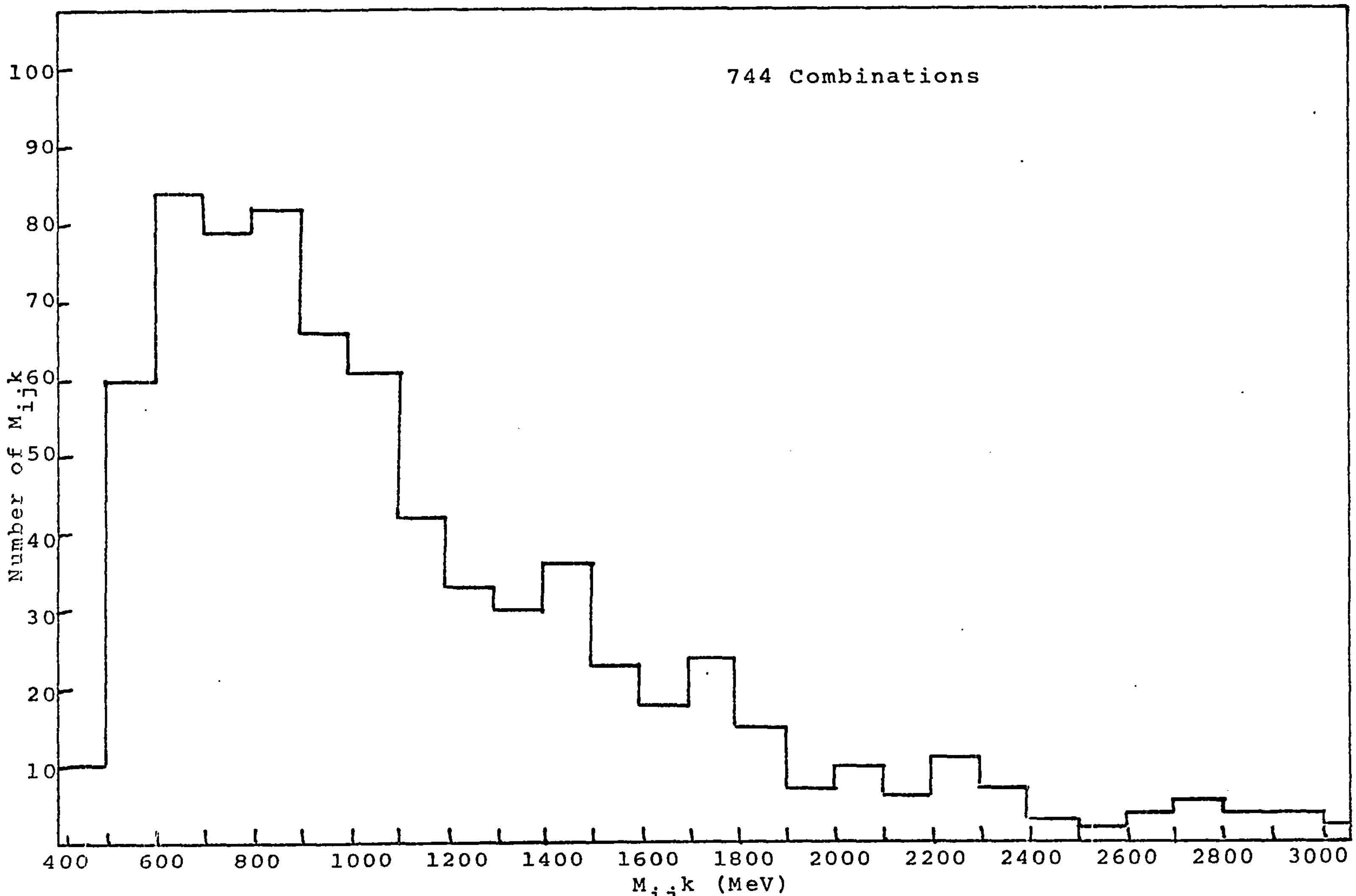

Fig. 19 π-π-π Correlation Histogram for 16.2 BeV π-Nucleus Interactions

the invariant mass distribution indicate the presence of resonant states. The invariant mass distributions in Figures 18 and 19 apparently exhibit none of these secondary peaks. This implies that multipion resonances may be relatively absent in the pion-nucleus interaction.

CHAPTER V

DISCUSSION OF RESULTS AND CONCLUSIONS

About one-half of the nucleons in a nucleus are "screened" out by other nucleons in a high energy collision. This screening results in the observed average cross-section per nucleon being lower than the cross-section which would be observed if the nucleons were in a free state. The fact that the observed pion-nucleon cross-section is smaller than the geometrical cross-section can be attributed to a transparency of the nucleon.

Various selection criteria were employed to separate (C-N-O) events from (Ag-Br) events. However, the angular distributions, the transverse momentum distributions, and the average transverse momentum for each method were almost the same for each group of events. Only one difference was noticeable, that being the average multiplicities of the secondary pions. Here Methods V and VI gave results which differed somewhat from those obtained using the other four criteria. Examination of Tables 13 and 14 in Chapter IV shows that $\langle n_s \rangle$ for Method V in the (C-N-O) group is significantly higher than the other values listed for the 16.2

BeV pion-nucleus interactions. This same behavior is exhibited by Method V in the (Ag-Br) events. It can be explained by the dependence of $<n_s>$ on N_h shown in Figure 4 in Chapter IV. Since the (C-N-O) group, according to Method V, contains all events with $N_h \leq 8$, one would expect the pion multiplicity to be somewhat higher than in the method which contains the next smallest number of heavy tracks--in this case the group with $N_h \leq 7$. On the other hand, the (Ag-Br) group, using Method V includes only events with $N_h > 8$. Since the smallest number of heavy tracks in any one event in this group is 9, one would expect the average multiplicity to be larger than the other methods. This is indeed the case. Method I classifies only events with $1 < N_h \leq 4$ as (C-N-O) events. Therefore, it includes only the events which have the lowest multiplicities of the six criteria. As a result $<n_s>$ is the smallest for Method I in the (C-N-O) group. Since events with $N_h = 6$ and $N_h = 7$ are included in Method VI in the (Ag-Br) group, the value of $<n_s>$ is the smallest for Method VI.

The events which were classified as (C-N-O) events actually contain interactions involving both light and heavy emulsion nuclei. At present, no reliable method exists which enables this group to be further separated according to the size of the target nucleus. Those methods which were discussed in Chapter IV are admittedly inaccurate.

As far as any one of the six selection criteria used in this analysis being preferred over the others, the similar results which each method yielded make this decision very difficult. Since the only real difference exhibited by the six methods occurred in the average pion multiplicities, it is necessary to examine the results given in Tables 13 and 14. From Table 13, only Method V shows agreement with previous experimental results. The other five criteria have values of $\langle n_s \rangle$ which are generally lower than the values found by other authors. This is somewhat surprising because the contamination of the (C-N-O) events by some events which actually involve (Ag-Br) nuclei should lead to higher multiplicities. Because of this, it can be concluded that the six selection criteria used in this analysis do not show enough differences in the observed characteristics to justify one being chosen as more acceptable than the others. All appear to be equally good methods of separating (C-N-O) and (Ag-Br) events.

The average pion multiplicity from the 16.2 BeV pion-nucleus interactions is significantly higher than those observed in high energy pion-nucleon interactions. This indicates that the pion-nucleus interactions should not be treated as a single collision between the incident pion and a nucleon of the target nucleus. The value of $\langle N_h \rangle$ was observed to increase linearly with n_s. However $\langle n_s \rangle$ increased more slowly with N_h. This latter observation is additional support for not treating pion-nucleus interactions as single pion-nucleon collisions which result in the creation of all the secondary particles. It was determined that, on the average, an incident pion undergoes approximately two collisions within an emulsion nucleus.

Figure 7, which shows the behavior of $<N_h>$ as a function of n_s for both the (C-N-O) and the (Ag-Br) events, can serve as a means of comparing the six selection criteria with those used by others. The plot for the (C-N-O) events shows that $<N_h>$ is a constant for this group. This behavior is an indication of the energy transferred to the target nucleus as was mentioned in Chapter IV. The constancy of $<N_h>$ for increasing n_s in the light nucleus events is expected and the results shown in Figure 7 also agree with previous results, e.g. Kohli et al.[41], show larger fluctuations in $<N_h>$ for increasing n_s than was observed in this experiment. Therefore, it can be concluded that the selection criteria used in this analysis were at least as good as the other methods which have been used to separate light and heavy nucleus events in emulsion.

None of the different transverse momentum distributions which were discussed in Chapter II gave a good fit to the raw p_T data from the 16.2 BeV pion-nucleus and pion-nucleon interactions. After using a cut-off at p_T>1200 MeV/c and considering the statistical error in observed frequencies, the linear distribution with the unbiased estimate for the parameter p_0 gave the best fit to the pion-nucleus p_T data. Although the (LD) also gave the best fit to the p_T data with cut-off from the pion-nucleon events, this fit was still fairly poor.

Since Friedlander[60] and Ho[103] have shown that the Boltzmann distribution (BD) is the only p_T distribution compatible with the assumption of axial symmetry and statistical independence of p_y and p_z, an attempt must be made to explain the discrepancy between this claim and the results of this experiment. In order to do this, the two assumptions underlying their results were examined directly using the data from the 16.2 pion-nucleus and pion-nucleon interactions.

Here a difference in notation should be noted. Since Friedlander[60] and Ho[103] designate the incident pion direction to be along the z-axis, p_x and p_y in their co-ordinate system denote the momentum components in a plane perpendicular to the incident pion direction. In this analysis the direction of the incident pion will be taken to be along the x-axis. This means that now p_y and p_z are the components of momentum in the plane perpendicular to the incident pion direction.

First p_y and p_z were determined from the projected angle ϕ, the dip angle δ, and the momentum p for each measured pion track:

$$p_y = p \sin \phi \cos \delta,$$

and $$p_z = p \sin \delta.$$

After these quantities were determined, it was possible to check the assumption of axial symmetry. Define the angle ψ as that angle which the projection of p_T on a plane perpendicular to the direction of the incident pion (x-axis) makes with p_z. Then ψ is given by

$$\tan \psi = \frac{p_y}{p_z}.$$

Using the p_T data, plots were made of p_y versus p_z for the two types of interactions. The graph from the pion-nucleus interactions showed a definite tendency for points to fall near the $p_z = 0$ axis, expecially in the region $p_z > 0$. The points on the graph for the pion-nucleon interactions were distributed more evenly, although there were several clusters of points along the p_y and p_z axes. Figure 20 shows the axial angular distribution for the secondary pions from the pion-nucleus interactions. According to Ho[(103)], an axially symmetric distribution is one whose distribution function does not change under rotation of the aximuth angle ψ about the z-axis. This implies that an axially symmetric ψ-distribution should show no peaks. Such is not the case in Figure 20. Therefore, the p_T data from the 16.2 BeV pion-nucleus experiment violates the assumption of axial symmetry. A similar result was obtained for the p_T data from the 16.2 BeV pion-nucleon interactions. Therefore, one would not expect the (BD) to fit the p_T histograms.

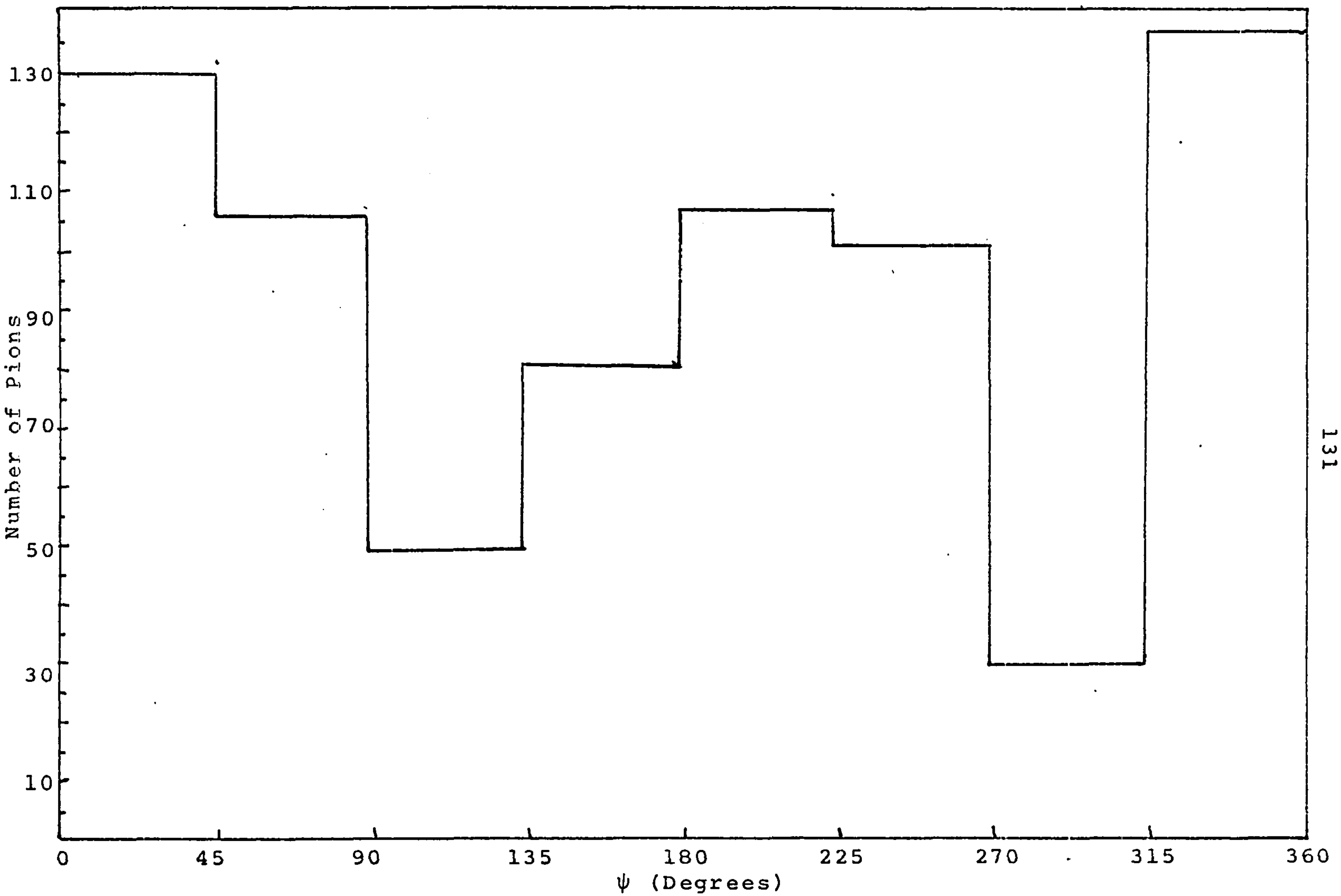

Fig. 20 Axial Distribution of Secondary Pions from 16.2 BeV π-Nucleus Interactions

The average value of transverse momentum of the secondary pions produced in the 16.2 BeV pion-nucleus interactions was 317±11 MeV/c. This value is in agreement with previous results, particularly, the global survey reported by Imaeda and Avidan(58). The behavior of $\langle p_T \rangle$ as a function of n_s is somewhat difficult to determine from Figure 15. Although, it would be possible to interpret $\langle p_T \rangle$ as being independent of n_s, nevertheless, the oscillations of $\langle p_T \rangle$ with increasing n_s are almost too regular to ignore. Considering Figure 16, poor statistics prevent any definite conclusion being made about the dependence of $\langle p_T \rangle$ on the emission angle θ. $\langle p_T \rangle$ does appear to increase with θ up to about $\theta \simeq 20^o$-30^o, the rate of increase being slower for $\theta > 15^o$. The same observations hold true for the behavior of $\langle p_T \rangle$ from the (Ag-Br) events in Figure 17. However, in the case of the (C-N-O) events, $\langle p_T \rangle$ does exhibit a dependence on θ. It increases with θ until $\theta \simeq 15^o$, then the curve begins to gradually decrease in slope. Although indications have been found that $\langle p_T \rangle$ is independent of n_s and θ, the results of this experiment do not agree with previous observations. The difference in the θ dependence can possibly be explained by poor statistics, but no reason can be given for the oscillating behavior of $\langle p_T \rangle$ with n_s.

Finally, the problem remains as to whether or not the results obtained in this analysis of pion-nucleus interactions can be explained by either of the two theoretical models: the tube model, or the cascade model. The average multiplicities were in good agreement with the cascade model. Since the tube model predictions covered such a wide range of values due to the different values of the proportionality constant in the expression for $<n_s>$, this reduces the significance of the results. The angular distributions were similar to the Monte Carlo calculations made using the cascade model. However, the ratio of the average multiplicity from the (Ag-Br) events to that of the (C-N-O) events gave reasonable agreement with the tube model predictions but differed significantly from those of the cascade model. The transverse momentum distributions did not agree with the only cascade model calculations available--those performed for 9 BeV proton-nucleus interactions[17]. The distribution function, the (PD), for transverse momentum derived from the hydrodynamical theory, which forms the basis for the tube model, did not give the best fit to the experimental p_T distribution. By its very nature, the cascade model must include the assumption of a particular model of multiple meson production. The only available calculations [17,20,29,30] of transverse momentum made using the cascade model do not indicate which transverse momentum distribution function best describes the results. Because of this, no comparison can be made between the p_T distribution function which was the best fit to the data obtained in this experiment (LD) and a corresponding function from the cascade model.

According to Matsumoto[46], the cascade model should not be able to explain the similarities between nucleon-nucleon p_T distributions and nucleon-nucleus p_T distributions. This statement should also apply to any similarities between p_T distributions from pion-nucleus and pion-nucleon interactions. As stated before, the cascade model consists of a series of high energy collisions between pions and the nucleons of the nucleus, initiated by a pion-nucleon interaction. If many similarities between the observed characteristics of pion-nucleus and pion-nucleon interactions occur, this could possibly mean that a pion-nucleus collision is a combination of two interaction mechanisms. It may consist of a pion-nucleon mechanism combined with either the cascade or the tube mechanism. If the contribution of the cascade or the tube mechanism were small, then the pion-nucleon part would dominate and the observed results would be similar to those of pion-nucleon interactions.

As a whole, the observed results seem to agree with the cascade model. However, it is possible, as was discussed in Chapter II, that the characteristics of the secondary particles produced in high energy particle-nucleus collisions may not be sensitive to the type of interaction mechanism which produced them. In addition, a scarcity of available analytical calculations (such as the Monte Carlo calculations using the cascade model) which use the tube model prevented a fair and direct comparison of the two models with some of the observed characteristics. For these reasons, one cannot conclude that either the tube model or the cascade model is the one which best describes the pion-nucleus interactions at 16.2 BeV.

APPENDIX A

DATA

TABLE 24

DATA

EVENT	TRK	P(MEV)	ϕ(°)	δ(°)	θ(°)
150060	1		25.9±0.1	35.2± 0.2	42.7± 0.2
150078	1	18316±7573	-0.2±0.1	1.2± 0.4	1.2± 0.4
150079	1	1216± 159	26.2±0.1	-2.4± 0.4	26.3± 0.1
150152	1	1478± 374	-0.9±0.1	5.1± 0.4	5.2± 0.4
150179	1		-35.9±0.1	-24.0± 0.4	42.3± 0.2
300194	2	9068±1770	-1.8±0.1	2.5± 0.4	3.1± 0.3
300216	1	1564± 143	-5.0±0.1	-1.1± 0.4	5.1± 0.1
300239	1		-0.4±0.1	0.0± 0.0	0.4± 0.1
310352	1	3935± 902	3.8±0.1	1.4± 0.4	4.0± 0.2
240411	1	10534±2416	-1.8±0.1	1.7± 0.4	2.5± 0.3
240416	1	4528± 435	6.9±0.1	0.0± 0.0	6.9± 0.1
240419	1	3828± 898	0.3±0.1	0.0± 0.0	0.3± 0.1
240422	1	10242±2931	-1.0±0.1	0.0± 0.0	1.0± 0.1
240445	1	8378±4758	-0.7±0.1	-1.3± 0.4	1.5± 0.4
240459	1	2849± 452	0.1±0.1	7.5± 0.4	7.5± 0.4
240469	1	10630±1492	-1.8±0.1	0.0± 0.0	1.8± 0.1
240532	1	7838±1173	0.7±0.1	-1.2± 0.4	1.4± 0.3
240534	1	6191±1001	0.0±0.1	-2.6± 0.4	2.6± 0.4
350741	1	1019± 239	0.3±0.1	0.0± 0.0	0.3± 0.1
481101	1	4113±1562	1.3±0.1	0.0± 0.0	1.3± 0.1
351217	1	5129± 703	-0.3±0.1	1.5± 0.4	1.5± 0.4
410001	1		33.4±0.1	-15.7± 0.3	36.5± 0.1
	2	567± 116	-37.8±0.1	6.7± 0.4	38.3± 0.1
410003	1	1283± 324	0.8±0.1	4.2± 0.4	4.3± 0.4
	2		26.0±0.1	-18.9± 0.3	31.8± 0.2

EVENT	TRK	P(MEV)	$\phi(°)$	$\delta(°)$	$\theta(°)$
150066	1	989± 38	17.6±0.1	3.0± 0.4	17.8± 0.1
	2	1353± 202	-4.4±0.1	-1.7± 0.4	4.7± 0.2
150067	1		146.1±0.1	-43.7± 0.2	126.9± 0.2
	2	1272± 282	-9.1±0.1	-5.5± 0.4	10.6± 0.2
150073	1		79.8±0.1	57.5± 0.4	84.5± 0.1
	2	8456±2141	1.2±0.1	11.4± 0.4	11.5± 0.4
150074	1	13260±1631	-0.6±0.1	3.4± 0.4	3.5± 0.4
	2		173.3±0.1	38.2± 0.2	141.3± 0.2
150075	1	975± 159	0.2±0.1	4.3± 1.0	4.3± 1.0
	2		-9.5±0.1	-16.3± 1.2	18.8± 1.0
150085	1	3253± 758	4.0±0.1	2.2± 0.6	4.6± 0.3
	2	4064± 254	4.0±0.1	0.0± 0.0	4.0± 0.1
150097	1		-6.3±0.1	11.8± 0.4	13.4± 0.4
	2		-117.4±0.1	-28.1± 0.3	113.9± 0.1
150099	1		4.3±0.1	-4.4± 0.4	6.1± 0.3
	2		-0.8±0.1	3.7± 0.4	3.8± 0.4
150182	1	2138± 517	3.3±0.1	-4.6± 0.4	5.7± 0.3
	2	3450±1524	-1.7±0.1	0.0± 0.0	1.7± 0.1
330183	1		-4.8±0.1	-3.3± 0.7	5.8± 0.4
	2	7633±2394	6.3±0.1	1.5± 0.4	6.5± 0.1
300199	1	548± 135	28.7±0.1	-4.2± 0.4	29.0± 0.1
	2		-11.9±0.1	24.7± 0.3	27.3± 0.3
300224	1	4537± 702	7.9±0.1	0.0± 0.0	7.9± 0.1
	2	585± 172	-50.1±0.1	7.6± 0.4	50.5± 0.1
310318	1	5473±1534	0.2±0.1	4.6± 0.4	4.6± 0.4
	2		-3.5±0.1	-47.2± 0.2	47.3± 0.2
310327	1	391± 84	7.6±0.1	2.1± 0.4	7.9± 0.1
	2	6310±1533	-6.7±0.1	0.0± 0.0	6.7± 0.1
310348	1	2386± 228	-1.9±0.1	5.9± 0.4	6.2± 0.4
	2	7479±3754	-3.5±0.1	-1.7± 0.4	3.9± 0.2
240402	1	4772± 348	6.1±0.1	2.6± 0.4	6.6± 0.2
	2	613± 61	2.2±0.1	10.3± 0.4	10.5± 0.4

EVENT	TRK	P(MEV)	ϕ(°)	δ(°)	θ(°)
240405	1	9999±1505	-0.8±0.1	0.0± 0.0	0.8± 0.1
	2		18.7±0.1	49.5± 0.2	52.0± 0.2
240432	1	7459± 997	-1.0±0.1	1.2± 0.4	1.5± 0.3
	2	3034± 638	-3.1±0.1	-1.9± 0.4	3.6± 0.2
240438	1	1281± 173	11.7±0.1	3.4± 0.4	12.2± 0.1
	2	274± 32	-4.0±0.1	-11.4± 0.4	12.1± 0.4
240460	1		64.1±0.1	-41.5± 1.3	70.9± 0.4
	2		-9.6±0.1	-3.8± 0.4	10.3± 0.2
240463	1	4259± 772	1.8±0.1	1.0± 0.4	2.1± 0.2
	2	7127±1079	-1.0±0.1	0.7± 0.4	1.2± 0.2
240495	1	5763± 792	0.7±0.1	1.5± 0.4	1.7± 0.4
	2		-19.1±0.1	-12.3± 0.4	22.6± 0.2
240500	1		33.6±0.1	-9.8± 0.4	34.9± 0.1
	2	1036± 229	-15.4±0.1	7.3± 0.4	17.0± 0.2
240503	1	271± 30	-6.0±0.1	12.6± 0.4	13.9± 0.4
	2	3124± 328	-10.3±0.1	2.1± 0.4	10.5± 0.1
240516	1		9.8±0.1	-40.6± 0.2	41.6± 0.2
	2	305± 44	-1.2±0.1	1.3± 0.4	1.8± 0.3
240520	1		4.4±0.1	-9.5± 0.4	10.5± 0.4
	2	1524± 66	-2.4±0.1	3.6± 0.4	4.3± 0.3
240543	1		-10.5±0.1	2.4± 0.4	10.8± 0.1
	2		-25.5±0.1	0.0± 0.0	25.5± 0.1
240550	1	1016± 44	6.0±0.1	0.0± 0.0	6.0± 0.1
	2	1270± 69	1.1±0.1	4.9± 0.4	5.0± 0.4
430938	1	5936± 855	6.6±0.1	-2.6± 0.4	7.1± 0.2
	2	2085± 822	-7.5±0.1	-5.4± 0.4	9.2± 0.2
461375	1		-2.4±0.1	-8.1± 0.4	8.4± 0.4
	2	490± 60	-12.8±0.1	6.3± 0.4	14.2± 0.2
410005	1	1805± 468	0.3±0.1	-4.6± 0.4	4.6± 0.4
	2	6421± 999	-1.8±0.1	-1.2± 0.4	2.2± 0.2
	3	626± 212	-9.3±0.1	5.2± 0.4	10.6± 0.2
150021	1	7335±1630	-1.1±0.1	2.3± 0.4	2.5± 0.4
	2	4598± 426	-3.6±0.1	0.0± 0.0	3.6± 0.1

EVENT	TRK	P(MEV)	$\phi(°)$	$\delta(°)$	$\theta(°)$
	3	1664± 263	-4.9±0.1	4.4± 0.4	6.6± 0.3
220022	1	1642± 702	4.0±0.1	-11.8± 0.4	12.5± 0.4
	2	1683± 276	-3.3±0.1	-7.4± 0.4	8.1± 0.4
	3	1667± 341	-3.8±0.1	3.6± 0.4	5.2± 0.3
150042	1	1592± 696	1.3±0.1	3.2± 0.4	3.5± 0.4
	2	2000± 571	-8.2±0.1	-12.1± 0.4	14.6± 0.3
	3	341± 56	-41.9±0.1	15.9± 0.3	44.3± 0.1
150045	1		20.5±0.1	-36.2± 0.5	40.9± 0.4
	2	1409±1027	0.1±0.1	-3.7± 0.4	3.7± 0.4
	3	1048± 150	-28.2±0.1	2.6± 0.4	28.3± 0.1
150076	1	7401±1997	3.3±0.1	0.0± 0.0	3.3± 0.1
	2	2478± 663	-3.3±0.1	-7.6± 0.4	8.3± 0.4
	3		-5.8±0.1	2.2± 0.4	6.2± 0.2
150089	1	8857±1687	-2.2±0.1	5.2± 0.4	5.6± 0.4
	2		-2.0±0.1	-19.7± 0.3	19.8± 0.3
	3	257± 39	-9.3±0.1	-2.8± 0.4	9.7± 0.1
150090	1	608± 127	10.6±0.1	9.9± 0.4	14.5± 0.3
	2	10406±3866	-5.4±0.1	0.0± 0.0	5.4± 0.1
	3		-66.1±0.1	-3.9± 0.4	66.2± 0.1
150115	1	598± 154	2.2±0.1	3.3± 0.4	4.0± 0.3
	2		-1.0±0.1	18.2± 0.3	18.2± 0.3
	3		-14.8±0.1	-21.0± 0.3	25.5± 0.2
150117	1		5.1±0.1	-25.6± 0.3	26.1± 0.3
	2	299± 39	-4.7±0.1	11.7± 0.4	12.6± 0.4
	3	1932± 484	-7.9±0.1	13.8± 0.3	15.9± 0.3
150174	1		138.3±0.1	40.0± 0.2	124.9± 0.1
	2		-0.5±0.1	40.4± 0.2	40.4± 0.2
	3		-13.8±0.1	-10.0± 0.4	17.0± 0.2
150180	1		40.0±0.1	-3.3± 0.4	40.1± 0.1
	2	1443± 361	23.9±0.1	-10.3± 0.4	25.9± 0.2
	3		-13.4±0.1	19.8± 0.3	23.9± 0.3
150185	1		4.6±0.1	-14.2± 0.4	14.9± 0.4
	2		2.7±0.1	-1.6± 0.4	3.1± 0.2
	3		-0.8±0.1	4.9± 0.4	5.0± 0.4
370199	3		-5.7±0.1	11.2± 0.4	12.6± 0.4
	4		-4.9±0.1	26.0± 0.3	26.4± 0.3

EVENT	TRK	P(MEV)	$\phi(°)$	$\delta(°)$	$\theta(°)$
	5		3.2±0.1	11.1± 0.3	11.5± 0.3
300209	1	10068±3559	13.2±0.1	-3.9± 0.4	13.8± 0.1
	2	3542±1471	-4.2±0.1	-3.7± 0.4	5.6± 0.3
	3		-23.5±0.1	26.7± 0.3	35.0± 0.2
300217	1		1.9±0.1	-5.9± 0.4	6.2± 0.4
	2		-62.1±0.1	37.5± 0.2	68.2± 0.1
	3		145.5±0.1	-23.2± 0.3	139.2± 0.2
300234	1	8347± 713	1.4±0.1	1.5± 0.4	2.1± 0.3
	2		1.7±0.1	-6.0± 0.4	6.2± 0.4
	3		-2.9±0.1	-13.7± 0.4	14.0± 0.4
300242	1		129.1±0.1	34.0± 0.3	121.5± 0.1
	2		-0.3±0.1	5.6± 0.4	5.6± 0.4
	4		-55.2±0.1	-56.9± 0.3	72.3± 0.2
300254	1	844± 212	4.3±0.1	6.6± 0.4	7.9± 0.3
	2	6522±1560	-3.4±0.1	-1.1± 0.4	3.6± 0.2
	3	1070± 147	-7.3±0.1	11.0± 0.4	13.2± 0.3
310301	1	685± 305	27.3±0.1	13.9± 0.4	30.4± 0.2
	2		-6.6±0.1	-28.3± 0.3	29.0± 0.3
	3		-26.3±0.1	-17.4± 0.3	31.2± 0.2
310303	1	3559± 943	1.3±0.1	0.0± 0.0	1.3± 0.1
	2		-0.5±0.1	1.6± 0.4	1.7± 0.4
	3		-8.1±0.1	-8.5± 0.4	11.7± 0.3
310321	1		66.3±0.1	39.9± 0.2	72.0± 0.1
	2	3726± 974	3.5±0.1	4.5± 0.4	5.7± 0.3
	3	1085± 318	-6.1±0.1	-6.1± 0.4	8.6± 0.3
310343	1		57.4±0.1	11.3± 0.4	58.1± 0.1
	2	9298±1906	-0.1±0.1	3.5± 0.4	3.5± 0.4
	3		-1.3±0.1	11.9± 0.4	12.0± 0.4
310356	1	1364± 283	0.0±0.1	5.5± 0.4	5.5± 0.4
	2	1368± 161	-1.5±0.1	-1.5± 0.4	2.1± 0.3
	3		-21.4±0.1	25.7± 0.3	33.0± 0.2
310367	1		10.3±0.1	-49.7± 0.2	50.5± 0.2
	2		-8.1±0.1	-6.0± 0.4	10.1± 0.2
	3		-28.6±0.1	-14.1± 0.4	31.6± 0.2
240406	1	1417± 192	43.5±0.1	0.0± 0.0	43.5± 0.1
	2		22.3±0.1	-56.9± 0.1	59.7± 0.1

EVENT	TRK	P(MEV)	ϕ(°)	δ(°)	θ(°)
	3	380± 66	-10.7±0.1	6.1± 0.4	12.3± 0.2
240434	1		32.8±0.1	7.9± 0.4	33.6± 0.1
	2		-19.2±0.1	-43.8± 0.2	47.0± 0.2
	3		-36.9±0.1	16.9± 0.3	40.1± 0.1
240441	1	1543± 295	9.2±0.1	-5.4± 0.4	10.7± 0.2
	2	3463± 795	0.5±0.1	3.5± 0.4	3.5± 0.4
	3	832± 108	-4.1±0.1	-7.9± 0.4	8.9± 0.4
240482	1	815± 158	6.2±0.1	9.6± 0.4	11.4± 0.3
	2	3388± 996	-4.1±0.1	0.0± 0.0	4.1± 0.1
	3		-6.5±0.1	22.5± 0.3	23.4± 0.3
240493	1	767± 108	8.8±0.1	8.5± 0.4	12.2± 0.3
	2	1980± 945	3.9±0.1	5.9± 0.4	7.1± 0.3
	3	3303± 642	-3.8±0.1	7.1± 0.4	8.0± 0.4
240506	1		0.2±0.1	-36.2± 0.2	36.2± 0.2
	2	4488±1336	-3.6±0.1	0.0± 0.0	3.6± 0.1
	3		-37.2±0.1	-46.4± 0.6	56.7± 0.4
240529	1		44.3±0.1	15.3± 0.3	46.3± 0.1
	2	6857± 558	-6.1±0.1	2.3± 0.4	6.5± 0.2
	3	1887± 475	-14.5±0.1	8.4± 0.4	16.7± 0.2
240540	1		27.3±0.1	2.6± 0.4	27.4± 0.1
	2	4806± 619	-3.1±0.1	-1.8± 0.4	3.6± 0.2
	3		-21.9±0.1	-14.4± 0.4	26.0± 0.2
240552	1		12.3±0.1	6.5± 0.4	13.9± 0.2
	2	3393± 646	-0.5±0.1	-2.1± 0.4	2.2± 0.4
	3		-18.9±0.1	-10.2± 0.4	21.4± 0.2
480562	1	710± 30	8.0±0.1	1.2± 0.4	8.1± 0.1
	2	7091±1923	-0.2±0.1	1.1± 0.4	1.1± 0.4
	3	1965± 242	-1.0±0.1	1.5± 0.4	1.8± 0.3
201021	1	549± 151	22.1±0.1	-8.8± 0.4	23.7± 0.2
	3	2585± 526	-3.7±0.1	-3.7± 0.4	5.2± 0.3
	4	887± 99	-40.0±0.1	7.9± 0.4	40.6± 0.1
201025	2	906± 136	-1.1±0.1	2.4± 0.4	2.6± 0.4
	3	1064± 290	-45.0±0.1	15.1± 0.3	46.9± 0.1
	4	558± 82	0.7±0.1	-8.1± 0.4	8.1± 0.4
201026	2	1868± 425	25.6±0.1	8.6± 0.4	26.9± 0.2
	3	379± 70	3.6±0.1	-9.8± 0.4	10.4± 0.4

EVENT	TRK	P(MEV)	$\phi(°)$	$\delta(°)$	$\theta(°)$
	4		-34.4±0.1	21.8± 0.5	40.0± 0.3
351304	1	336± 21	7.4±0.1	0.0± 0.0	7.4± 0.1
	2	2560± 282	1.8±0.1	1.7± 0.4	2.5± 0.3
	3	3499± 834	-6.0±0.1	5.8± 0.4	8.3± 0.3
461373	1	2706± 158	4.9±0.1	1.5± 0.4	5.1± 0.2
	2		-1.5±0.1	-6.2± 0.4	6.4± 0.4
	3	2955± 633	-44.5±0.1	-2.5± 0.4	44.6± 0.1
461384	1		10.7±0.1	-12.2± 0.3	16.2± 0.2
	2		2.0±0.1	-2.4± 0.4	3.1± 0.3
	3	376± 17	-4.6±0.1	7.5± 0.4	8.8± 0.3
461389	1	9430±1246	2.5±0.1	0.0± 0.0	2.5± 0.1
	2	764± 51	-3.5±0.1	5.6± 0.4	6.6± 0.3
	3	3692± 235	-5.4±0.1	0.0± 0.0	5.4± 0.1
461397	1		4.4±0.1	38.3± 0.6	38.5± 0.6
	2	4746± 878	-0.8±0.1	2.2± 0.4	2.3± 0.4
	3	1728± 561	-3.8±0.1	-3.9± 0.4	5.4± 0.3
410007	1		61.2±0.1	32.1± 0.3	65.9± 0.1
	2		13.3±0.1	4.7± 0.4	14.1± 0.2
	3	868± 287	5.7±0.1	-9.5± 0.4	11.1± 0.3
	4	4073± 508	-5.9±0.1	-0.9± 0.4	6.0± 0.1
150026	1	1257± 456	2.8±0.1	9.7± 0.4	10.1± 0.4
	2	4013± 487	1.3±0.1	0.0± 0.0	1.3± 0.1
	3	2230± 240	-1.8±0.1	1.2± 0.4	2.2± 0.2
	4	2306± 490	-11.1±0.1	1.3± 0.4	11.2± 0.1
150034	1		16.7±0.1	24.4± 0.3	29.3± 0.2
	2		7.3±0.1	-7.4± 0.4	10.4± 0.3
	3	1353± 178	4.4±0.1	7.1± 0.4	8.3± 0.3
	4	287± 25	-69.7±0.1	-9.1± 0.4	70.0± 0.1
150039	1	6999± 941	0.4±0.1	1.5± 0.4	1.6± 0.4
	2		-0.9±0.1	-7.5± 0.4	7.6± 0.4
	3		-2.0±0.1	-5.0± 0.4	5.4± 0.4
	4		-2.8±0.1	-16.6± 0.3	16.8± 0.3
150046	1	4476± 847	-2.1±0.1	-3.7± 0.4	4.3± 0.4
	2		-8.0±0.1	8.3± 0.4	11.5± 0.3
	3	360± 52	-46.2±0.1	13.9± 0.3	47.9± 0.1
	4		-77.1±0.1	-16.3± 0.3	77.6± 0.1

EVENT	TRK	P(MEV)	ϕ(°)	δ(°)	θ(°)
150049	1	835± 89	16.7±0.1	12.0± 0.4	20.5± 0.2
	2	274± 21	6.2±0.1	6.4± 0.4	8.9± 0.3
	3	4372± 959	1.2±0.1	2.6± 0.4	2.9± 0.4
	4		-2.8±0.1	17.2± 0.3	17.4± 0.3
150050	1		167.2±0.1	27.9± 0.3	149.5± 0.3
	2		56.9±0.1	18.1± 0.3	58.7± 0.1
	3	18619±5019	-2.1±0.1	-4.0± 0.4	4.5± 0.4
	4		-9.7±0.1	-31.3± 0.3	32.6± 0.3
150054	1		57.7±0.1	-16.9± 0.3	59.3± 0.1
	2	1050± 94	4.5±0.1	1.8± 0.4	4.9± 0.2
	3	972± 83	-14.9±0.1	6.9± 0.4	16.4± 0.2
	4	1036± 340	-15.9±0.1	13.1± 0.4	20.5± 0.3
150070	1	3937± 903	13.6±0.1	2.2± 0.4	13.9± 0.1
	2	1086± 274	8.7±0.1	-2.1± 0.4	9.0± 0.1
	3		-7.9±0.1	-10.3± 0.4	13.0± 0.3
	4	5088± 892	-16.7±0.1	0.0± 0.0	16.7± 0.1
150103	1	1377± 389	-0.5±0.1	7.1± 0.4	7.1± 0.4
	2	4357± 440	-2.1±0.1	3.7± 0.4	4.3± 0.4
	3	2428± 609	-6.7±0.1	-6.6± 0.4	9.4± 0.3
	4		0.3±0.1	12.1± 0.4	12.1± 0.4
150123	1	2367± 335	3.8±0.1	-2.4± 0.4	4.5± 0.2
	2	6126± 849	0.8±0.1	2.1± 0.4	2.2± 0.4
	3		-72.6±0.1	-32.8± 0.3	75.4± 0.1
	4		142.7±0.1	66.7± 0.3	108.3± 0.2
150181	1		81.9±0.1	-52.2± 0.3	85.0± 0.1
	2		5.0±0.1	-46.0± 0.2	46.2± 0.2
	3		-9.6±0.1	40.9± 0.2	41.8± 0.2
	4		34.5±0.1	-59.2± 0.2	65.0± 0.2
300193	1		146.7±0.1	-15.6± 0.4	143.6± 0.2
	2	3639± 866	6.9±0.1	0.0± 0.0	6.9± 0.1
	3	1480± 285	-2.6±0.1	2.4± 0.4	3.5± 0.3
	4	574± 116	-33.4±0.1	12.0± 0.4	35.3± 0.2
300204	1		36.5±0.1	-25.3± 0.3	43.4± 0.2
	2	2658± 352	19.2±0.1	2.4± 0.4	19.3± 0.1
	3	6809±1633	1.9±0.1	-0.9± 0.4	2.1± 0.2
	4		-9.4±0.1	9.7± 0.4	13.5± 0.3
300213	1		20.8±0.1	-73.7± 0.2	74.8± 0.2
	2		6.2±0.1	-23.6± 0.3	24.4± 0.3

EVENT	TRK	P(MEV)	ϕ(°)	δ(°)	θ(°)
	3	2205± 465	5.8±0.1	-2.4± 0.4	6.3± 0.2
	4		2.9±0.1	-23.3± 0.3	23.5± 0.3
300214	1		19.5±0.1	-9.7± 0.4	21.7± 0.2
	2	3759±1354	5.0±0.1	3.6± 0.4	6.2± 0.2
	3	3173± 976	-0.1±0.1	7.4± 0.4	7.4± 0.4
	4	1235± 154	-3.9±0.1	3.9± 0.4	5.5± 0.3
300219	1		94.9±0.1	-13.1± 0.4	94.8± 0.1
	2	4806±2567	4.8±0.1	0.0± 0.0	4.8± 0.1
	3	4315±2293	-1.4±0.1	0.0± 0.0	1.4± 0.1
	4	3898± 737	-8.1±0.1	0.0± 0.0	8.1± 0.1
300238	1	159± 23	51.2±0.1	6.3± 0.4	51.5± 0.1
	2	6339±2947	-1.1±0.1	-2.2± 0.4	2.5± 0.4
	3	2446±1033	-5.5±0.1	1.3± 0.4	5.7± 0.1
	4	2518± 454	-8.0±0.1	1.7± 0.4	8.2± 0.1
300265	1	1895± 456	53.3±0.1	-7.5± 0.4	53.7± 0.1
	2		12.4±0.1	-24.2± 0.3	27.0± 0.3
	3		8.6±0.1	-12.9± 0.4	15.5± 0.3
	4	2702± 814	6.3±0.1	0.0± 0.0	6.3± 0.1
310304	2		17.5±0.1	-16.7± 0.3	24.0± 0.2
	3		10.1±0.1	14.4± 0.4	17.5± 0.3
	4	5713±1199	-3.1±0.1	-3.6± 0.4	4.7± 0.3
	5		-8.5±0.1	-12.8± 0.4	15.3± 0.3
310338	1		89.0±0.1	-36.9± 0.2	89.2± 0.1
	2		34.3±0.1	-12.4± 0.3	36.2± 0.1
	3		-22.4±0.1	15.8± 0.6	27.2± 0.3
	4		-87.4±0.1	40.2± 0.2	88.0± 0.1
240497	1		58.9±0.1	26.7± 0.3	62.5± 0.1
	2		10.3±0.1	7.1± 0.4	12.5± 0.2
	3		10.3±0.1	4.4± 0.4	11.2± 0.2
	4		16.2±0.1	-23.4± 0.3	28.2± 0.2
240498	1	3858± 295	10.5±0.1	3.5± 0.4	11.1± 0.2
	2	479± 70	8.7±0.1	-1.8± 0.4	8.9± 0.1
	3	2024± 590	-2.6±0.1	-4.6± 0.4	5.3± 0.4
	4		-29.1±0.1	-14.4± 0.3	32.2± 0.2
240501	1		-0.8±0.1	-6.9± 0.6	6.9± 0.6
	2		-2.3±0.1	-4.6± 0.4	5.1± 0.4
	3		-27.3±0.1	-9.3± 0.4	28.4± 0.1
	4		-150.7±0.1	54.7± 0.4	120.3± 0.3

EVENT	TRK	P(MEV)	ϕ(°)	δ(°)	θ(°)
240513	1	4005± 410	5.9±0.1	0.0± 0.0	5.9± 0.1
	2	775± 101	-0.2±0.1	7.8± 0.4	7.8± 0.4
	3		-40.6±0.1	-23.9± 0.3	46.0± 0.2
	4		-60.0±0.1	-29.8± 0.3	64.3± 0.1
240522	1		19.2±0.1	2.3± 0.4	19.3± 0.1
	2	3408± 145	2.0±0.1	1.4± 0.4	2.4± 0.2
	3	4723± 665	-7.0±0.1	-1.8± 0.4	7.2± 0.1
	4		-33.2±0.1	-24.7± 0.3	40.5± 0.2
240553	1		49.0±0.1	-46.3± 0.2	63.0± 0.1
	2	762± 54	1.7±0.1	0.0± 0.0	1.7± 0.1
	3		-8.5±0.1	-11.3± 0.4	14.1± 0.3
	4		-38.2±0.1	33.0± 0.3	48.8± 0.2
481142	1		12.9±0.1	40.5± 0.5	42.2± 0.5
	2	3448±1840	-3.3±0.1	6.6± 0.4	7.4± 0.4
	3		-5.2±0.1	14.7± 0.4	15.6± 0.4
	4	1870± 400	-8.0±0.1	4.8± 0.4	9.3± 0.2
351201	1		4.1±0.1	-7.6± 0.4	8.6± 0.4
	2	1139± 284	2.1±0.1	7.6± 0.4	7.9± 0.4
	3		-3.7±0.1	-16.8± 0.3	17.2± 0.3
	4	1196± 345	-16.4±0.1	-4.4± 0.4	17.0± 0.1
461400	1	320± 34	-17.5±0.1	-2.3± 0.4	17.6± 0.1
	2		-16.2±0.1	-6.1± 0.4	17.3± 0.2
	3		-2.0±0.1	-29.2± 0.3	29.3± 0.3
	4		24.1±0.1	-22.4± 0.3	32.4± 0.2
183048	1		-1.1±0.1	7.7± 0.4	7.8± 0.4
	2	2919± 338	-0.7±0.1	0.0± 0.0	0.7± 0.1
	3		3.4±0.1	4.1± 0.4	5.3± 0.3
	4	4268± 302	3.4±0.1	-2.3± 0.4	4.1± 0.2
410004	1		51.6±0.1	-22.6± 0.3	55.0± 0.1
	2		3.6±0.1	-12.3± 0.4	12.8± 0.4
	3	2344± 645	-2.0±0.1	-7.3± 0.4	7.6± 0.4
	4		-9.1±0.1	-1.2± 0.4	9.2± 0.1
	5	146± 26	-93.3±0.1	-6.3± 0.4	93.3± 0.1
150051	1		11.5±0.1	34.1± 0.3	35.8± 0.3
	2	1405± 155	8.7±0.1	0.0± 0.0	8.7± 0.1
	3		6.7±0.1	3.9± 0.4	7.7± 0.2
	4		-74.6±0.1	26.7± 0.3	76.3± 0.1

EVENT	TRK	P(MEV)	ϕ(°)	δ(°)	θ(°)
	5	320± 38	-78.5±0.1	11.7± 0.4	78.7± 0.1
150059	1		4.6±0.1	-13.8± 0.3	14.5± 0.3
	2	1231± 322	3.8±0.1	6.5± 0.4	7.5± 0.3
	3	3539± 963	-0.5±0.1	5.0± 0.4	5.0± 0.4
	4	2943± 408	-1.7±0.1	-2.7± 0.4	3.2± 0.3
	5	4298± 732	-9.4±0.1	4.9± 0.4	10.6± 0.2
150069	1	869± 158	17.9±0.1	-6.7± 0.4	19.1± 0.2
	2	746± 196	13.5±0.1	10.8± 0.4	17.2± 0.3
	3		3.9±0.1	-30.3± 0.3	30.5± 0.3
	4	1011± 207	2.3±0.1	8.9± 0.4	9.2± 0.4
	5	3784± 532	-11.2±0.1	4.8± 0.4	12.2± 0.2
150072	1		92.4±0.1	21.2± 0.4	92.2± 0.1
	2		8.1±0.1	4.4± 0.4	9.2± 0.2
	3	4637± 826	5.5±0.1	0.0± 0.0	5.5± 0.1
	4	5444± 239	-2.9±0.1	1.3± 0.4	3.2± 0.2
	5		-74.6±0.1	-58.0± 0.5	81.9± 0.1
150088	1		12.0±0.1	-20.7± 0.3	23.8± 0.3
	2	683± 307	9.3±0.1	-5.3± 0.4	10.7± 0.2
	3	3471±1231	2.5±0.1	-6.2± 0.4	6.7± 0.4
	4	601± 75	-15.3±0.1	6.7± 0.4	16.7± 0.2
	5		-63.2±0.1	81.7± 0.1	86.3± 0.0
150121	1		10.7±0.1	-12.5± 0.3	16.4± 0.2
	2	499± 160	1.9±0.1	-1.7± 0.4	2.5± 0.3
	3	5093± 416	-0.6±0.1	0.0± 0.0	0.6± 0.1
	4		-4.2±0.1	46.4± 0.2	46.5± 0.2
	5		-12.6±0.1	-25.9± 0.3	28.6± 0.3
150134	1		113.6±0.1	-48.8± 0.2	105.3± 0.1
	2		21.7±0.1	30.9± 0.3	37.1± 0.2
	3	2124± 356	14.8±0.1	0.0± 0.0	14.8± 0.1
	4		0.2±0.1	-13.2± 0.4	13.2± 0.4
	5		-10.2±0.1	-2.4± 0.4	10.5± 0.1
150137	1	2275± 303	3.1±0.1	1.4± 0.4	3.4± 0.2
	2	1751± 399	-3.9±0.1	-1.7± 0.4	4.3± 0.2
	3		-9.5±0.1	14.9± 0.3	17.6± 0.3
	4		-34.6±0.1	18.5± 0.3	38.7± 0.2
	5		-35.6±0.1	21.0± 0.3	40.6± 0.2
150138	1		31.9±0.1	-38.6± 0.2	48.4± 0.2
	2	1095± 103	20.7±0.1	-1.2± 0.4	20.7± 0.1
	3	869± 112	13.0±0.1	-5.5± 0.4	14.1± 0.2

EVENT	TRK	P(MEV)	$\phi(^\circ)$	$\delta(^\circ)$	$\theta(^\circ)$
	4		-2.5±0.1	-10.9± 0.4	11.2± 0.4
	5		-2.6±0.1	-36.3± 1.2	36.4± 1.2
150150	1		66.3±0.1	6.0± 0.4	66.4± 0.1
	2		64.4±0.1	10.4± 0.4	64.8± 0.1
	3		59.7±0.1	5.7± 0.4	59.9± 0.1
	4		8.0±0.1	20.6± 1.1	22.0± 1.0
	5	4585± 657	2.3±0.1	-2.6± 0.4	3.5± 0.3
150162	1		43.6±0.1	-46.6± 0.2	60.2± 0.1
	2		21.8±0.1	14.5± 0.3	26.0± 0.2
	3	4258±2108	8.7±0.1	-3.8± 0.4	9.5± 0.2
	4	6585±2474	5.8±0.1	0.0± 0.0	5.8± 0.1
	5	5754±1729	2.4±0.1	0.0± 0.0	2.4± 0.1
150167	1	2372± 532	4.6±0.1	-12.9± 0.3	13.7± 0.3
	2	2201± 196	2.7±0.1	-1.1± 0.4	2.9± 0.2
	4		-3.5±0.1	14.9± 0.3	15.3± 0.3
	3	3035± 264	1.6±0.1	0.0± 0.0	1.6± 0.1
	5	2470± 500	-7.4±0.1	-10.0± 0.7	12.4± 0.6
150184	1		122.0±0.1	18.0± 0.3	120.3± 0.1
	2	4588±1660	29.9±0.1	-6.1± 0.4	30.5± 0.1
	3	2572± 987	2.2±0.1	4.8± 0.4	5.3± 0.4
	4	3609± 361	1.1±0.1	-2.0± 0.4	2.3± 0.4
	5		-26.4±0.1	-38.0± 0.2	45.1± 0.2
300190	1		72.5±0.1	-23.8± 1.0	74.0± 0.2
	2	2058± 423	30.5±0.1	2.7± 0.4	30.6± 0.1
	3		-4.2±0.1	-2.4± 0.4	4.8± 0.2
	4		9.6±0.1	32.1± 0.3	33.4± 0.3
	5		-55.1±0.1	-15.7± 0.4	56.6± 0.1
300191	1		26.6±0.1	-30.7± 0.3	39.7± 0.2
	2	2231± 294	7.9±0.1	1.2± 0.4	8.0± 0.1
	3	1492± 238	3.9±0.1	0.9± 0.4	4.0± 0.1
	4	6538± 921	-0.3±0.1	2.3± 0.4	2.3± 0.4
	5		-12.0±0.1	-21.6± 0.3	24.6± 0.3
300196	1		32.5±0.1	-38.8± 0.2	48.9± 0.2
	2	1440± 99	9.2±0.1	-1.8± 0.4	9.4± 0.1
	3	5348± 657	1.6±0.1	0.0± 0.0	1.6± 0.1
	4		-3.7±0.1	-23.2± 0.3	23.5± 0.3
	5		-124.9±0.1	24.6± 0.3	121.3± 0.1
300220	1		74.5±0.1	-32.1± 0.3	76.9± 0.1
	2	603± 131	10.0±0.1	-2.6± 0.4	10.3± 0.1
	3	876± 262	3.9±0.1	8.9± 0.4	9.7± 0.4

EVENT	TRK	P(MEV)	ϕ(°)	δ(°)	θ(°)
	4	609± 106	-0.6±0.1	11.3± 0.4	11.3± 0.4
	5	891± 216	-3.0±0.1	12.6± 0.4	12.9± 0.4
300230	1	143± 12	91.4±0.1	0.0± 0.0	91.4± 0.1
	2		-20.3±0.1	-6.9± 0.4	21.4± 0.2
	3		-32.4±0.1	20.4± 0.3	37.7± 0.2
	4	164± 15	-36.7±0.1	6.0± 0.4	37.1± 0.1
	5		-148.9±0.1	37.1± 0.3	133.1± 0.2
300256	1	838± 150	15.7±0.1	-8.9± 0.5	18.0± 0.3
	2	250± 8	14.0±0.1	3.3± 0.5	14.4± 0.1
	3	615± 73	-5.6±0.1	-12.7± 0.4	13.9± 0.4
	4	2376± 323	-6.1±0.1	-11.8± 0.4	13.3± 0.4
	5	1599± 290	-10.6±0.1	6.2± 0.4	12.3± 0.2
300261	1		30.8±0.1	-20.1± 0.3	36.2± 0.2
	2	4457±1041	2.9±0.1	-2.8± 0.4	4.0± 0.3
	3		-14.5±0.1	39.3± 0.2	41.5± 0.2
	4	2806± 372	-11.8±0.1	-7.3± 0.4	13.8± 0.2
	5	1363± 85	-43.5±0.1	0.0± 0.0	43.5± 0.1
300281	1		3.1±0.1	-11.4± 0.4	11.8± 0.4
	2	1141± 219	-5.6±0.1	-1.6± 0.4	5.8± 0.1
	3	4550±1036	-6.8±0.1	0.0± 0.0	6.8± 0.1
	4	702± 123	-11.6±0.1	7.8± 0.4	13.9± 0.2
	5		-31.9±0.1	-32.2± 0.3	44.1± 0.2
310295	1		98.6±0.1	-17.9± 0.3	98.2± 0.1
	2	2670± 569	8.3±0.1	-10.8± 0.4	13.6± 0.3
	3	2788± 386	0.3±0.1	-2.3± 0.4	2.3± 0.4
	4		-3.2±0.1	15.0± 0.3	15.3± 0.3
	5	3822±1662	-14.0±0.1	2.0± 0.4	14.1± 0.1
310317	1		5.9±0.1	-14.4± 1.1	15.5± 1.0
	2	3577± 567	2.1±0.1	6.0± 0.4	6.4± 0.4
	3	2928±1372	-4.7±0.1	7.4± 0.4	8.8± 0.3
	4		-34.4±0.1	-20.5± 1.6	39.4± 0.7
	5		-3.6±0.1	-24.8± 0.9	25.0± 0.9
310330	1		37.3±0.1	-24.7± 0.3	43.7± 0.2
	2	1062± 279	-15.4±0.1	-0.9± 0.4	15.4± 0.1
	3	369± 121	-16.5±0.1	5.7± 0.4	17.4± 0.2
	4		2.1±0.1	0.0± 0.0	2.1± 0.1
	5	47± 1	-173.9±0.1	61.4± 0.1	118.4± 0.1
310340	2	132± 25	78.1±0.1	-2.4± 0.4	78.1± 0.1
	3	280± 50	16.0±0.1	14.8± 0.3	21.7± 0.2
	4		12.6±0.1	-14.2± 0.4	18.9± 0.3

EVENT	TRK	P(MEV)	ϕ(°)	δ(°)	θ(°)
	5		-2.5±0.1	-40.2± 0.2	40.3± 0.2
	6		-28.1±0.1	-49.3± 0.2	54.9± 0.2
310344	1	3030± 629	8.8±0.1	3.6± 0.4	9.5± 0.2
	2	1340± 311	5.6±0.1	-5.0± 0.4	7.5± 0.3
	3	2399±1225	3.1±0.1	-7.0± 0.4	7.7± 0.4
	4		-0.2±0.1	-13.7± 0.3	13.7± 0.3
	5		-95.7±0.1	-24.7± 0.3	95.2± 0.1
240403	1		20.9±0.1	-12.4± 0.4	24.2± 0.2
	2		18.8±0.1	18.9± 0.3	26.4± 0.2
	3	2444± 77	9.9±0.1	2.0± 0.4	10.1± 0.1
	4	296± 35	2.4±0.1	14.7± 0.3	14.9± 0.3
	5		-3.7±0.1	27.6± 0.3	27.8± 0.3
240462	1	1244± 326	13.4±0.1	2.6± 0.4	13.6± 0.1
	2	1642± 263	11.0±0.1	-2.0± 0.4	11.2± 0.1
	3		6.6±0.1	22.3± 0.3	23.2± 0.3
	4	4055± 418	-3.2±0.1	-2.1± 0.4	3.8± 0.2
	5		-31.6±0.1	37.7± 0.2	47.6± 0.2
240476	1	275± 35	169.3±0.1	0.0± 0.0	169.3± 0.1
	2		48.5±0.1	-33.5± 1.3	56.5± 0.6
	3	7316±2370	-0.5±0.1	-1.4± 0.4	1.5± 0.4
	4		-1.6±0.1	-6.5± 0.4	6.7± 0.4
	5	692± 181	-16.6±0.1	13.2± 0.3	21.1± 0.2
240479	1	2575± 190	7.8±0.1	-1.7± 0.4	8.0± 0.1
	2	729± 131	5.3±0.1	3.4± 0.4	6.3± 0.2
	3	880± 247	3.0±0.1	6.7± 0.4	7.3± 0.4
	4	484± 73	-20.3±0.1	-13.3± 0.4	24.1± 0.2
	5	785± 127	-59.2±0.1	-11.2± 0.4	59.8± 0.1
240489	1	176± 11	24.9±0.1	25.9± 0.3	35.3± 0.2
	2		24.1±0.1	9.4± 0.4	25.8± 0.2
	3	171± 11	16.7±0.1	15.9± 0.3	22.9± 0.2
	4	1742± 556	12.5±0.1	-6.1± 0.4	13.9± 0.2
	5	1107± 195	-37.7±0.1	-22.1± 0.3	42.9± 0.2
240490	1	1409± 120	9.0±0.1	-3.9± 0.4	9.8± 0.2
	2	876± 379	0.3±0.1	2.6± 0.4	2.6± 0.4
	3	529± 95	-9.5±0.1	-11.0± 0.4	14.5± 0.3
	4		90.3±0.1	25.4± 0.4	90.3± 0.1
	5		-80.6±0.1	-37.5± 0.4	82.6± 0.1
240509	1	452± 24	5.0±0.1	-9.8± 0.4	11.0± 0.4
	2	3287± 188	1.4±0.1	0.0± 0.0	1.4± 0.1
	3	1054± 91	-4.9±0.1	-5.4± 0.4	7.3± 0.3

EVENT	TRK	P(MEV)	ϕ(°)	δ(°)	θ(°)
	4		−10.0±0.1	29.1± 0.3	30.6± 0.3
	5		−18.9±0.1	21.3± 0.3	28.2± 0.2
240511	1		0.8±0.1	−43.2± 0.2	43.2± 0.2
	2	1709± 149	−1.5±0.1	0.0± 0.0	1.5± 0.1
	3		−1.9±0.1	−8.4± 0.4	8.6± 0.4
	4		−52.2±0.1	−44.4± 0.5	64.0± 0.2
	5		−2.5±0.1	−15.7± 0.3	15.9± 0.3
240526	1	390± 44	71.8±0.1	11.3± 0.4	72.2± 0.1
	2	781± 156	0.0±0.1	12.9± 0.4	12.9± 0.4
	3	1398± 246	−14.0±0.1	8.0± 0.4	16.1± 0.2
	4		−26.7±0.1	−16.1± 0.3	30.9± 0.2
	5		−94.0±0.1	−59.5± 0.1	92.0± 0.1
240528	1		6.1±0.1	−12.5± 0.4	13.9± 0.4
	2		0.1±0.1	−9.7± 0.4	9.7± 0.4
	3		−10.1±0.1	−14.8± 0.4	17.9± 0.3
	4		−14.5±0.1	−9.1± 0.4	17.1± 0.2
	5		−56.2±0.1	23.8± 0.3	59.4± 0.1
240538	1		21.4±0.1	14.2± 0.3	25.5± 0.2
	2		16.1±0.1	3.9± 0.4	16.6± 0.1
	3		2.0±0.1	4.4± 0.4	4.8± 0.4
	4	2914± 103	−3.7±0.1	−1.9± 0.4	4.2± 0.2
	5	1167± 178	−23.8±0.1	−4.3± 0.4	24.2± 0.1
240556	1		87.2±0.1	54.0± 0.1	88.4± 0.1
	2		19.3±0.1	−8.0± 0.4	20.8± 0.2
	3		−7.5±0.1	−26.2± 0.3	27.2± 0.3
	5	562± 78	−19.2±0.1	9.3± 0.4	21.3± 0.2
	6	630± 70	−44.2±0.1	4.8± 0.4	44.4± 0.1
240559	1		108.4±0.1	12.1± 0.4	108.0± 0.1
	2	800± 134	81.0±0.1	−3.7± 0.4	81.0± 0.1
	3		2.4±0.1	−24.3± 0.3	24.4± 0.3
	4	720± 79	−26.5±0.1	0.0± 0.0	26.5± 0.1
	5		−174.6±0.1	32.6± 0.3	147.0± 0.3
201022	1	315± 56	98.1±0.1	−17.6± 0.4	97.7± 0.1
	3	474± 188	22.6±0.1	5.4± 0.4	23.2± 0.1
	5	2644± 635	5.3±0.1	15.6± 0.4	16.5± 0.4
	6		1.6±0.1	−19.6± 0.3	19.7± 0.3
	7	2383± 392	−1.7±0.1	−2.5± 0.4	3.0± 0.3
201024	1	157± 20	163.8±0.1	−16.1± 0.4	157.3± 0.3
	2	3557± 211	−6.1±0.1	−1.9± 0.4	6.4± 0.2
	3	868± 178	−8.3±0.1	−8.2± 0.4	11.6± 0.3

EVENT	TRK	P(MEV)	ϕ(°)	δ(°)	θ(°)
	4	1404± 287	-11.5±0.1	-7.2± 0.4	13.5± 0.2
	5		94.7±0.1	61.0± 0.1	92.3± 0.0
351216	1		15.8±0.1	-11.4± 0.4	19.4± 0.2
	2	4335±1525	7.3±0.1	-6.7± 0.4	9.9± 0.3
	3		-1.1±0.1	9.2± 0.4	9.3± 0.4
	4	5893± 749	-1.8±0.1	-2.3± 0.4	2.9± 0.3
	5		-58.6±0.1	17.0± 0.3	60.1± 0.1
461363	1		3.1±0.1	1.2± 0.4	3.3± 0.2
	2		3.4±0.1	3.1± 0.4	4.6± 0.3
	3		6.6±0.1	8.9± 0.4	11.1± 0.3
	4		10.2±0.1	-23.3± 0.3	25.3± 0.3
	5		15.6±0.1	13.5± 0.3	20.5± 0.2
461430	1	676± 50	-27.6±0.1	4.6± 0.4	28.0± 0.1
	2		-21.7±0.1	-13.1± 0.3	25.2± 0.2
	3		12.4±0.1	10.2± 0.4	16.0± 0.3
	4		13.9±0.1	-27.1± 0.3	30.2± 0.3
	5	1494± 133	36.2±0.1	0.0± 0.0	36.2± 0.1
150005	1		56.3±0.1	-18.2± 0.4	58.2± 0.1
	2	136± 8	46.4±0.1	-11.5± 0.4	47.5± 0.1
	3	299± 43	10.6±0.1	-14.2± 0.3	17.7± 0.2
	4	773± 134	9.2±0.1	7.3± 0.4	11.7± 0.3
	5	2561± 613	6.5±0.1	11.1± 0.4	12.8± 0.3
	6		-9.8±0.1	-17.8± 0.3	20.2± 0.3
410006	1		28.1±0.1	15.7± 0.3	31.9± 0.2
	2	163± 38	15.6±0.1	4.7± 0.4	16.3± 0.1
	3	1110± 446	-0.9±0.1	-10.5± 0.4	10.5± 0.4
	4		-96.9±0.1	-23.5± 0.3	96.3± 0.1
	5		-137.9±0.1	-30.7± 0.3	129.6± 0.2
	6	2635± 620	-3.2±0.1	-4.1± 0.4	5.2± 0.3
150016	1		42.6±0.1	-53.5± 0.3	64.0± 0.2
	2		23.0±0.1	18.2± 0.4	29.0± 0.2
	4	958± 218	11.6±0.1	-1.8± 0.4	11.7± 0.1
	5		6.6±0.1	-5.1± 0.4	8.3± 0.3
	6		-21.4±0.1	-30.6± 0.9	36.7± 0.7
	7		11.9±0.1	-18.3± 0.3	21.7± 0.3
150018	1	383± 59	18.6±0.1	16.1± 0.3	24.4± 0.2
	2	984± 326	11.2±0.1	8.4± 0.4	14.0± 0.3
	3	6711±4251	-9.8±0.1	-2.5± 0.4	10.1± 0.1
	4	914± 155	-24.1±0.1	-7.8± 0.4	25.3± 0.1

EVENT	TRK	P(MEV)	$\phi(°)$	$\delta(°)$	$\theta(°)$
	5	673± 118	-29.0±0.1	-6.2± 0.4	29.6± 0.1
	6		-108.9±0.1	-17.1± 0.4	108.0± 0.1
150068	1	1136± 368	10.9±0.1	9.3± 0.4	14.3± 0.3
	2		5.2±0.1	-19.4± 1.0	20.1± 1.0
	3		1.8±0.1	-5.3± 0.4	5.6± 0.4
	4	9412±1557	-1.3±0.1	1.2± 0.4	1.8± 0.3
	5		-4.6±0.1	-19.0± 1.0	19.5± 1.0
	6	830± 132	-15.9±0.1	10.3± 0.4	18.9± 0.2
150083	1	1072± 137	25.5±0.1	7.9± 0.4	26.6± 0.1
	2		21.9±0.1	28.5± 0.7	35.4± 0.5
	3	6055±1159	0.3±0.1	-1.0± 0.4	1.0± 0.4
	4		-10.9±0.1	28.7± 0.7	30.5± 0.7
	5	1717± 156	-12.4±0.1	-2.0± 0.4	12.6± 0.1
	6		-67.2±0.1	25.3± 0.3	69.5± 0.1
150087	1		93.8±0.1	-56.0± 0.3	92.1± 0.1
	2	796± 161	22.5±0.1	-25.3± 0.3	33.4± 0.2
	3	843± 170	17.3±0.1	6.2± 0.4	18.3± 0.2
	4		0.6±0.1	27.1± 0.3	27.1± 0.3
	5		-10.5±0.1	7.6± 0.4	12.9± 0.2
	6		-4.8±0.1	-23.0± 0.3	23.5± 0.3
150131	1	393± 34	28.2±0.1	-6.1± 0.4	28.8± 0.1
	2		24.7±0.1	5.7± 0.4	25.3± 0.1
	3		7.6±0.1	32.3± 0.3	33.1± 0.3
	4		-0.9±0.1	4.2± 0.4	4.3± 0.4
	5	1750± 456	-1.2±0.1	-3.8± 0.4	4.0± 0.4
	6		-43.9±0.1	17.8± 0.3	46.7± 0.1
150173	1		25.9±0.1	12.9± 0.4	28.7± 0.2
	2	1106± 226	13.5±0.1	9.0± 0.4	16.2± 0.2
	3	816± 263	-15.1±0.1	10.0± 0.4	18.0± 0.2
	4	437± 43	-22.9±0.1	12.6± 0.4	26.0± 0.2
	5	1187± 118	-30.2±0.1	4.6± 0.4	30.5± 0.1
	6		-33.3±0.1	-26.0± 0.3	41.3± 0.2
150176	1		17.7±0.1	-26.9± 0.3	31.8± 0.3
	2		8.1±0.1	0.0± 0.0	8.1± 0.1
	3		5.8±0.1	-13.1± 0.4	14.3± 0.4
	4	5121±1499	-3.8±0.1	8.3± 0.4	9.1± 0.4
	5		-4.7±0.1	-28.9± 0.3	29.2± 0.3
	6		-17.1±0.1	-29.2± 0.3	33.5± 0.3

EVENT	TRK	P(MEV)	$\phi(^\circ)$	$\delta(^\circ)$	$\theta(^\circ)$
300211	1	1217± 169	13.9±0.1	4.8± 0.4	14.7± 0.2
	2	11048±1506	-0.1±0.1	2.6± 0.4	2.6± 0.4
	3		-0.6±0.1	-8.2± 0.4	8.2± 0.4
	4		-5.0±0.1	22.3± 0.3	22.8± 0.3
	5	1790± 378	-5.4±0.1	-6.1± 0.4	8.1± 0.3
	6	1294± 402	-15.7±0.1	3.9± 0.4	16.2± 0.1
300223	2	554± 48	24.9±0.1	-3.9± 0.4	25.2± 0.1
	4		9.0±0.1	-20.6± 0.3	22.4± 0.3
	5	3290± 356	5.8±0.1	-1.2± 0.4	5.9± 0.1
	6	3114± 538	-1.2±0.1	-2.5± 0.4	2.8± 0.4
	7	3706±1431	-4.8±0.1	5.4± 0.4	7.2± 0.3
	8	2661± 697	-9.7±0.1	-6.6± 0.4	11.7± 0.2
300225	1	6724±3527	12.6±0.1	0.0± 0.0	12.6± 0.1
	2	1800± 397	7.6±0.1	-5.2± 0.4	9.2± 0.2
	3	6408±1631	-0.8±0.1	-3.3± 0.4	3.4± 0.4
	4		-7.4±0.1	11.1± 0.4	13.3± 0.3
	5		-25.8±0.1	8.9± 0.4	27.2± 0.2
	6	199± 23	-79.0±0.1	-12.1± 0.4	79.2± 0.1
300226	1		37.2±0.1	19.9± 0.3	41.5± 0.1
	2		18.0±0.1	18.1± 0.3	25.3± 0.2
	4	2073± 276	-4.0±0.1	-4.9± 0.4	6.3± 0.3
	5	2581± 378	-7.4±0.1	0.0± 0.0	7.4± 0.1
	6		-8.9±0.1	-13.2± 0.4	15.9± 0.3
	7	769± 137	-16.8±0.1	-7.8± 0.4	18.5± 0.2
300260	1	5725±1241	5.2±0.1	2.2± 0.4	5.6± 0.2
	2		4.1±0.1	-24.3± 0.3	24.6± 0.3
	3	1938± 329	-8.9±0.1	6.7± 0.4	11.1± 0.3
	4		-22.6±0.1	34.3± 0.3	40.3± 0.2
	5		-47.0±0.1	-24.6± 0.3	51.7± 0.1
	6	1447± 308	-47.3±0.1	-10.2± 0.4	48.1± 0.1
310298	1		17.9±0.1	-20.6± 0.3	27.0± 0.2
	2		14.1±0.1	-4.7± 0.4	14.8± 0.2
	3		4.2±0.1	-8.2± 0.4	9.2± 0.4
	4	2831± 517	2.8±0.1	-2.5± 0.4	3.8± 0.3
	5	4410± 664	-1.7±0.1	2.2± 0.4	2.8± 0.3
	6	440± 90	-10.4±0.1	8.3± 0.4	13.3± 0.3
310308	1		78.9±0.1	18.7± 0.3	79.5± 0.1
	2		46.0±0.1	33.4± 0.3	54.6± 0.2
	3		21.1±0.1	-13.3± 0.4	24.8± 0.2

EVENT	TRK	P(MEV)	$\phi(^\circ)$	$\delta(^\circ)$	$\theta(^\circ)$
	4	442± 124	3.3±0.1	7.5± 0.4	8.2± 0.4
	5		-48.9±0.1	-10.2± 0.4	49.7± 0.1
	6		17.6±0.1	-41.4± 0.2	44.4± 0.2
310337	1		13.1±0.1	-27.6± 0.3	30.3± 0.3
	2	416± 21	11.5±0.1	0.6± 0.4	11.5± 0.1
	3		0.3±0.1	3.1± 0.4	3.1± 0.4
	4		-3.1±0.1	-8.9± 0.4	9.4± 0.4
	5	875± 280	-6.5±0.1	-7.2± 0.4	9.7± 0.3
	6		-51.8±0.1	18.3± 0.3	54.0± 0.1
310357	1	2592± 486	14.3±0.1	2.3± 0.4	14.5± 0.1
	2	241± 39	12.2±0.1	6.2± 0.4	13.7± 0.2
	3	1031± 162	11.4±0.1	-2.4± 0.4	11.6± 0.1
	4	2514± 787	7.3±0.1	3.6± 0.4	8.1± 0.2
	5	1283± 233	-2.5±0.1	-7.5± 0.4	7.9± 0.4
	6	722± 106	-5.6±0.1	-9.5± 0.4	11.0± 0.3
240412	1		41.1±0.1	-10.4± 0.4	42.2± 0.1
	2		25.3±0.1	18.0± 0.3	30.7± 0.2
	3		18.4±0.1	45.6± 0.2	48.4± 0.2
	4	252± 49	8.2±0.1	6.2± 0.4	10.3± 0.3
	5	9909±1503	-3.9±0.1	2.1± 0.4	4.4± 0.2
	6		-52.8±0.1	-42.0± 0.2	63.3± 0.1
240425	1		18.8±0.1	-26.8± 0.7	32.3± 0.6
	2	1098± 153	9.0±0.1	7.9± 0.4	12.0± 0.3
	3		4.8±0.1	-2.1± 0.4	5.2± 0.2
	4	3936± 623	-5.7±0.1	2.2± 0.4	6.1± 0.2
	5		-9.8±0.1	-14.5± 0.4	17.4± 0.3
	6		-16.0±0.1	-11.4± 0.4	19.6± 0.2
240429	1		104.1±0.1	-39.2± 0.7	100.9± 0.1
	2		93.8±0.1	-18.1± 0.7	93.6± 0.1
	3	490± 57	20.1±0.1	6.8± 0.1	21.2± 0.1
	4		5.4±0.1	-3.2± 0.4	6.3± 0.2
	5	768± 130	-22.6±0.1	3.2± 0.4	22.8± 0.1
	6	1174± 219	-26.2±0.1	5.6± 0.4	26.7± 0.1
240440	1		18.6±0.1	13.1± 0.3	22.6± 0.2
	2	3853± 616	0.3±0.1	2.2± 0.4	2.2± 0.4
	3		-8.8±0.1	13.6± 0.3	16.2± 0.3
	4		-10.2±0.1	17.3± 0.3	20.0± 0.3
	5		-72.7±0.1	-7.3± 0.4	72.8± 0.1
	6		-147.1±0.1	-42.4± 0.2	128.3± 0.2

EVENT	TRK	P(MEV)	ϕ(°)	δ(°)	Θ(°)
240465	1	1306± 221	18.4±0.1	-3.6± 0.4	18.7± 0.1
	2	7471± 903	-0.7±0.1	2.2± 0.4	2.3± 0.4
	3		-1.8±0.1	-18.4± 0.3	18.5± 0.3
	4		-7.0±0.1	17.9± 0.3	19.2± 0.3
	5	509± 24	-5.5±0.1	-6.6± 0.4	8.6± 0.3
	6	65± 1	0.0±0.1	89.7± 0.0	89.7± 0.0
240468	1		91.1±0.1	-74.8± 0.2	90.3± 0.0
	2	1028± 40	12.6±0.1	0.0± 0.0	12.6± 0.1
	3	3883± 493	6.4±0.1	0.0± 0.0	6.4± 0.1
	4		-2.5±0.1	-11.6± 0.4	11.9± 0.4
	5	604± 52	-6.1±0.1	8.1± 0.4	10.1± 0.3
	6		-63.5±0.1	-35.0± 0.3	68.6± 0.1
240477	1		61.6±0.1	-22.2± 0.3	63.9± 0.1
	2	324± 86	12.9±0.1	-3.1± 0.4	13.3± 0.1
	3	2866± 781	1.5±0.1	4.2± 0.4	4.5± 0.4
	4	674± 71	-16.4±0.1	3.8± 0.4	16.8± 0.1
	5	433± 95	-35.7±0.1	4.4± 0.4	35.9± 0.1
	6		-66.4±0.1	-62.5± 0.4	79.3± 0.2
240486	1		27.7±0.1	15.8± 0.4	31.6± 0.2
	2		27.1±0.1	-22.0± 0.3	34.4± 0.2
	3		9.9±0.1	-10.6± 0.4	14.5± 0.3
	4		9.1±0.1	16.4± 0.3	18.7± 0.3
	5	6092± 404	-2.5±0.1	0.0± 0.0	2.5± 0.1
	6		-9.1±0.1	-12.3± 0.3	15.3± 0.2
240517	1		13.3±0.1	-11.2± 0.5	17.3± 0.3
	2		12.9±0.1	-50.4± 0.4	51.6± 0.4
	3	2944± 254	1.4±0.1	3.7± 0.4	4.0± 0.4
	4	4444±1878	-7.3±0.1	-2.5± 0.4	7.7± 0.2
	5		-8.0±0.1	20.0± 0.4	21.5± 0.4
	6	2214± 272	-7.2±0.1	3.3± 0.4	7.9± 0.2
240530	1		66.1±0.1	13.8± 0.3	66.8± 0.1
	2		51.0±0.1	-37.1± 0.6	59.9± 0.3
	3	1681± 384	19.4±0.1	-4.2± 0.4	19.8± 0.1
	4	632± 73	5.3±0.1	6.7± 0.4	8.5± 0.3
	5		-7.8±0.1	17.9± 0.4	19.5± 0.4
	6		-104.4±0.1	28.2± 0.3	102.7± 0.1
240557	1	374± 38	5.1±0.1	7.6± 0.4	9.1± 0.3
	2	849± 106	4.5±0.1	9.1± 0.5	10.1± 0.4
	3	3007± 286	3.8±0.1	-4.6± 0.4	6.0± 0.3
	4	1273± 232	-5.7±0.1	-3.5± 0.4	6.7± 0.2

EVENT	TRK	P(MEV)	ϕ(°)	δ(°)	θ(°)
	5		−25.1±0.1	−11.3± 0.3	27.4± 0.1
	6		−61.8±0.1	11.6± 0.3	62.4± 0.1
240558	1		18.2±0.1	−26.3± 0.3	31.6± 0.2
	2	299± 52	11.6±0.1	−11.1± 0.3	16.0± 0.2
	3	1005± 78	−10.5±0.1	0.0± 0.0	10.5± 0.1
	4		−15.3±0.1	29.2± 0.3	32.6± 0.3
	5	3313± 884	−16.5±0.1	−2.9± 0.4	16.7± 0.1
	6		−125.4±0.1	37.4± 0.2	117.4± 0.1
150031	1		4.3±0.1	−12.2± 0.4	12.9± 0.4
	2		2.1±0.1	25.6± 0.3	25.7± 0.3
	3		0.0±0.1	−7.7± 0.4	7.7± 0.4
	4	575± 125	−11.8±0.1	12.1± 0.4	16.8± 0.3
	5	1035± 495	−12.3±0.1	−3.1± 0.4	12.7± 0.1
	6	2696±1590	−17.6±0.1	9.7± 0.4	20.0± 0.2
	7		−59.2±0.1	−35.6± 0.2	65.4± 0.1
150040	1		13.8±0.1	15.9± 0.4	20.9± 0.3
	2	1557± 393	8.4±0.0	−3.2± 0.3	9.0± 0.1
	3	1416± 388	2.5±0.1	12.3± 0.4	12.5± 0.4
	4		−6.7±0.1	−17.3± 0.3	18.5± 0.3
	5	794± 62	−20.0±0.1	−15.0± 0.3	24.8± 0.2
	6		−66.3±0.1	36.8± 0.2	71.2± 0.1
	7		13.1±0.1	−23.6± 0.3	26.8± 0.3
150043	1		−10.1±0.1	16.8± 0.3	19.5± 0.3
	2		−14.3±0.1	19.1± 0.3	23.7± 0.2
	3		−17.7±0.1	47.9± 0.2	50.3± 0.2
	4		−27.4±0.1	−49.0± 0.4	54.4± 0.3
	5	465± 36	−38.4±0.1	2.7± 0.4	38.5± 0.1
	6		−53.2±0.1	−9.1± 0.4	53.7± 0.1
	7		−46.4±0.1	50.7± 0.2	64.1± 0.1
150110	1	1109± 272	38.7±0.1	8.6± 0.4	39.5± 0.1
	2		9.0±0.1	15.5± 0.3	17.9± 0.3
	3	1359± 131	4.4±0.1	4.8± 0.4	6.5± 0.3
	4		−3.0±0.1	−18.5± 0.3	18.7± 0.3
	5		−2.6±0.1	−10.4± 0.4	10.7± 0.4
	6	124± 16	−53.5±0.1	15.7± 0.4	55.1± 0.1
	7		−58.7±0.1	23.0± 0.3	61.4± 0.1
150125	1		42.0±0.1	−18.0± 0.3	45.0± 0.1
	2		28.4±0.1	−12.7± 0.4	30.9± 0.2
	3	3829± 933	−2.2±0.1	1.3± 0.4	2.6± 0.2
	4		−5.9±0.1	19.0± 0.3	19.9± 0.3

EVENT	TRK	P(MEV)	$\phi(^\circ)$	$\delta(^\circ)$	$\theta(^\circ)$
	5	457± 80	-15.8±0.1	-9.0± 0.4	18.1± 0.2
	6		-34.8±0.1	-14.3± 0.3	37.3± 0.1
	7	706± 163	-53.4±0.1	2.2± 0.4	53.4± 0.1
150136	1		67.5±0.1	-25.4± 0.3	69.8± 0.1
	2	312± 56	16.6±0.1	-6.2± 0.4	17.7± 0.2
	3		13.1±0.1	-5.7± 0.4	14.3± 0.2
	4	1695± 514	8.9±0.1	-4.3± 0.4	9.9± 0.2
	5	4119± 398	4.0±0.1	2.2± 0.4	4.6± 0.2
	6	2466± 515	5.2±0.1	-4.4± 0.4	6.8± 0.3
	7		-45.4±0.1	-9.0± 0.4	46.1± 0.1
150156	1		7.8±0.1	-16.8± 0.3	18.5± 0.3
	2	5585±1053	6.9±0.1	-6.6± 0.4	9.5± 0.3
	3	1110± 377	3.0±0.1	-6.4± 0.4	7.1± 0.4
	4	1677± 417	-2.8±0.1	-9.0± 0.4	9.4± 0.4
	5	2452± 610	-11.5±0.1	3.7± 0.4	12.1± 0.2
	6		-24.0±0.1	10.7± 0.4	26.1± 0.2
	7		-14.4±0.1	10.9± 0.4	18.0± 0.3
150157	1		91.2±0.1	-2.3± 0.4	91.2± 0.1
	2		3.2±0.1	8.8± 0.4	9.4± 0.4
	3	2114± 183	-1.0±0.1	3.1± 0.4	3.3± 0.4
	4		-8.7±0.1	20.4± 0.3	22.1± 0.3
	5	1805± 418	-11.6±0.1	5.9± 0.4	13.0± 0.2
	6		-18.6±0.1	11.6± 0.4	21.8± 0.2
	7		-26.7±0.1	7.9± 0.4	27.8± 0.1
300195	1	285± 54	42.9±0.1	-7.4± 0.4	43.4± 0.1
	2	1953± 189	-1.3±0.1	2.3± 0.4	2.6± 0.4
	3		-28.9±0.1	-41.9± 0.2	49.3± 0.2
	4	616± 44	32.4±0.1	0.3± 0.3	32.4± 0.1
	5	624± 43	13.9±0.1	2.6± 0.4	14.1± 0.1
	6		11.2±0.1	-49.4± 0.2	50.3± 0.2
	7		9.2±0.1	-23.3± 0.4	25.0± 0.4
300231	1		50.3±0.1	34.1± 0.2	58.1± 0.1
	2		37.2±0.1	60.7± 0.3	67.1± 0.2
	3		25.6±0.1	34.7± 0.2	42.1± 0.2
	4	734± 39	-3.3±0.1	0.0± 0.0	3.3± 0.1
	5	371± 107	-5.1±0.1	4.6± 0.4	6.9± 0.3
	6	1738± 450	-9.5±0.1	-5.9± 0.4	11.2± 0.2
	7	953± 114	-18.0±0.1	-4.6± 0.4	18.6± 0.1

EVENT	TRK	P(MEV)	$\phi(^\circ)$	$\delta(^\circ)$	$\theta(^\circ)$
300235	1	1342± 312	22.0±0.1	2.6± 0.4	22.1± 0.1
	2		16.6±0.1	-16.0± 0.3	22.9± 0.2
	3	2051± 348	6.9±0.1	-17.9± 0.3	19.1± 0.3
	4	2042± 603	5.4±0.1	5.0± 0.4	7.4± 0.3
	5		6.4±0.1	-3.7± 0.4	7.4± 0.2
	6		-3.9±0.1	18.7± 0.4	19.1± 0.4
	7	4667± 868	-7.5±0.1	-3.7± 0.4	8.4± 0.2
300269	1	525± 33	36.6±0.1	10.7± 0.4	37.9± 0.1
	2	2278± 585	32.6±0.1	-12.8± 0.4	34.9± 0.2
	3	706± 144	20.6±0.1	-18.5± 0.3	27.4± 0.2
	4	1300± 145	14.2±0.1	1.5± 0.4	14.3± 0.1
	5	840± 185	5.5±0.1	-10.1± 0.4	11.5± 0.4
	6	391± 49	-38.7±0.1	-13.3± 0.4	40.6± 0.1
	7		-60.7±0.1	-13.2± 0.4	61.5± 0.1
310299	1		97.3±0.1	-17.6± 0.3	97.0± 0.1
	2		10.6±0.1	-7.9± 0.4	13.2± 0.2
	3		9.7±0.1	-7.3± 0.4	12.1± 0.3
	4	1052± 263	1.5±0.1	6.1± 0.4	6.3± 0.4
	5		-6.3±0.1	18.2± 0.3	19.2± 0.3
	6	906± 114	-8.5±0.1	0.0± 0.0	8.5± 0.1
	7		-16.0±0.1	19.3± 0.3	24.9± 0.2
310309	1	1881± 666	4.7±0.1	-1.3± 0.4	4.9± 0.1
	2		-3.3±0.1	-5.6± 0.4	6.5± 0.3
	3	1847± 552	-6.0±0.1	11.4± 0.4	12.9± 0.4
	4	622± 125	-6.7±0.1	-1.8± 0.4	6.9± 0.1
	5		-8.8±0.1	-7.3± 0.4	11.4± 0.3
	6		-42.2±0.1	-35.7± 0.2	53.0± 0.1
	7		26.5±0.1	-20.8± 0.3	33.2± 0.2
310312	1		5.2±0.1	16.3± 0.4	17.1± 0.4
	2	5035± 341	0.3±0.1	1.7± 0.4	1.7± 0.4
	3	3281± 861	-6.7±0.1	6.2± 0.4	9.1± 0.3
	4		-34.3±0.1	-6.2± 0.4	34.8± 0.1
	5		-34.6±0.1	-20.6± 0.3	39.6± 0.2
	6		-52.7±0.1	43.3± 0.2	63.8± 0.1
	7		-141.3±0.1	-39.0± 0.2	127.3± 0.1
240407	1		14.0±0.1	-10.6± 0.4	17.5± 0.3
	2		-0.1±0.1	15.7± 0.4	15.7± 0.4
	3	3435± 291	-1.5±0.1	-1.7± 0.4	2.3± 0.3
	4	476± 45	-2.1±0.1	-7.4± 0.4	7.7± 0.4
	5	1391± 222	-8.8±0.1	-1.7± 0.4	9.0± 0.1

EVENT	TRK	P(MEV)	$\phi(^\circ)$	$\delta(^\circ)$	$\theta(^\circ)$
	6	987± 67	-12.1±0.1	0.0± 0.0	12.1± 0.1
	7		-26.8±0.1	27.4± 0.3	37.5± 0.2
240437	1		15.3±0.1	9.6± 0.4	18.0± 0.2
	2		6.9±0.1	-12.9± 0.4	14.6± 0.4
	3	833± 85	-1.5±0.1	-6.4± 0.4	6.6± 0.4
	4		-2.9±0.1	-38.9± 0.2	39.0± 0.2
	5		-6.0±0.1	-28.3± 0.3	28.9± 0.3
	6	1064± 167	-15.9±0.1	-5.9± 0.4	16.9± 0.2
	7		12.1±0.1	4.5± 0.4	12.9± 0.2
240455	1		40.7±0.1	14.5± 0.4	42.8± 0.1
	2	3781± 300	-8.6±0.1	0.0± 0.0	8.6± 0.1
	3		-21.0±0.1	-18.3± 0.3	27.6± 0.2
	4		-45.8±0.1	10.4± 0.4	46.7± 0.1
	5		-40.2±0.1	-16.9± 0.4	43.0± 0.2
	6		104.8±0.1	21.9± 0.3	103.7± 0.1
	7		-57.8±0.1	39.3± 0.2	65.6± 0.1
240457	1	149± 10	82.1±0.1	-1.3± 0.4	82.1± 0.1
	2		1.7±0.1	17.0± 0.4	17.1± 0.4
	3	927± 317	0.7±0.1	9.1± 0.4	9.1± 0.4
	4		-1.6±0.1	-9.2± 0.4	9.3± 0.4
	5	2113± 649	-6.3±0.1	-1.0± 0.4	6.4± 0.1
	6		-8.3±0.1	-3.4± 0.4	9.0± 0.2
	7	5316±1118	-9.4±0.1	-1.6± 0.4	9.5± 0.1
240521	1	531± 85	16.9±0.1	-3.6± 0.4	17.3± 0.1
	2		12.6±0.1	-3.7± 0.4	13.1± 0.1
	3		8.8±0.1	-11.8± 0.4	14.7± 0.3
	4	344± 33	8.9±0.1	10.2± 0.4	13.5± 0.3
	5	3517± 243	-1.0±0.1	2.6± 0.4	2.8± 0.4
	6		-4.9±0.1	-5.0± 0.4	7.0± 0.3
	7	376± 42	-8.9±0.1	9.7± 0.4	13.1± 0.3
461352	1	152± 27	-102.1±0.1	10.1± 0.4	101.9± 0.1
	2		20.8±0.1	-4.0± 0.4	21.2± 0.1
	3	778± 77	8.1±0.1	4.8± 0.4	9.4± 0.2
	4	1636± 130	0.5±0.1	2.3± 0.4	2.4± 0.4
	5		4.5±0.1	-12.3± 0.3	13.1± 0.3
	6	1329± 244	10.8±0.1	0.0± 0.0	10.8± 0.1
	7	500± 32	14.0±0.1	6.5± 0.4	15.4± 0.2
182966	1		-16.3±0.1	7.8± 0.4	18.0± 0.2
	2		-0.7±0.1	12.0± 0.4	12.0± 0.4
	3	5688±2503	0.3±0.1	-5.9± 0.4	5.9± 0.4
	4		6.9±0.1	-9.3± 0.4	10.7± 0.3

EVENT	TRK	P(MEV)	$\phi(^\circ)$	$\delta(^\circ)$	$\theta(^\circ)$
	5	3773± 178	6.8±0.1	0.0± 0.0	6.8± 0.1
	6		18.3±0.1	23.4± 0.3	29.4± 0.2
	7		34.3±0.1	-42.3± 0.2	52.3± 0.2
150019	1		55.1±0.1	-41.7± 0.2	64.7± 0.1
	2		35.1±0.1	-39.1± 0.6	49.9± 0.4
	3	2421± 340	-3.4±0.1	0.0± 0.3	3.4± 0.1
	4		-6.7±0.1	-5.5± 0.4	8.7± 0.3
	5		-12.6±0.1	-58.4± 0.1	59.2± 0.1
	6	1051± 69	-13.5±0.1	0.0± 0.0	13.5± 0.1
	7		-40.2±0.1	-26.7± 0.3	47.0± 0.2
	8		-45.5±0.1	28.2± 0.3	51.8± 0.1
150024	1	2160± 521	18.2±0.1	16.7± 0.3	24.5± 0.2
	2	420± 47	9.2±0.1	-9.2± 0.4	13.0± 0.3
	3	3982± 983	5.5±0.1	2.4± 0.4	6.0± 0.2
	4		3.7±0.1	-17.7± 0.3	18.1± 0.3
	5	1588± 305	0.9±0.1	5.0± 0.4	5.1± 0.4
	6	688± 359	0.8±0.1	-13.7± 0.3	13.7± 0.3
	7	837± 91	-7.1±0.1	0.0± 0.0	7.1± 0.1
	8		-36.3±0.1	-13.6± 0.4	38.4± 0.2
150057	1		24.6±0.1	17.0± 0.4	29.6± 0.2
	2	132± 26	13.3±0.1	16.1± 0.2	20.8± 0.2
	3	9017±1942	4.0±0.1	4.6± 0.4	6.1± 0.3
	4		-0.8±0.1	11.3± 0.4	11.3± 0.4
	5		-9.4±0.1	10.5± 0.7	14.1± 0.5
	6	233± 25	-19.2±0.1	0.0± 0.0	19.2± 0.1
	7	473± 28	-22.0±0.1	-2.3± 0.2	22.1± 0.1
	8		-52.9±0.1	41.6± 0.2	63.2± 0.1
150094	1		23.9±0.1	-45.1± 0.2	49.8± 0.2
	2		22.1±0.1	16.1± 0.3	27.1± 0.2
	3		15.6±0.1	-24.1± 0.3	28.5± 0.3
	4		5.9±0.1	28.4± 0.3	29.0± 0.3
	5		-10.6±0.1	-26.0± 0.3	27.9± 0.3
	6	846± 526	-21.2±0.1	12.9± 0.3	24.7± 0.2
	7	489± 99	-32.3±0.1	-14.9± 0.3	35.2± 0.1
	8	185± 27	-124.6±0.1	14.3± 0.6	123.4± 0.1
150165	1		27.0±0.1	-17.8± 0.5	32.0± 0.3
	2		22.4±0.1	-31.1± 1.3	37.7± 1.0
	3		12.9±0.1	35.1± 0.2	37.1± 0.2
	4		-3.2±0.1	33.4± 0.3	33.5± 0.3
	5		-7.4±0.1	-9.3± 0.4	11.9± 0.3

EVENT	TRK	P(MEV)	ϕ(°)	δ(°)	θ(°)
	6		-29.5±0.1	-28.8± 1.5	40.3± 1.0
	7		-35.7±0.1	-23.9± 1.0	42.1± 0.5
	8		-47.2±0.1	-1.4± 0.4	47.2± 0.1
300200	1	1335± 352	10.7±0.1	6.4± 0.4	12.4± 0.2
	2		5.9±0.1	-16.0± 0.2	17.0± 0.3
	3	6131±2036	-3.3±0.1	6.6± 0.4	7.4± 0.4
	4	986± 46	-6.2±0.1	2.8± 0.4	6.8± 0.2
	5		-11.6±0.1	-9.2± 0.4	14.8± 0.3
	6	2414± 756	-12.3±0.1	8.7± 0.4	15.0± 0.2
	7	323± 67	-150.2±0.1	11.4± 0.4	148.3± 0.2
	8		-11.4±0.1	-29.4± 0.3	31.3± 0.3
300221	1		13.0±0.1	-14.3± 0.4	19.2± 0.3
	2	3444± 451	0.6±0.1	1.9± 0.4	2.0± 0.4
	3		-1.3±0.1	9.7± 0.4	9.8± 0.4
	4	662± 120	-2.3±0.1	-1.5± 0.4	2.7± 0.2
	5	2525± 493	-3.2±0.1	-3.0± 0.4	4.4± 0.3
	6		-12.0±0.1	16.0± 0.4	19.9± 0.3
	7	698± 217	-12.4±0.1	2.4± 0.4	12.6± 0.1
	8		-12.4±0.1	25.0± 0.3	27.7± 0.3
300229	1		106.3±0.1	-23.8± 0.3	104.9± 0.1
	2		102.9±0.1	6.1± 0.4	102.8± 0.1
	3	311± 74	81.7±0.1	-5.4± 0.4	81.7± 0.1
	4		20.6±0.1	36.9± 0.2	41.5± 0.2
	5		2.7±0.1	26.1± 0.3	26.2± 0.3
	6		-5.5±0.1	25.2± 0.3	25.8± 0.3
	7		-46.4±0.1	19.6± 0.3	49.5± 0.1
	8		-47.7±0.1	-71.9± 0.1	77.9± 0.1
300289	1	459± 151	98.0±0.1	-8.2± 0.4	97.9± 0.1
	2		27.7±0.1	17.4± 0.3	32.3± 0.2
	3	129± 15	24.4±0.1	5.3± 0.4	24.9± 0.1
	4		21.9±0.1	11.5± 0.4	24.6± 0.2
	5		12.4±0.1	-19.5± 0.3	23.0± 0.3
	6	185± 21	9.1±0.1	-10.4± 0.4	13.9± 0.3
	7	2582±1478	4.5±0.1	-6.4± 0.4	7.8± 0.3
	8		-38.4±0.1	31.8± 0.3	48.2± 0.2
310306	1	595± 103	99.5±0.1	-3.8± 0.4	99.5± 0.1
	2		80.1±0.1	-17.6± 0.2	80.3± 0.1
	3		9.7±0.1	22.9± 0.3	24.8± 0.3
	4	710± 119	0.8±0.1	-4.6± 0.4	4.7± 0.4
	5		-6.7±0.1	11.1± 0.4	12.9± 0.3

EVENT	TRK	P(MEV)	$\phi(^\circ)$	$\delta(^\circ)$	$\theta(^\circ)$
	6		-20.7±0.1	-27.0± 0.3	33.5± 0.2
	7		-36.3±0.1	17.9± 0.3	39.9± 0.1
	8		-62.5±0.1	31.7± 0.3	66.9± 0.1
310326	1	1127± 214	29.8±0.1	7.3± 0.4	30.6± 0.1
	2	5511±1690	-5.0±0.1	3.2± 0.4	5.9± 0.2
	3		-10.2±0.1	-29.2± 0.3	30.8± 0.3
	4	293± 44	-10.2±0.1	-5.4± 0.4	11.5± 0.2
	5	837± 171	-14.0±0.1	-4.8± 0.4	14.8± 0.2
	6		-16.2±0.1	-17.0± 0.3	23.3± 0.2
	7		-18.1±0.1	-11.4± 0.4	21.3± 0.2
	8		35.0±0.1	-45.9± 0.2	55.2± 0.2
310339	1	546± 22	48.0±0.1	2.7± 0.4	48.1± 0.1
	2		7.9±0.1	-27.0± 0.3	28.0± 0.3
	3		3.7±0.1	-7.5± 0.4	8.4± 0.4
	4	5415± 918	-0.8±0.1	0.0± 0.0	0.8± 0.1
	5	2298± 701	-11.4±0.1	8.5± 0.4	14.2± 0.2
	6	2720± 466	-15.8±0.1	11.0± 0.4	19.2± 0.2
	7	666± 132	-34.7±0.1	-1.3± 0.4	34.7± 0.1
	8		34.3±0.1	23.8± 0.3	40.9± 0.2
310342	1		27.7±0.1	22.6± 0.3	35.2± 0.2
	2	1176± 258	22.4±0.1	10.2± 0.4	24.5± 0.2
	3		11.8±0.1	-0.2± 0.4	14.9± 0.3
	4		7.0±0.1	-7.0± 0.4	9.9± 0.3
	5		2.8±0.1	25.5± 0.3	25.6± 0.3
	6	151± 20	-4.6±0.1	10.1± 0.4	11.1± 0.4
	7		-4.8±0.1	-7.9± 0.4	9.2± 0.3
	8		-99.2±0.1	35.8± 0.2	97.4± 0.1
310355	1		137.9±0.1	-24.9± 0.2	132.3± 0.2
	2		21.1±0.1	-11.8± 0.4	24.0± 0.2
	3		15.3±0.1	-21.2± 0.3	25.9± 0.2
	4		-4.7±0.1	-2.2± 0.4	5.2± 0.2
	5	886± 306	-7.0±0.1	8.6± 0.4	11.1± 0.3
	6	2446± 536	-14.3±0.1	3.2± 0.4	14.6± 0.1
	7		-77.0±0.1	12.8± 0.4	77.3± 0.1
	8		-31.9±0.1	37.6± 0.2	47.7± 0.2
240404	1		76.3±0.1	-28.7± 0.3	78.0± 0.1
	2		12.5±0.1	7.8± 0.4	14.7± 0.2
	3		2.0±0.1	6.3± 0.4	6.6± 0.4
	4	1275± 166	-0.5±0.1	-5.7± 0.4	5.7± 0.4
	5	2826± 970	-1.8±0.1	1.7± 0.4	2.5± 0.3

EVENT	TRK	P(MEV)	$\phi(^\circ)$	$\delta(^\circ)$	$\theta(^\circ)$
	6		-5.4±0.1	11.7± 0.3	12.9± 0.3
	7		-16.6±0.1	-27.6± 0.3	31.9± 0.3
	8		-109.2±0.1	-24.6± 0.3	107.4± 0.1
240423	1		45.0±0.1	-9.1± 0.4	45.7± 0.1
	2		32.9±0.1	-61.1± 0.4	66.1± 0.3
	3		0.9±0.1	22.9± 0.3	22.9± 0.3
	4	402± 86	-0.3±0.1	2.3± 0.4	2.3± 0.4
	5		17.1±0.1	-14.2± 0.3	22.1± 0.2
	6		-21.6±0.1	-2.3± 0.4	21.7± 0.1
	7	759± 160	-32.9±0.1	6.7± 0.4	33.5± 0.1
	8		-37.9±0.1	69.5± 0.2	74.0± 0.2
240424	1		32.3±0.1	17.0± 0.3	36.1± 0.2
	3		17.8±0.1	-9.1± 0.4	19.9± 0.2
	4	2180± 986	-5.2±0.1	-6.3± 0.5	8.2± 0.4
	5		-8.9±0.1	-13.9± 0.3	16.5± 0.3
	6		-9.9±0.1	-16.7± 0.3	19.3± 0.3
	7		-16.4±0.1	-10.5± 0.4	19.4± 0.2
	8		-30.7±0.1	37.7± 0.2	47.1± 0.2
	9		-101.5±0.1	43.4± 0.2	98.3± 0.1
240448	1		73.6±0.1	-14.3± 0.3	74.1± 0.1
	2	852± 243	45.4±0.1	5.0± 0.4	45.6± 0.1
	3	486± 82	22.6±0.1	0.0± 0.0	22.6± 0.1
	4		15.2±0.1	31.1± 0.3	34.3± 0.3
	5	934± 408	5.8±0.1	-1.9± 0.4	6.1± 0.2
	6	582± 68	1.1±0.1	8.6± 0.4	8.7± 0.4
	7		-3.7±0.1	-9.1± 0.4	9.8± 0.4
	8	1031± 218	-4.6±0.1	4.7± 0.4	6.6± 0.3
240470	1		36.1±0.1	-25.3± 0.3	43.1± 0.2
	2	317± 44	29.2±0.1	7.7± 0.4	30.1± 0.1
	3		14.2±0.1	26.4± 0.3	29.7± 0.3
	4		8.0±0.1	21.0± 0.3	22.4± 0.3
	5		-18.3±0.1	-41.7± 0.3	44.9± 0.3
	6		-19.7±0.1	73.6± 0.1	74.6± 0.1
	7		-33.7±0.1	-26.9± 0.3	42.1± 0.2
	8		-109.4±0.1	-21.4± 0.3	108.0± 0.1
240496	1	461± 89	27.3±0.1	6.2± 0.4	27.9± 0.1
	2		19.0±0.1	-18.3± 0.3	26.1± 0.2
	3	276± 13	18.3±0.1	11.5± 0.4	21.5± 0.2
	4	1559± 672	15.1±0.1	-1.0± 0.4	15.1± 0.1
	5	910± 68	1.9±0.1	0.0± 0.0	1.9± 0.1

EVENT	TRK	P(MEV)	$\phi(^\circ)$	$\delta(^\circ)$	$\theta(^\circ)$
	6		-4.4±0.1	-7.9± 0.4	9.0± 0.4
	7	726± 160	-15.4±0.1	4.6± 0.4	16.1± 0.1
	8	220± 23	-57.5±0.1	3.9± 0.4	57.6± 0.1
240535	1		9.4±0.1	25.4± 0.3	27.0± 0.3
	2		6.4±0.1	0.0± 0.0	6.4± 0.1
	3	2067± 222	6.0±0.1	-2.4± 0.4	6.5± 0.2
	4	3237±1039	5.4±0.1	-7.1± 0.4	8.9± 0.3
	5	476± 52	3.2±0.1	9.8± 0.4	10.3± 0.4
	6		-4.8±0.1	-35.9± 0.2	36.2± 0.2
	7		-16.7±0.1	17.7± 0.3	24.1± 0.2
	9		-43.0±0.1	-28.7± 0.3	50.1± 0.2
240554	1		161.3±0.1	25.4± 0.3	148.9± 0.2
	2		72.2±0.1	-17.0± 0.3	73.0± 0.1
	3	314± 13	58.1±0.1	0.0± 0.0	58.1± 0.1
	4	845± 251	10.6±0.1	6.9± 0.4	12.6± 0.2
	5	346± 83	7.6±0.1	-5.7± 0.4	9.5± 0.3
	6	3958± 697	4.1±0.1	-0.8± 0.4	4.2± 0.1
	7		-8.6±0.1	17.8± 0.4	19.7± 0.4
	8	1048± 184	-19.0±0.1	-4.6± 0.4	19.5± 0.1
201020	1	246± 20	24.1±0.1	-13.4± 0.3	27.4± 0.2
	2	1575± 495	21.3±0.1	-2.0± 0.4	21.4± 0.1
	3	2270± 922	16.3±0.1	9.3± 0.5	18.7± 0.3
	4	394± 92	16.3±0.1	13.3± 0.5	20.9± 0.3
	5	2367± 701	-13.5±0.1	6.3± 0.4	14.9± 0.2
	6	235± 34	-31.2±0.1	11.1± 0.4	32.9± 0.2
	7		-126.9±0.1	-31.1± 0.3	120.9± 0.1
	8		-17.8±0.1	31.0± 0.3	35.3± 0.3
201023	1		5.7±0.1	22.6± 0.3	23.3± 0.3
	2	729± 143	2.6±0.1	4.1± 0.4	4.9± 0.3
	3		-7.5±0.1	54.2± 0.3	54.6± 0.3
	4	1836± 228	-10.2±0.1	-2.3± 0.4	10.5± 0.1
	5		-21.2±0.1	22.7± 0.3	30.7± 0.2
	6		-30.0±0.1	-83.0± 0.0	83.9± 0.0
	7	583± 220	-67.2±0.1	15.6± 0.3	68.1± 0.1
	8		115.2±0.1	41.9± 0.7	108.5± 0.2
461392	1		80.0±0.1	43.5± 0.5	92.9± 0.1
	2		14.4±0.1	-31.2± 0.3	34.1± 0.3
	3		6.7±0.1	26.2± 0.3	27.0± 0.3
	4	1719± 229	-3.2±0.1	2.9± 0.4	4.3± 0.3
	5	1207± 167	-7.0±0.1	0.0± 0.0	7.0± 0.1

EVENT	TRK	P(MEV)	$\phi(^\circ)$	$\delta(^\circ)$	$\theta(^\circ)$
	6	4458± 490	-7.9±0.1	1.9± 0.4	8.1± 0.1
	7	241± 60	-18.3±0.1	6.4± 0.4	19.4± 0.2
	8		6.5±0.1	35.8± 0.2	36.3± 0.2
150030	1		169.2±0.1	-53.6± 0.3	125.7± 0.3
	2		44.8±0.1	26.0± 0.3	50.4± 0.1
	4		22.6±0.1	21.7± 0.3	30.9± 0.2
	5		-9.6±0.1	-29.8± 0.3	31.2± 0.3
	6	2108± 501	-10.7±0.1	-2.8± 0.4	11.1± 0.1
	7		-16.6±0.1	-18.7± 0.3	24.9± 0.2
	8		-22.4±0.1	2.1± 0.4	22.5± 0.1
	9	275± 45	-48.9±0.1	1.1± 0.1	48.9± 0.1
	11		-173.1±0.1	-44.9± 0.2	134.7± 0.2
150035	1	1872± 112	25.1±0.1	13.5± 0.4	28.3± 0.2
	2		11.7±0.1	-9.2± 0.4	14.8± 0.3
	3		10.6±0.1	16.9± 0.3	19.9± 0.3
	4		4.4±0.1	-10.7± 0.4	11.6± 0.4
	5	2778± 976	1.7±0.1	6.9± 0.4	7.1± 0.4
	6	2297±1255	-5.6±0.1	-3.7± 0.4	6.7± 0.2
	7	2244± 662	-9.3±0.1	-2.9± 0.4	9.7± 0.2
	8	659± 228	-19.7±0.1	-8.1± 0.4	21.2± 0.2
	9	602± 96	-21.2±0.1	-1.6± 0.4	21.3± 0.1
150037	1		18.5±0.1	-15.9± 0.3	24.2± 0.2
	2	4382±1998	-0.3±0.1	-3.7± 0.4	3.7± 0.4
	3		-0.9±0.1	-13.2± 0.4	13.2± 0.4
	4	12198±2489	-1.9±0.1	-1.7± 0.4	2.5± 0.3
	5	1127± 324	-10.1±0.1	-6.4± 0.4	11.9± 0.2
	6		-19.0±0.1	-7.9± 0.4	20.5± 0.2
	7	1023± 408	-19.4±0.1	23.9± 0.3	30.4± 0.2
	8		-68.9±0.1	33.6± 0.3	72.6± 0.1
	9	729± 144	-76.4±0.1	-6.4± 0.4	76.5± 0.1
150096	1	2396± 622	9.0±0.1	8.9± 0.4	12.6± 0.3
	2	2370± 234	3.7±0.1	0.0± 0.0	3.7± 0.1
	3		2.7±0.1	11.1± 0.4	11.4± 0.4
	4	5030±1131	-2.3±0.1	-5.3± 0.4	5.8± 0.4
	5		-4.8±0.1	-9.1± 0.4	10.3± 0.4
	6	204± 41	-10.3±0.1	6.8± 0.4	12.3± 0.2
	7	1209± 200	-11.5±0.1	-4.3± 0.4	12.3± 0.2
	8	144± 43	-19.2±0.1	-1.8± 0.4	19.3± 0.1

EVENT	TRK	P(MEV)	ϕ(°)	δ(°)	θ(°)
	9	321± 62	-70.6±0.1	-16.2± 0.3	71.4± 0.1
150120	1		35.7±0.1	-20.5± 0.3	40.5± 0.2
	2	905± 44	20.9±0.1	0.0± 0.0	20.9± 0.1
	3	1032± 517	20.4±0.1	-9.3± 0.4	22.3± 0.2
	4		20.9±0.1	-15.9± 0.4	26.0± 0.2
	5		6.2±0.1	52.9± 0.1	53.2± 0.1
	6		1.9±0.1	-45.0± 0.6	45.0± 0.6
	7		-2.6±0.1	-14.1± 0.4	14.3± 0.4
	8		-37.8±0.1	65.6± 0.3	70.9± 0.2
	10		5.8±0.1	-48.1± 0.2	48.4± 0.2
300192	1	2850± 953	7.5±0.1	-9.6± 0.4	12.2± 0.3
	2		6.3±0.1	25.5± 0.3	26.2± 0.3
	3		2.4±0.1	1.1± 0.4	2.6± 0.2
	4		-15.2±0.1	-1.6± 0.4	15.3± 0.1
	5	441± 89	-24.7±0.1	-4.1± 0.4	25.0± 0.1
	6		-53.0±0.1	-19.5± 0.3	55.4± 0.1
	7		-176.5±0.1	-45.8± 0.2	134.1± 0.2
	8	1520± 289	-179.4±0.1	0.0± 0.0	179.4± 0.1
	9		-21.6±0.1	8.2± 0.4	23.0± 0.2
300215	1		69.0±0.1	-7.6± 0.4	69.2± 0.1
	2		26.2±0.1	29.9± 0.2	38.9± 0.2
	3	362± 26	22.4±0.1	-1.2± 0.4	22.4± 0.1
	4		0.3±0.1	11.8± 0.4	11.8± 0.4
	5	1506± 229	-1.6±0.1	-5.2± 0.4	5.5± 0.4
	6	4280± 612	-6.7±0.1	-1.7± 0.4	6.9± 0.1
	7		-52.5±0.1	-18.1± 0.3	54.6± 0.1
	8		-68.0±0.1	34.0± 0.3	71.9± 0.1
	9	277± 20	-129.9±0.1	-1.4± 0.4	129.9± 0.1
400245	1		-86.4±0.1	-22.8± 0.3	86.7± 0.1
	2		-35.9±0.1	-16.8± 0.3	39.2± 0.1
	3	539± 49	-7.7±0.1	1.9± 0.4	7.9± 0.1
	4	4067± 562	-3.9±0.1	-3.5± 0.4	5.2± 0.3
	5	899± 291	-2.8±0.1	-3.5± 0.4	4.5± 0.3
	6		4.4±0.1	20.3± 0.3	20.8± 0.3
	7		6.0±0.1	10.9± 0.4	12.4± 0.4
	8	5359±1039	6.3±0.1	0.0± 0.0	6.3± 0.1
	9		-7.7±0.1	-12.4± 0.3	14.6± 0.3

EVENT	TRK	P(MEV)	$\phi(°)$	$\delta(°)$	$\theta(°)$
300255	1	990± 250	20.3±0.1	9.0± 0.4	22.1± 0.2
	2	368± 36	18.2±0.1	15.1± 0.3	23.5± 0.2
	4	3777± 706	8.8±0.1	5.8± 0.4	10.5± 0.2
	5	765± 127	5.4±0.1	-3.7± 0.4	6.5± 0.2
	6	749± 118	5.3±0.1	3.8± 0.4	6.5± 0.2
	7	427± 55	-6.2±0.1	-5.5± 0.4	8.3± 0.3
	8		-18.8±0.1	24.6± 0.3	30.6± 0.2
	9	351± 54	-32.8±0.1	6.0± 0.4	33.3± 0.1
	10		-70.8±0.1	-23.6± 0.3	72.5± 0.1
310302	1		98.3±0.1	14.1± 0.3	98.0± 0.1
	2		33.8±0.1	16.8± 0.3	37.3± 0.1
	3		5.3±0.1	-9.1± 0.4	10.5± 0.3
	4	5389± 536	-2.8±0.1	0.0± 0.0	2.8± 0.1
	5	1609± 170	-12.6±0.1	3.0± 0.4	12.9± 0.1
	6		-15.6±0.1	15.6± 0.3	21.9± 0.2
	7	872± 71	-57.6±0.1	1.9± 0.4	57.6± 0.1
	8	151± 27	-104.5±0.1	9.5± 0.4	104.3± 0.1
	9	383± 34	-156.7±0.0	9.8± 0.3	154.8± 0.1
310336	1		111.9±0.1	-33.1± 0.3	108.2± 0.1
	2		86.6±0.1	-55.6± 0.1	88.1± 0.1
	3		20.0±0.1	-9.1± 0.4	21.9± 0.2
	4	409± 160	19.5±0.1	6.2± 0.4	20.4± 0.2
	5	1215± 407	9.1±0.1	-5.3± 0.4	10.5± 0.2
	6		3.8±0.1	-19.9± 0.3	20.2± 0.3
	7		-6.9±0.1	31.0± 0.3	31.7± 0.3
	8		-9.0±0.1	14.5± 0.3	17.0± 0.3
	9		25.6±0.1	-57.9± 0.1	61.4± 0.1
310351	1	320± 50	68.9±0.1	-1.4± 0.4	68.9± 0.1
	2		56.1±0.1	-25.2± 0.3	59.7± 0.1
	3	614± 216	17.7±0.1	-9.5± 0.4	20.0± 0.2
	4		0.9±0.1	-16.8± 0.3	16.8± 0.3
	5		-7.9±0.1	6.6± 0.4	10.3± 0.3
	6		-82.3±0.1	0.0± 0.0	82.3± 0.1
	7	1227± 312	-84.7±0.1	10.7± 0.4	84.8± 0.1
	8		121.1±0.1	-12.3± 0.4	120.3± 0.1
	9		-18.9±0.1	28.5± 0.3	33.8± 0.2
240396	1		21.2±0.1	-12.5± 0.3	24.5± 0.2
	2		19.1±0.1	18.1± 0.3	26.1± 0.2
	3	2491± 99	9.9±0.1	1.6± 0.4	10.0± 0.1
	4		2.5±0.1	14.1± 0.4	14.3± 0.4
	5		-9.9±0.1	-29.4± 0.3	30.9± 0.3

EVENT	TRK	P(MEV)	ϕ(°)	δ(°)	θ(°)
	6	1502± 362	-12.4±0.1	0.0± 0.0	12.4± 0.1
	7		-36.8±0.1	25.2± 0.3	43.6± 0.2
	8		-102.3±0.1	-39.5± 0.2	99.5± 0.1
	9		-28.3±0.1	37.8± 0.2	45.0± 0.2
240400	1		28.1±0.1	16.0± 0.3	32.0± 0.2
	2		23.1±0.1	29.3± 0.3	36.7± 0.2
	3		6.1±0.1	37.7± 0.2	38.1± 0.2
	4	2747± 403	5.5±0.1	3.2± 0.4	6.4± 0.2
	5		3.7±0.1	-14.7± 0.4	15.1± 0.4
	6	240± 33	0.4±0.1	3.4± 0.4	3.4± 0.4
	7	1402± 50	-3.7±0.1	0.0± 0.0	3.7± 0.1
	8	741± 78	-35.8±0.1	0.0± 0.0	35.8± 0.1
	9		12.8±0.1	-51.5± 0.1	52.6± 0.1
240409	1		11.0±0.1	11.2± 0.4	15.6± 0.3
	2		6.3±0.1	8.3± 0.4	10.4± 0.3
	3	669± 58	6.3±0.1	-6.6± 0.4	9.1± 0.3
	4		5.3±0.1	12.6± 0.4	13.7± 0.4
	5		5.0±0.1	5.5± 0.4	7.4± 0.3
	6	4208± 835	-2.7±0.1	3.6± 0.4	4.5± 0.3
	7	840± 170	-7.3±0.1	-8.3± 0.4	11.0± 0.3
	8		-23.6±0.1	-34.5± 0.2	41.0± 0.2
	9		-41.9±0.1	8.9± 0.4	42.7± 0.1
240453	1	454± 81	8.1±0.1	-3.3± 0.4	8.7± 0.2
	2	1108± 122	5.6±0.1	-2.1± 0.4	6.0± 0.2
	3	670± 51	5.0±0.1	9.1± 0.4	10.4± 0.4
	4	5937±1291	0.5±0.1	0.0± 0.0	0.5± 0.1
	5	1523± 606	-1.1±0.1	-7.8± 0.4	7.9± 0.4
	6	2811± 180	-2.6±0.1	0.0± 0.0	2.6± 0.1
	7		-5.9±0.1	10.1± 0.4	11.7± 0.3
	8	1171± 187	-25.5±0.1	-3.3± 0.4	25.7± 0.1
	9		-85.9±0.1	25.5± 0.3	86.3± 0.1
240472	1		29.8±0.1	-14.2± 0.4	32.7± 0.2
	2		27.3±0.1	-60.4± 0.4	64.0± 0.3
	3	627± 71	10.0±0.1	0.0± 0.0	10.0± 0.1
	4		5.5±0.1	-13.4± 0.4	14.5± 0.4
	5	1184± 165	-5.3±0.1	0.0± 0.0	5.3± 0.1
	7		-9.0±0.1	50.8± 0.1	51.4± 0.1
	8		-17.0±0.1	-5.5± 0.4	17.8± 0.2
	9		-63.2±0.1	-18.0± 0.4	64.6± 0.1

EVENT	TRK	P(MEV)	$\phi(^\circ)$	$\delta(^\circ)$	$\theta(^\circ)$
	10	6935±3349	8.8±0.1	-1.3± 0.4	8.9± 0.1
240484	1		98.6±0.1	16.3± 0.3	98.3± 0.1
	2		58.9±0.1	18.9± 0.3	60.7± 0.1
	4	851± 96	11.7±0.1	-4.9± 0.4	12.7± 0.2
	5	1035± 127	3.0±0.1	-2.6± 0.4	4.0± 0.3
	6		-15.0±0.1	14.2± 0.4	20.5± 0.3
	7	1955± 431	-33.1±0.1	6.5± 0.4	33.7± 0.1
	8	1146± 104	-36.3±0.1	-2.6± 0.4	36.4± 0.1
	9		-122.1±0.1	20.3± 0.3	119.9± 0.1
	10		-146.0±0.1	-59.8± 0.5	114.6± 0.4
240499	1	505± 90	78.9±0.1	-3.9± 0.4	78.9± 0.1
	2	315± 30	54.8±0.1	10.1± 0.4	55.4± 0.1
	3		32.1±0.1	-54.4± 0.1	60.5± 0.1
	4		8.0±0.1	21.1± 0.3	22.5± 0.3
	5	403± 35	-2.2±0.1	9.8± 0.4	10.0± 0.4
	6		-2.6±0.1	-12.0± 0.4	12.3± 0.4
	7	670± 141	-7.8±0.1	2.3± 0.4	8.1± 0.1
	8		-7.8±0.1	-5.9± 0.4	9.8± 0.3
	9		-10.4±0.1	-6.2± 0.4	12.1± 0.2
240523	1		24.7±0.1	-16.3± 0.3	29.3± 0.2
	2	939± 289	21.2±0.1	-5.4± 0.4	21.8± 0.1
	3	695± 177	18.2±0.1	-8.2± 0.4	19.9± 0.2
	4		5.1±0.1	28.7± 0.3	29.1± 0.3
	5	929± 86	-1.1±0.1	-5.1± 0.4	5.2± 0.4
	6	1614± 267	-10.6±0.1	-7.9± 0.4	13.2± 0.2
	7		-29.3±0.1	-36.7± 1.4	45.6± 1.0
	8		-106.3±0.1	10.9± 0.4	106.0± 0.1
	9		-153.8±0.1	40.8± 0.2	132.8± 0.2
240549	1		37.4±0.1	-56.6± 0.1	64.1± 0.1
	3		22.2±0.1	12.8± 0.3	25.5± 0.2
	4		3.2±0.1	22.5± 0.3	22.7± 0.3
	5		-8.1±0.1	-33.4± 0.3	34.3± 0.3
	6		-8.6±0.1	13.6± 0.3	16.0± 0.3
	7		-11.0±0.1	-16.7± 0.3	19.9± 0.3
	8		-16.0±0.1	16.7± 0.3	23.0± 0.2
	9		-33.4±0.1	32.4± 0.3	45.2± 0.2
	10		-47.9±0.1	-45.6± 0.2	62.0± 0.1

EVENT	TRK	P(MEV)	ϕ(°)	δ(°)	θ(°)
150003	1		35.0±0.1	23.9± 0.3	41.5± 0.2
	2	333± 23	8.1±0.1	0.0± 0.0	8.1± 0.1
	3	653± 69	-5.2±0.1	1.0± 0.4	5.3± 0.1
	4		-8.2±0.1	-15.7± 0.3	17.7± 0.3
	5		-21.2±0.1	-11.5± 0.4	24.0± 0.2
	6	857± 149	-26.4±0.1	-8.6± 0.4	27.7± 0.1
	7	871± 186	-30.0±0.1	-6.9± 0.4	30.7± 0.1
	8		-21.3±0.1	35.9± 0.2	41.0± 0.2
	9		94.7±0.1	38.6± 0.7	93.7± 0.1
	10		-169.7±0.1	-19.9± 0.3	157.7± 0.3
150027	1		112.6±0.1	-17.1± 0.3	111.5± 0.1
	2		57.6±0.1	-52.0± 0.1	70.7± 0.1
	3		16.2±0.1	28.6± 0.3	32.5± 0.3
	4		7.8±0.1	14.8± 0.3	16.7± 0.3
	5		5.8±0.1	12.5± 0.4	13.8± 0.4
	6	1891± 600	4.4±0.1	-10.9± 0.4	11.7± 0.4
	7	1030± 297	2.4±0.1	-12.5± 0.3	12.7± 0.3
	8		0.3±0.1	46.5± 0.6	46.5± 0.6
	9		-6.2±0.1	11.3± 0.4	12.9± 0.4
	10	2093± 611	-22.8±0.1	-12.9± 0.4	26.0± 0.2
150029	1	222± 44	48.6±0.1	10.4± 0.4	49.4± 0.1
	2		36.8±0.1	-23.1± 0.5	42.6± 0.2
	3		13.8±0.1	-2.7± 0.4	14.1± 0.1
	4	642± 134	11.2±0.1	8.1± 0.4	13.8± 0.2
	5		8.0±0.1	-12.6± 0.4	14.9± 0.3
	6	1591± 266	3.9±0.1	1.8± 0.4	4.3± 0.2
	7	159± 37	3.0±0.1	0.0± 0.0	3.0± 0.1
	8		-5.7±0.1	-1.1± 0.4	5.8± 0.1
	9		-28.5±0.1	-3.6± 0.4	28.7± 0.1
	10	870± 192	-51.1±0.1	12.5± 0.3	52.2± 0.1
150033	1		43.9±0.1	-83.9± 0.0	85.6± 0.0
	2		35.8±0.1	-23.4± 0.3	41.9± 0.2
	3		33.4±0.1	-17.3± 0.3	37.1± 0.2
	4		0.2±0.1	57.6± 0.4	57.6± 0.4
	5		0.1±0.1	-21.6± 0.3	21.6± 0.3
	6		-27.7±0.1	45.6± 0.2	51.7± 0.2
	7		-43.3±0.1	-13.9± 0.3	45.1± 0.1
	8		-56.9±0.1	-31.1± 0.3	62.1± 0.1

EVENT	TRK	P(MEV)	ϕ(°)	δ(°)	θ(°)
	9		-75.5±0.1	19.6± 0.3	76.4± 0.1
	10		-101.2±0.1	-27.4± 0.3	99.9± 0.1
150155	1	2166± 457	24.8±0.1	-1.4± 0.4	24.8± 0.1
	2		19.1±0.1	2.0± 0.4	19.2± 0.1
	3	223± 36	4.5±0.1	-3.9± 0.4	6.0± 0.3
	4	1046± 134	0.8±0.1	2.8± 0.4	2.9± 0.4
	5	1724± 147	-7.9±0.1	6.2± 0.4	10.0± 0.3
	6	1321± 281	-11.1±0.1	6.0± 0.4	12.6± 0.2
	7		-12.4±0.1	-15.4± 0.4	19.7± 0.3
	8		-30.6±0.1	-38.5± 0.6	47.7± 0.4
	9	1154± 80	-35.2±0.1	0.9± 0.4	35.2± 0.1
	10	436± 98	-81.6±0.1	-5.3± 0.4	81.6± 0.1
300208	1		148.5±0.1	-14.5± 0.3	145.6± 0.1
	2		35.3±0.1	-27.7± 0.3	43.7± 0.2
	3		3.2±0.1	-33.9± 0.3	34.0± 0.3
	4		-2.3±0.1	23.3± 0.3	23.4± 0.3
	5		-6.1±0.1	-13.6± 0.4	14.9± 0.4
	6	1157± 334	-9.9±0.1	-10.0± 0.4	14.0± 0.3
	7	3647±1214	-11.7±0.1	-6.9± 0.4	13.6± 0.2
	8		-22.1±0.1	46.7± 0.2	50.5± 0.2
	9		-50.4±0.1	66.2± 0.3	75.1± 0.2
	10		-102.1±0.1	20.8± 0.3	101.3± 0.1
300236	1		13.2±0.1	27.9± 0.3	30.6± 0.3
	2		95.9±0.1	75.3± 0.1	91.5± 0.0
	3		50.4±0.1	16.6± 0.3	52.3± 0.1
	4	4657±2406	6.3±0.1	-3.4± 0.4	7.2± 0.2
	5		-3.8±0.1	-39.4± 0.2	39.6± 0.2
	6	399± 41	-6.9±0.1	-3.0± 0.4	7.5± 0.2
	7	2946± 861	-11.2±0.1	-5.8± 0.4	12.6± 0.2
	8		-18.1±0.1	-32.0± 0.3	36.3± 0.3
	9		-44.8±0.1	-2.6± 0.4	44.9± 0.1
	10		-48.0±0.1	-21.9± 0.3	51.6± 0.1
310294	1		79.8±0.1	65.2± 0.2	85.7± 0.1
	2	2204± 465	5.3±0.1	-3.9± 0.4	6.6± 0.2
	3		5.0±0.1	12.0± 0.4	13.0± 0.4
	4		3.2±0.1	11.7± 0.4	12.1± 0.4
	5	705± 83	-8.4±0.1	2.0± 0.4	8.6± 0.1
	6		-10.0±0.1	-14.9± 0.3	17.9± 0.3
	7		-30.0±0.1	6.5± 0.4	30.6± 0.1

EVENT	TRK	P(MEV)	$\phi(^{\circ})$	$\delta(^{\circ})$	$\theta(^{\circ})$
	8		−145.3±0.1	27.7± 0.3	136.7± 0.2
	9		−147.6±0.1	18.4± 0.4	143.2± 0.2
	10		−168.2±0.1	22.5± 0.4	154.7± 0.4
240444	1		113.5±0.1	−23.4± 0.3	111.5± 0.1
	2		25.4±0.1	−18.5± 0.4	31.1± 0.2
	3		15.4±0.1	11.6± 0.4	19.2± 0.2
	4	906± 209	15.2±0.1	−9.4± 0.4	17.8± 0.2
	5	2114± 488	14.4±0.1	−5.4± 0.4	15.4± 0.2
	6		8.7±0.1	17.3± 0.3	19.3± 0.3
	7		−3.7±0.1	14.3± 0.3	14.8± 0.3
	8		−113.8±0.1	38.5± 0.2	108.4± 0.1
	9		−160.3±0.1	22.7± 0.3	150.3± 0.2
	10		−11.0±0.1	38.6± 0.2	39.9± 0.2
461343	1		−20.4±0.1	−6.3± 0.4	21.3± 0.1
	2	1418± 373	−8.0±0.1	5.5± 0.4	9.7± 0.2
	3	1162± 149	−7.8±0.1	−2.4± 0.4	8.2± 0.2
	4		−3.2±0.1	−5.0± 0.4	5.9± 0.3
	5	522± 50	4.0±0.1	6.0± 0.4	7.2± 0.3
	6	391± 20	8.6±0.1	7.9± 0.4	11.7± 0.3
	7	818± 138	9.4±0.1	1.3± 0.4	9.5± 0.1
	8	729± 54	9.4±0.1	1.3± 0.4	9.5± 0.1
	9		10.7±0.1	−7.0± 0.4	12.8± 0.2
	10		102.3±0.1	50.6± 0.1	97.8± 0.1
410002	1	107± 21	140.5±0.1	10.5± 0.4	139.3± 0.1
	2	820± 147	19.4±0.1	−1.9± 0.4	19.5± 0.1
	3		7.9±0.1	7.4± 0.4	10.8± 0.3
	4	632± 114	7.2±0.1	0.7± 0.4	7.2± 0.1
	5	511± 176	5.8±0.1	−9.7± 0.4	11.3± 0.3
	6		−0.7±0.1	−1.4± 0.4	1.6± 0.4
	7	1211± 517	−1.0±0.1	5.8± 0.4	5.9± 0.4
	8		−10.8±0.1	10.6± 0.4	15.1± 0.3
	9		−21.4±0.1	−17.7± 0.3	27.5± 0.2
	10	8317±3075	6.6±0.1	−5.7± 0.4	8.7± 0.3
	11		−124.0±0.1	19.4± 0.3	121.8± 0.1
150009	1		72.4±0.1	−39.5± 0.2	76.5± 0.1
	2	2247± 268	14.0±0.1	−1.3± 0.4	14.1± 0.1
	3		9.7±0.1	6.2± 0.4	11.5± 0.2
	4		6.3±0.1	19.8± 0.3	20.7± 0.3
	5		−3.4±0.1	21.7± 0.3	22.0± 0.3
	6		−2.6±0.1	2.0± 0.4	3.3± 0.3

EVENT	TRK	P(MEV)	ϕ(°)	δ(°)	θ(°)
	7	803± 162	-11.4±0.1	-11.9± 0.4	16.4± 0.3
	8	966± 265	-16.6±0.1	-11.9± 0.4	20.3± 0.2
	9		-27.0±0.1	22.3± 0.3	34.5± 0.2
	10		-35.7±0.1	-18.9± 0.3	39.8± 0.2
	11		8.9±0.1	-26.1± 0.3	27.5± 0.3
150135	1		89.1±0.1	6.1± 0.4	89.1± 0.1
	2	307± 59	59.2±0.1	-9.2± 0.4	59.6± 0.1
	3		42.4±0.1	21.9± 0.3	46.8± 0.1
	4		28.6±0.1	-24.3± 0.3	36.9± 0.2
	5		21.9±0.1	28.6± 0.3	35.4± 0.2
	6	440± 60	5.9±0.1	-9.0± 0.4	10.7± 0.3
	7		-28.8±0.1	-22.2± 0.3	35.8± 0.2
	8		-30.2±0.1	15.5± 0.4	33.6± 0.2
	9		-109.4±0.1	-22.4± 0.3	107.9± 0.1
	10	8078± 668	2.2±0.1	-3.5± 0.4	4.1± 0.3
	11		-14.2±0.1	19.0± 0.3	23.6± 0.2
150188	1	430± 95	51.9±0.1	1.6± 0.4	51.9± 0.1
	2		28.7±0.1	23.0± 0.3	36.2± 0.2
	3		22.7±0.1	-6.3± 0.4	23.5± 0.1
	4		7.3±0.1	-38.2± 1.1	38.8± 1.1
	5		6.9±0.1	-2.8± 0.4	7.4± 0.2
	6		-0.7±0.1	-1.7± 0.4	1.8± 0.4
	7	831± 196	-8.0±0.1	12.4± 0.4	14.7± 0.3
	8		-11.7±0.1	65.9± 0.2	66.4± 0.2
	9		-17.5±0.1	-3.0± 0.4	17.7± 0.1
	10		-94.7±0.1	-21.1± 0.4	94.4± 0.1
	11	1813± 152	-13.3±0.1	4.7± 0.4	14.1± 0.2
300257	1		53.8±0.1	44.8± 0.2	65.2± 0.1
	2		27.9±0.1	24.7± 0.3	36.6± 0.2
	3		15.8±0.1	11.1± 0.4	19.2± 0.2
	4	1971± 183	11.0±0.1	-1.7± 0.4	11.1± 0.1
	5		8.6±0.1	29.1± 0.3	30.2± 0.3
	6		7.5±0.1	-34.0± 0.3	34.7± 0.3
	7		1.4±0.1	-19.6± 0.3	19.6± 0.3
	8		-20.7±0.1	28.1± 0.3	34.4± 0.2
	9	4195±1199	-20.2±0.1	-4.3± 0.4	20.6± 0.1
	10		-20.9±0.1	-30.1± 0.3	36.1± 0.2

EVENT	TRK	P(MEV)	ϕ(°)	δ(°)	θ(°)
	11		−40.9±0.1	15.7± 0.3	43.3± 0.1
300271	1		61.9±0.1	−8.0± 0.4	62.2± 0.1
	2		42.0±0.1	−8.3± 0.4	42.7± 0.1
	3		29.0±0.1	−18.8± 0.7	34.1± 0.4
	4		22.1±0.1	−3.5± 0.5	22.4± 0.1
	5	347± 75	21.8±0.1	14.3± 0.4	25.9± 0.2
	6	5173±1722	7.7±0.1	6.3± 0.4	9.9± 0.3
	7	1203± 83	6.4±0.1	0.0± 0.0	6.4± 0.1
	8	2372± 294	5.1±0.1	0.0± 0.0	5.1± 0.1
	9		−0.7±0.1	19.3± 1.0	19.3± 1.0
	10	1110± 132	−28.5±0.1	3.8± 0.4	28.7± 0.1
	11		−62.1±0.1	31.7± 0.3	66.5± 0.1
300274	1	1111± 212	36.0±0.1	7.2± 0.4	36.6± 0.1
	2		29.1±0.1	−23.3± 0.3	36.6± 0.2
	3	646± 284	18.1±0.1	−5.5± 0.4	18.9± 0.1
	4	1518± 260	16.3±0.1	−2.7± 0.4	16.5± 0.1
	5		6.7±0.1	9.7± 0.4	11.8± 0.3
	6	2920± 161	3.7±0.1	0.0± 0.0	3.7± 0.1
	7	814± 275	−22.1±0.1	5.2± 0.4	22.7± 0.1
	8		−32.2±0.1	18.1± 0.3	36.5± 0.2
	9	220± 36	−87.9±0.1	4.0± 0.4	87.9± 0.1
	10	498± 80	−134.3±0.1	0.0± 0.0	134.3± 0.1
	11		−166.6±0.1	54.5± 0.3	124.4± 0.3
310293	1		16.0±0.1	50.7± 0.1	52.5± 0.1
	2		9.6±0.1	−24.3± 0.4	26.0± 0.4
	3		9.4±0.1	−21.2± 0.3	23.1± 0.3
	4		4.5±0.1	−11.9± 0.4	12.7± 0.4
	5		−3.1±0.1	−13.4± 0.4	13.7± 0.4
	6	606± 35	−14.6±0.1	2.1± 0.4	14.7± 0.1
	7		−21.5±0.1	−18.2± 0.3	27.9± 0.2
	8		−44.6±0.1	−76.1± 0.1	80.2± 0.1
	9	557± 110	−42.3±0.1	−9.7± 0.4	43.2± 0.1
	10		−16.8±0.1	−23.5± 0.3	28.6± 0.2
	11		11.2±0.1	−23.5± 0.4	25.9± 0.4
150047	2	1153± 265	6.1±0.1	5.9± 0.4	8.5± 0.3
	3		10.3±0.1	−31.1± 0.3	32.6± 0.3
	4	1850± 644	1.3±0.1	6.0± 0.4	6.1± 0.4
	5	788± 94	−5.8±0.1	6.6± 0.4	8.8± 0.3
	6	2513± 287	−6.5±0.1	0.0± 0.0	6.5± 0.1
	7		−10.1±0.1	−11.6± 0.4	15.3± 0.3

EVENT	TRK	P(MEV)	$\phi(^\circ)$	$\delta(^\circ)$	$\theta(^\circ)$
	8	611± 158	-16.6±0.1	13.4± 0.4	21.2± 0.3
	9		-18.5±0.1	-31.6± 0.3	36.1± 0.3
	10		-33.5±0.1	41.9± 0.2	51.6± 0.2
	11		-88.9±0.1	36.0± 0.2	89.1± 0.1
	12		-175.6±0.1	-29.2± 0.3	150.5± 0.3
	13		2.5±0.1	31.1± 0.3	31.2± 0.3
300218	1		53.0±0.1	-16.3± 0.3	54.7± 0.1
	3	333± 63	29.3±0.1	6.5± 0.4	29.9± 0.1
	4		22.2±0.1	28.1± 0.3	35.2± 0.2
	5		12.4±0.1	20.7± 0.5	24.0± 0.4
	6		7.1±0.1	-20.2± 0.4	21.4± 0.4
	7		6.1±0.1	35.1± 0.2	35.6± 0.2
	8	880± 181	3.4±0.1	10.2± 0.4	10.7± 0.4
	9	8628±2528	-0.5±0.1	7.0± 0.4	7.0± 0.4
	10	1119± 106	-23.9±0.1	0.0± 0.0	23.9± 0.1
	11		-23.9±0.1	-24.9± 0.3	34.0± 0.2
	12	657± 48	-62.3±0.1	0.0± 0.0	62.3± 0.1
	13	265± 27	-114.3±0.1	-2.8± 0.4	114.3± 0.1
150032	1		79.2±0.1	-52.6± 0.1	83.5± 0.1
	2		35.2±0.1	-12.3± 0.4	37.0± 0.1
	3		31.8±0.1	-5.8± 0.4	32.3± 0.1
	4	1916± 656	25.0±0.1	4.9± 0.4	25.4± 0.1
	5		18.5±0.1	-47.9± 0.4	50.5± 0.4
	6		11.9±0.1	-15.7± 0.3	19.6± 0.2
	7		-1.6±0.1	-9.6± 0.4	9.7± 0.4
	8		-27.7±0.1	15.9± 0.3	31.6± 0.2
	9		-32.5±0.1	27.9± 0.3	41.8± 0.2
	10		-35.9±0.1	22.0± 0.8	41.3± 0.4
	11		-63.1±0.1	17.8± 0.3	64.5± 0.1
	12		-67.4±0.1	39.2± 0.8	72.7± 0.2
	13		-75.2±0.1	48.7± 0.5	80.3± 0.1
240415	1	198± 42	83.8±0.1	-2.6± 0.4	83.8± 0.1
	2		62.4±0.1	-25.7± 0.3	65.3± 0.1
	3		44.8±0.1	4.1± 0.4	44.9± 0.1
	4	3611± 477	13.2±0.1	0.0± 0.0	13.2± 0.1
	5	463± 104	2.7±0.1	0.0± 0.0	2.7± 0.1
	6		-8.5±0.1	11.3± 0.4	14.1± 0.3
	7		-19.2±0.1	-14.4± 0.4	23.8± 0.2
	8		-20.1±0.1	-14.6± 0.3	24.7± 0.2

EVENT	TRK	P(MEV)	$\phi(°)$	$\delta(°)$	$\theta(°)$
	9		-19.6±0.1	11.6± 0.4	22.7± 0.2
	10		-67.0±0.1	6.4± 0.4	67.2± 0.1
	11	597± 114	-76.5±0.1	1.8± 0.4	76.5± 0.1
	12		-90.2±0.1	29.2± 0.3	90.2± 0.1
	13		-102.9±0.1	22.1± 0.3	101.9± 0.1
150056	1		60.0±0.1	37.3± 0.6	66.6± 0.2
	2	650± 39	26.5±0.1	-2.4± 0.5	26.6± 0.1
	3		24.5±0.1	-28.0± 0.4	36.5± 0.3
	4	456± 84	22.3±0.1	11.1± 0.4	24.8± 0.2
	5		20.6±0.1	-36.0± 0.2	40.8± 0.2
	6		10.8±0.1	23.0± 0.3	25.3± 0.3
	7		9.6±0.1	15.3± 0.3	18.0± 0.3
	8	479± 92	4.2±0.1	-14.7± 0.4	15.3± 0.4
	9		-7.5±0.1	11.8± 0.7	14.0± 0.6
	10	757± 72	-14.9±0.1	-2.5± 0.4	15.1± 0.1
	11	976± 208	-22.4±0.1	14.9± 0.3	26.7± 0.2
	12		-26.1±0.1	-20.2± 0.3	32.6± 0.2
	13		-13.6±0.1	-37.5± 0.2	39.5± 0.2
	14		20.6±0.1	0.0± 0.0	20.6± 0.1
240492	1		91.6±0.1	-59.9± 0.2	90.8± 0.1
	2		49.7±0.1	55.0± 0.6	68.2± 0.3
	3		39.3±0.1	-46.5± 0.9	57.8± 0.6
	4	310± 37	24.6±0.1	9.3± 0.4	26.2± 0.2
	5	832± 286	14.9±0.1	-3.1± 0.4	15.2± 0.1
	6		10.2±0.1	25.9± 0.3	27.7± 0.3
	7		8.5±0.1	-20.8± 0.3	22.4± 0.3
	8		3.8±0.1	-17.2± 0.3	17.6± 0.3
	9	410± 94	-0.6±0.1	-2.6± 0.4	2.7± 0.4
	10	312± 47	-14.2±0.1	12.4± 0.3	18.8± 0.2
	11		-26.1±0.1	22.8± 0.3	34.1± 0.2
	12		-43.6±0.1	-19.5± 0.3	46.9± 0.1
	13		-53.7±0.1	-11.4± 0.4	54.5± 0.1
	14	1727± 138	-1.4±0.1	4.8± 0.4	5.0± 0.4
240542	2		33.1±0.1	-8.0± 0.4	33.9± 0.1
	3		23.1±0.1	6.8± 0.4	24.0± 0.1
	4		16.6±0.1	19.6± 0.3	25.5± 0.2
	5		13.0±0.1	18.5± 0.3	22.5± 0.2
	6	574± 149	9.8±0.1	-15.1± 0.4	17.9± 0.3
	7		10.1±0.1	-7.2± 0.4	12.4± 0.2
	8	1903± 800	5.7±0.1	3.9± 0.4	6.9± 0.2

EVENT	TRK	P(MEV)	ϕ(°)	δ(°)	θ(°)
	9		-1.6±0.1	-44.8± 0.2	44.8± 0.2
	10		-6.8±0.1	-20.4± 0.3	21.5± 0.3
	11	1515± 401	-7.3±0.1	-3.5± 0.4	8.1± 0.2
	12		-21.9±0.1	15.6± 0.4	26.7± 0.2
	13		-37.1±0.1	9.8± 0.4	38.2± 0.1
	14		-51.2±0.1	-46.9± 0.2	64.6± 0.1
	15		-69.4±0.1	36.4± 0.3	73.5± 0.1
	16		-114.9±0.1	14.2± 0.3	114.1± 0.1
150055	1		60.0±0.1	-23.2± 0.3	62.6± 0.1
	2		24.8±0.1	51.4± 0.1	55.5± 0.1
	3	601± 76	16.2±0.1	8.9± 0.4	18.4± 0.2
	4	211± 22	11.5±0.1	1.6± 0.4	11.6± 0.1
	5		8.5±0.1	-9.3± 0.4	12.6± 0.3
	6		6.6±0.1	-20.7± 0.3	21.7± 0.3
	7		-14.5±0.1	-9.6± 0.4	17.3± 0.2
	8		-17.6±0.1	-54.9± 0.3	56.8± 0.3
	9		-40.6±0.1	61.0± 0.1	68.4± 0.1
	10		-43.9±0.1	-63.2± 0.2	71.0± 0.1
	11		-81.4±0.1	-41.2± 0.2	83.5± 0.1
	12	441± 49	-122.3±0.1	16.4± 0.3	120.8± 0.1
	13		-129.3±0.1	-32.7± 0.3	122.2± 0.1
	14		-126.2±0.1	36.5± 0.2	118.3± 0.1
	15		-151.2±0.1	-41.3± 0.2	131.2± 0.2
	16		-17.3±0.1	35.8± 0.2	39.3± 0.2
240512	1		78.9±0.1	-13.4± 0.3	79.2± 0.1
	2		76.9±0.1	-59.9± 0.3	83.5± 0.1
	3		75.9±0.1	-50.9± 0.4	81.2± 0.1
	4	1583± 327	76.2±0.1	-8.2± 0.4	76.3± 0.1
	5		68.6±0.1	-48.8± 0.3	76.1± 0.1
	6		53.2±0.1	-55.0± 0.3	69.9± 0.2
	7	374± 84	24.2±0.1	-4.9± 0.4	24.7± 0.1
	8		22.3±0.1	-26.0± 0.3	33.7± 0.2
	9		12.8±0.1	-42.1± 0.2	43.7± 0.2
	10		11.2±0.1	-11.2± 0.4	15.8± 0.3
	11		10.5±0.1	-10.8± 0.4	15.0± 0.3
	12		11.1±0.1	18.8± 0.4	21.7± 0.3

EVENT	TRK	P(MEV)	$\phi(°)$	$\delta(°)$	$\theta(°)$
	13	1023± 64	10.3±0.1	0.0± 0.0	10.3± 0.1
	14		5.4±0.1	-10.7± 0.4	12.0± 0.4
	15		1.9±0.1	-25.3± 0.3	25.4± 0.3
	16	9155±1404	-8.2±0.1	0.0± 0.0	8.2± 0.1
	17		-15.8±0.1	15.5± 0.4	22.0± 0.3
	18	394± 27	-61.6±0.1	-2.2± 0.4	61.6± 0.1
	19	473± 114	-75.4±0.1	0.4± 0.4	75.4± 0.1
	20		-81.0±0.1	52.3± 0.3	84.5± 0.1

Filmed as received

without page(s) 178, 179 .

UNIVERSITY MICROFILMS.

LIST OF REFERENCES

1. Heisenberg, W., Kosmische Strahlung (Berlin, 1943)
2. Serber, R., Phys. Rev. 72, 1114 (1947)
3. Denisov, F. P. et al., Soviet J. Nuclear Phys. 1, 234 (1965)
4. Artykov, I.Z., Barashenkov, V. S., and Eliseev, S. M., Nucl. Phys. 87, 83 (1966)
5. Goldberger, M.R., Phys. Rev. 74, 1268 (1948)
6. Rozental', I. L., and Chernavskii, D. S., Usp. Fiz. Nauk. 52, 185 (1954)
7. Fermi, E., Prog. Theor. Phys. 5, 570 (1950)
8. Heisenberg, W., Z. Phys. 126, 560 (1949)
9. Landau, L. D., Izv. Akad. Nauk. SSSR Ser. Fiz. 17, 51 (1953)
10. Feinberg, E. L., Soviet Phys. JETP 1, 176 (1955)
11. Belen'kji, S. Z., and Landau, L. D., Suppl. Nuovo Cimento 3, 15(1956)
12. Belen'kji, S. Z., and Milekhin, G. A., Soviet Phys. JETP 2, 15 (1956)
13. Milekhin, G. A., Soviet Phys. JETP 8, 829 (1959)
14. Tolstov, K. D., Nucl. Phys. 47, 11 (1963)
15. Barashenkov, V. S., et al., Nucl. Phys. 55, 79 (1964)
16. Barashenkov, V. S., et al., Nucl. Phys. 14, 522 (1959-60)
17. Barashenkov, V. S., Maltsev, V. M., and Mikhul, E. K., Nucl. Phys. 24, 642 (1961)
18. Tolstov, K. D., Nucl. Phys. 27, 144 (1961)

LIST OF REFERENCES (Cont.)

19. Barashenkov, V. S., et al., Soviet Atomic Energy 16, 636 (1964)

20. Artykov, I. Z., Barashenkov, V. S., and Eliseev, S. M. Soviet J. Nucl. Phys. 4, 113 (1967)

21. Metropolis, N., et al., Phys. Rev. 110, 204 (1958)

22. Dostrovsky, I., Fraenkel, Z., and Winsberg, L., Phys. Rev. 118, 781 (1960)

23. Mora, U., and Yekutieli, G., Nuovo Cimento 17, 45 (1960)

24. Sitte, K., Encyclopedia of Physics Vol. XLVI/1, 157 (1961)

25. Fujimoto, Y., and Hayakawa, S., Encyclopedia of Physics Vol. XLVI/2, 115 (1967)

26. Pinkau, K., Forschr. Phys. 12, 139 (1964)

27. Rozental', I. L., and Chernavskii, D. S., Fortschr. Phys. 4, 560 (1956)

28. Koba, Z.,and Takagi, S., Fortschr. Phys. 7, 1 (1959)

29. Barashenkov, V. S., Maltsev, V. M., and Zinovjev, G. M. Acta Phys. Polon. 33, 315 (1968)

30. Artykov, I. Z., Barashenkov, V. S., and Eliseev, S. M., Nucl. Phys. B6, 11 (1968)

31. Winzeler, H. W., et al., Nuovo Cimento 17, 8 (1969)

32. Jain, P. L., and Glahe, H. C., Phys. Rev. 116, 458 (1959)

33. Bricman, C., et al., Nuovo Cimento 20, 1017 (1961)

34. Boos, E. G., et al., Soviet Physics JETP 20, 1371 (1962)

35. Galtieri Barbaro, A., et al., Nuovo Cimento 20, 1012 (1961)

36. Lim, Y. K., Nuovo Cimento 26, 1221 (1962)

37. Cvijanovich, G., et al., Nuovo Cimento 20, 1012 (1961)

38. Bogdanowicz, J., et al., Nucl. Phys. 40, 270 (1963)

LIST OF REFERENCES (Cont.)

39. Garbowska, K., _et al._, Nucl. Phys. _60_, 654 (1964)

40. Hoffman, L., _et al._, Nucl. Phys. _66_, 657 (1965)

41. Kohli, J. M., Mittra, I. S., Singh, M. B., J. Phys. Soc. Japan _22_, 1 (1967)

42. Friedlander, E. M., Nuovo Cimento _14_, 796 (1959)

43. Farley, F. J. M., Nuovo Cimento _16_, 209 (1960)

44. Bogachev, N. P., _et al._, Soviet Physics JETP _11_, 317 (1960)

45. Lohrmann, E., Teucher, M. W., Schein, M., Phys. Rev. _122_, 672 (1961)

46. Matsumoto, S., J. Phys. Soc. Japan _17_, 1 (1962)

47. Lohrmann, E. and Teucher, M. W., Nuovo Cimento _25_, 957 (1952)

48. Lim Y. K., Nuovo Cimento _26_, 1221 (1962)

49. Meyer, H., Teucher, H. W., and Lohrmann, E., Nuovo Cimento _28_, 1399 (1963)

50. Jain, P. L., _et al._, Nucl. Phys. _67_, 641 (1965)

51. Kohli, J. M., Mittra, I. S., and Singh, M. B., Nucl. Phys. _B2_, 164 (1967)

52. Shen, M. L., Nucl. Phys. _B3_, 77 (1967)

53. Rao, G. K., Rao, P. D. K., and Kamal, A. A., Canad. J. Phys. _45_, 3211 (1967)

54. Azimov, S. A., _et al._, Soviet J. Nucl. Phys. _8_, 542 (1969)

55. Gil, D., _et al._, Nucl. Phys. _82_, 662 (1966)

56. Pinkau, K., Phil. Mag. _6_, 657 (1961)

57. Imaeda, K., Nuovo Cimento _28_, 908 (1963)

58. Imaeda, K., and Avidan, J., Nuovo Cimento _32_, 1497

59. Aly, H. H., Kaplon, M. F., and Shen, M. O., Nuovo Cimento _32_, 905 (1964)

LIST OF REFERENCES (Cont.)

60. Friedlander, E. M., Nuovo Cimento 41, 417 (1966)

61. Wayland, J. R., and Bowen, T., Nuovo Cimento 48A, 663 (1967)

62. Cocconi, G., Nuovo Cimento 57A, 837 (1968)

63. Ijaz, M. A., and Campbell, J. E., Nuovo Cimento 61A 307 (1969)

64. Hagedorn, R., Suppl. Nuovo Cimento 3, 147 (1965)

65. Kajzar F., Acta. Phys. Polon. 31, 231 (1937)

66. Aly, H. H., Duthie, J. G. M., and Fisher, C. M., Phil. Mag. 4, 993 (1954)

67. Ohba, I., and Kobayashi, T., Prog. Theor. Phys. Suppl. 41-42, 90 (1967)

68. Malhotra, P. K., Nucl. Phys. 59, 551 (1964)

69. Spergel, M. S., Lieber, M., and Milford, S. N., Nuovo Cimento 42, 255 (1966)

70. Ciurlo, S., *et al.*, Nuovo Cimento 27, 791 (1963)

71. Yajima, N., and Hasegawa, S., Prog. Theor, Phys. 33, 184 (1965)

72. Edwards, B., *et al.*, Phil. Mag. 3, 237 (1957)

73. Aachen-Birmingham-Bonn-Hamburg-London-Munich Collaboration-Nuovo Cimento 31, 485 (1964)

74. Bellini, G., *et al.*, Nuovo Cimento 40, 948 (1948)

75. Petrzilka, S., *Proceedings of the International Conference on High Energy Physics* (Rochester, (1960) p.82

76. Friedlander, E. M., Marcu, M., and Spirchez, M., Nuovo Cimento 18, 623 (1960)

77. Bozoki, G., *et al.*, Nuovo Cimento 24, 29 (1962)

78. Biswas, N. N., *et al.*, Phys. Rev. 134, B901 (1964)

79. Kohli, J. M., Nucl. Phys. B4, 443 (1968)

LIST OF REFERENCES (Cont.)

80. Goldsack, S. G., et al., Nuovo Cimento 23,941 (1962)

81. Dubey, D. P., and Kohli, J. M., preprint (to be published)

82. Huson, F. R., and Fretter, W. B., Nuovo Cimento, 33, 1 (1964)

83. Bellini, G., et al., Nuovo Cimento 27, 816 (1963)

84. Belyukov, V. A., et al., Soviet Phys. JETP 39, 937(1960)

85. Grote, L.C., et al., Nucl. Phys. 24, 300 (1961)

86. Ferrero, M. I., et al., Nuovo Cimento 27, 1069 (1962)

87. Ferbel, T., and Taft, H., Nuovo Cimento 28, 1214(1963)

88. Proceedings of the Second Topical Conference, Resonant Particles (Ohio University, Athens, Ohio, 1965)

89. Williams, W. S. C., Introduction to Elementary Particles (Academic Press, New York, 1965)

90. Barkas, W. H., Nuclear Research Emulsions (Academic Press, New York, 1963)

91. Barkas, W. H., Private communication

92. Kinzer, R. L., Ph.D. Dissertation (University of Oklahoma, Norman, Oklahoma, 1967)

93. Samimi, J., Ph.D. Dissertation (University of Oklahoma, Norman, Oklahoma, 1969)

94. Burwell, J. R., Proceedings of the VI International Conference on Corpuscular Photography (1966)

95. Enge, H. A., Introduction to Nuclear Physics (Addison-Wesley, Reading, Massachusetts, 1966)

96. Barashenkov, V. S., et al., Fortshr. Phys. 14, 357(1966)

97. Barashenkov, V. S., and Maltsev, V. M., Fortshr. Phys. 15, 435 (1967)

98. Going, H., Nucl. Phys. 43, 662 (1963)

99. Finney, P.J., and Major, J.V., Nuovo Cimento 41, A771 (1966)

LIST OF REFERENCES (Cont.)

100. Wine, R.L., Statistics for Scientists and Engineers (Prentice-Hall, Englewood Cliffs, New Jersey, 1964)

101. Zhdanov, G.B., *et al.*, Soviet Phys. JETP, 10, 433(1960)

102. Samimi, J., M.S. Thesis (University of Oklahoma, Norman, Oklahoma, 1966)

103. Ho, S. K., M. S. Thesis (University of Oklahoma, Norman, Oklahoma, 1968)

104. Barkow, A., *et al.*, Phys. Rev. 122, 617 (1961)

105. Grote, C., *et al.*, Nucl. Phys. 34, 685 (1962)

106. Jain, P. L., *et al.*, Nuovo Cimento 32, 873 (1964)